

## OSTRACODS FROM THE LATE TRIASSIC (NORIAN) OF YUKON, CANADA: NEW TAXONOMIC AND PALAEOBIOGEOGRAPHIC INSIGHTS

MARIE-BÉATRICE FOREL<sup>1\*</sup>, NICOLÒ DEL PIERO<sup>2</sup>, SYLVAIN RIGAUD<sup>3</sup>  
& ROSSANA MARTINI<sup>2</sup>

<sup>1</sup>Centre de Recherche en Paléontologie – Paris (CR2P), Muséum national d'Histoire naturelle, 8 rue Buffon, 75005 Paris (France)

<sup>2</sup>University of Geneva, Department of Earth Sciences, Rue des Maraîchers 13, CH-1205 Genève (Switzerland)

<sup>3</sup>Asian School of the Environment, 62 Nanyang Drive, 637459 (Singapore)

\*Corresponding Author.

Associate Editor: Ilaria Mazzini.

To cite this article: Forel M.-B., Del Piero N., Rigaud S. & Martini R. (2022) - Ostracods from the Late Triassic (Norian) of Yukon, Canada: new taxonomic and palaeobiogeographic insights. *Riv. It. Paleontol. Strat.*, 128(2): 325-368.

**Keywords:** marine ostracods; Norian; Panthalassa; ostracod-algae association; palaeobiogeography.

*Abstract.* The present work investigates the significance of Late Triassic ostracods from the Yukon Territory, Canada, and adds to the scientific knowledge of the taxonomy of these organisms during the Norian, which remain poorly documented and understood. Fifteen limestone samples representing distinct marine palaeoenvironments cropping out at Lime Peak, Stikinia terrane, provided 90 species, including 9 newly described: *Alatobairdia? sobni* n. sp., *Bairdia aksala* n. sp., *B. taan* n. sp., *B. yukonensis* n. sp., *Cornutobairdia yukonella* n. sp., *Lobobairdia whitella* n. sp., *Mirabairdia canadia* n. sp., *Hungarella limella* n. sp., *Leviella riedeli* n. sp. Most assemblages point to neritic conditions in the photic zone. A similarity analysis demonstrates the distinct composition of reef-related and algae-related ostracod assemblages. The ostracod-algae associations in Lime Peak reveal that the affinity of Bairdiidae for algae (Dasycladaleans in the case of Lime Peak) was already established in the Norian. A faunal link is identified during the Norian between eastern and western Panthalassa and Japan, in line with studies on other taxa. The flux of species between eastern Panthalassa and Tethyan areas appears very unbalanced in the Late Triassic with most migrations originating from the Tethys. Further data from other Middle and Upper Triassic Panthalassan localities and stages (i.e. Ladinian and Carnian) are needed to confirm whether this apparent trend is due to sampling bias or reflects real dispersal fluxes.

## INTRODUCTION

The Triassic is unique in Phanerozoic history: it is bracketed by the major end-Permian and end-Triassic biotic extinction events, provided the oldest roots of the Mesozoic Marine Revolution and was thus pivotal in the emergence, shaping

and structuring of modern marine ecosystems (e.g. Klompaker et al. 2016; Forel et al. 2018; Lukeneder et al. 2020). It is now well-established that marine ostracods, after having gone through a major crisis at the end of the Permian, underwent a major re-organisation during the Triassic (e.g. McKenzie 1982; Crasquin & Forel 2014; Forel & Crasquin 2020). However, the knowledge of Triassic ostracods remains dominated by western Tethys localities and the significance of eastern Tethys and

Received: April 13, 2021; accepted: November 03, 2021

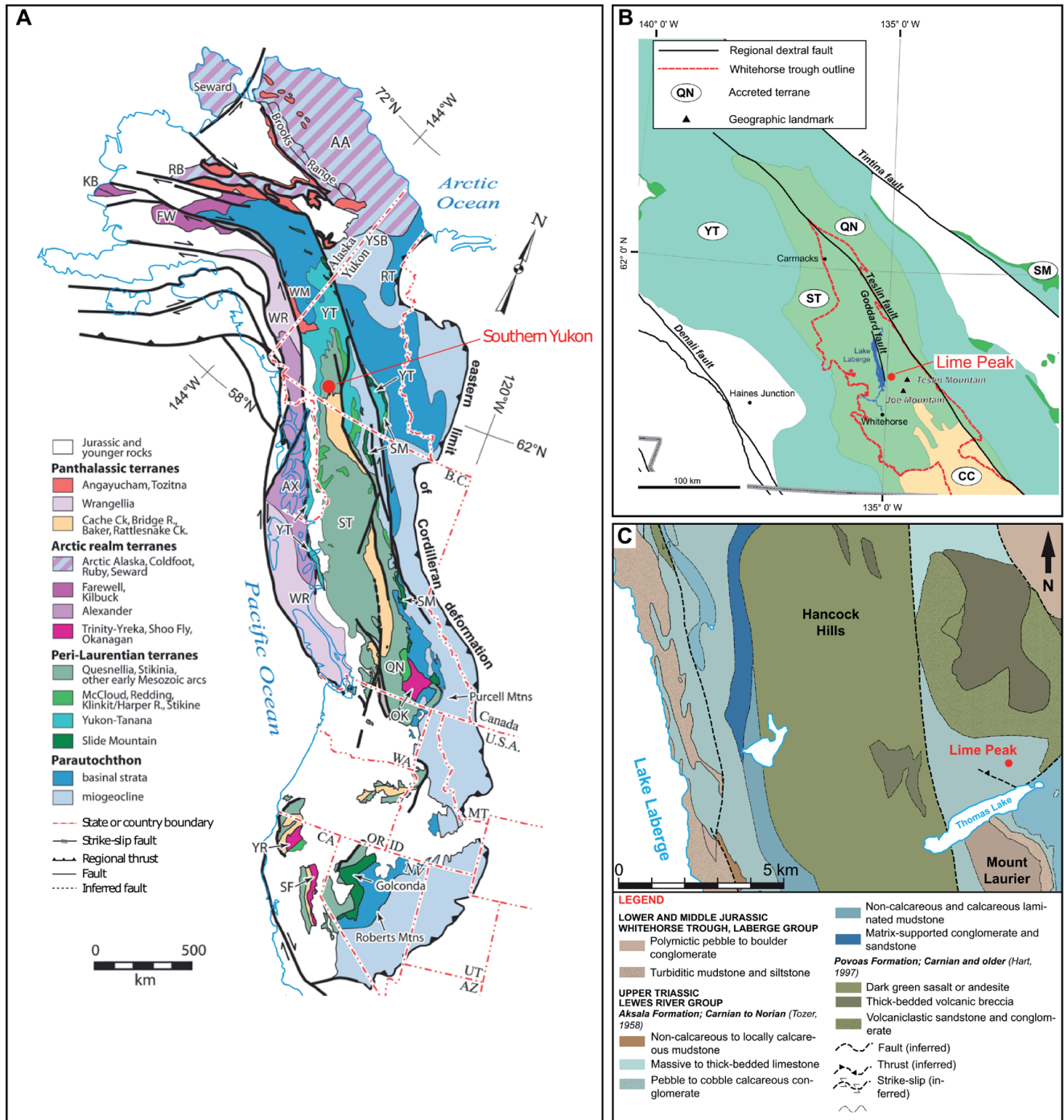


Fig. 1 - Geological and tectonic settings of the study area. A. Terranes map of the North American Cordillera showing the study location (modified from Del Piero et al. in prep. after Colpron & Nelson 2011). B. Terranes configuration within the Intermontane terranes: YT = Yukon-Tanana, ST = Stikina, QN = Quesnellia, SM = Slide Mountain, CC = Cache Creek, NA = ancestral North America (modified from Del Piero et al. in prep. after Bordet, 2016). C. Bedrock map of the western side of Lake Laberge where Lime Peak is located (modified from Del Piero et al. in prep. after Bordet 2017).

Panthalassa data is largely overlooked, as discussed for instance by Bate (1977), Lord (1988), Forel et al. (2019a), Forel & Moix (2020). The Late Triassic witnessed key events in the evolution of ostracods, among these, are: major radiations of ornate Bairdiidae, maximum of diversity of Cytherellidae and

Cytheruridae in the Carnian, acme of Bairdiidae, Cytheruridae and Healdiidae as well as the earliest occurrences of Progonocytheridae and Cytheridae in the Rhaetian (Forel & Crasquin 2020). Until now, isolated specimens of Norian ostracods have been reported and sometimes only illustrated from

Alaska (Sohn 1964, 1984, 1987), the Alps (Kollmann 1963; Kristan-Tollmann 1969, 1970, 1971a, 1973; Tollmann & Kristan-Tollmann 1970; Bunza & Kozur 1971; Kozur 1973a; Urlichs 1972; Zorn 2010), Canada (Reid 1985; Arias & Lord 2000; Sohn 1987), Exmouth Plateau (Kristan-Tollmann & Gramann 1992), Hungary (Bunza & Kozur 1971; Monostori & Tóth 2014) and Slovakia (Kozur 1996). However, they remain among the most poorly known for the entire Triassic as only rare complete assemblages have been studied so far. The present investigation of ostracods from the Upper Norian of Lime Peak in Whitehorse area, Yukon Territory, Canada is a unique opportunity to fill in these temporal and geographic gaps. The assemblages obtained allow us to investigate and discuss their taxonomy and diversity as well as palaeoenvironmental and palaeogeographic implications.

## GEOLOGICAL SETTING AND STUDIED SAMPLES

More than 70% of the North American Cordillera is made up by a “puzzle” of various crustal fragments and oceanic remnants that have been grouped into distinct tectonostratigraphic terranes (Jones et al. 1977; Coney et al. 1980; Wheeler & McFeeley 1991; Colpron et al. 2007). Most of these terranes are thought to be exotic to North America: originally formed or sedimented in the Panthalassa Ocean, they travelled towards the North American craton prior to their accretion onto it in the Mesozoic (e.g. Jones et al. 1977; Coney et al. 1980; Wheeler & McFeeley 1991; Colpron et al. 2007; Fig. 1A). Their exact palaeoposition, along with the total amount and trajectory of their displacement, however, remain poorly constrained and a widely debated issue (e.g. Aberhan 1999; Belasky et al. 2002; Schroeder-Adams & Haggart 2006; Smith 2006; Colpron et al. 2007; Beranek & Mortensen 2011; Golding et al. 2016a, 2016b; Golding 2019).

South-central Yukon and British Columbia are located in the Intermontane terranes belt (Colpron et al. 2007; Colpron & Nelson 2011). Within this belt, Mesozoic rocks of Stikinia and Quesnelia terranes bound the Cache Creek accretionary complex (Wheeler & McFeeley 1991; Colpron &

Nelson 2011; Fig. 1A & B). In southern Yukon, where Lime Peak is located, the Triassic succession of Stikinia is dominated by the Upper Triassic Lewes River Group (LRG). The basal part of the LRG is characterized by volcanic and volcanoclastic rocks (Povoas Formation) mainly of Carnian age that represent the product of the volcanism within Stikinia (Fig. 1C). Towards the end of the volcanism, the carbonate sedimentation took over (Aksala Formation; White et al. 2012; Bordet 2017; Bordet et al. 2019) and, according to Bordet et al. (2019), occurred in different sub-basins within Stikinia.

The Lime Peak area was the subject of several manuscripts, particularly the south-west face of the mountain (Fig. 1C), which is the best preserved (e.g. Reid 1985, 1988; Reid & Ginsburg 1986; Reid & Tempelman-Kluit 1987; Senowbari-Daryan & Reid 1987) in terms of rock quality and depositional relationships. A more recent sedimentological and micropalaeontological investigation (Del Piero et al., in prep.) highlighted the presence of contiguous depositional environments in the Lime Peak area and allowed for a better understanding of the local carbonate system.

## MATERIAL AND METHODS

The studied material comes from 15 limestone samples (OST3, 4, 6-10, 12, 13, WH227, 232, 234, 235, 236, 259), collected at Lime Peak, Whitehorse area, Yukon Territory, Canada (Fig. 1 C; see supplementary data for precise sampling locations). The samples have been treated by hot acetolysis technique (Lethiers & Crasquin-Soleau 1988; Crasquin-Soleau et al. 2005) for ostracod extraction and all have been productive. Note, “sample” OST13 corresponds to several samples dissolved together representing different silicified facies, mixed palaeoenvironments: for this reason, it is only considered for taxonomic purposes but not discussed for palaeoenvironment and paleobiogeography. In the present contribution, we follow the general classification of ostracods of Moore (1961), Becker (2002) and Horne et al. (2002). The taxonomy of Cytheroidea is based on the revisions of Whatley & Boomer (2000).

Ninety species distributed into 31 genera and 11 families have been identified during this investigation (Tab. 1). Several taxonomic issues are still unresolved regarding Triassic ostracods so that all species are illustrated to enable future comparisons (Plates 1-6). The synonymy (list of synonymized species) and cressonymy (list of occurrences of the species) of known species are provided and species kept in open nomenclature or referred to other species are only discussed when necessary. Following Maddocks (2015), the degree of slope of the antero-dorsal and postero-dorsal margins were measured on external lateral views of the carapaces/valves, with 0 being horizontal. Bairdiidae are highly homeomorphic ostracods (e.g. Maddocks 1969) for which diagnostic features are complex to characterize and describe. Characters are here quantified as much as possible and the length convention of carapaces/valves

Class <b>Ostracoda</b> Latreille, 1806	Superfamily <b>Cytheroidea</b> Baird, 1850
Subclass <b>Podocopa</b> Müller, 1894	Family <b>Bythocytheridae</b> Sars, 1866
Superfamily <b>Bairdioidea</b> Sars, 1887	<i>Patellacythere?</i> sp. [Pl. 5U; sample WH227]
Family <b>Bairdiidae</b> Sars, 1887	Family <b>Cytheruridae</b> Müller, 1894
Subfamily <b>Bairdiinae</b> Sars, 1923	<i>Judahella dizhuense</i> Kristan-Tollmann in Kristan-Tollmann et al., 1980 [Pl. 5P; samples OST6, 13]
<i>Acratia</i> sp. 1 [Pl. 1A; samples OST4, 6, 13]	<i>Judahella nodosa nodosa</i> (Kozur in Bunza & Kozur, 1971 sensu Kristan-Tollmann 1989) [Pl. 5Q, R; sample OST6]
<i>Acratia</i> sp. 2 [Pl. 1B; sample OST6]	<i>Judahella</i> sp. [Pl. 5S; sample OST6]
<i>Alatobairdia?</i> <i>sohni</i> Forel n. sp. [Pl. 1C-P; samples OST6, 13]	Family <b>Limnocytheridae</b> Klie, 1938
<i>Bairdia aksala</i> Forel n. sp. [Pl. 1Q-T, 2A-D; samples OST6, 12, WH227, 234, 235]	<i>Lutkevichinella?</i> sp. [Pl. 5T; sample WH236]
<i>Bairdia taan</i> Forel n. sp. [Pl. 2E-L; samples OST6, WH227, 232, 234, 235]	Family indet.
<i>Bairdia yukonensis</i> Forel n. sp. [Pl. 2M-Q; sample OST6]	Genus et sp. indet. [Pl. 4AF; sample WH234]
<i>Bairdia</i> sp. 7 in Forel et al. 2019b [Pl. 2R, S; samples OST7, WH227, 234, 235, 236]	Superfamily <b>Macrocypridoidea</b> Müller, 1912
<i>Bairdia</i> sp. A in Dépêche & Crasquin-Soleau, 1992 [Pl. 2T, U; samples OST3, 6, 7, 10, WH227, 235, 236]	Family <b>Macrocyprididae</b> Sars, 1866
<i>Bairdia</i> cf. <i>balatonica</i> Mehes, 1911 [Pl. 2V, W; samples OST7, WH227, 235, 259]	<i>Praemacrocypris</i> sp. 1 [Pl. 5V; sample OST6]
<i>Bairdia</i> sp. 1 [Pl. 2X; sample OST4]	<i>Praemacrocypris?</i> sp. 2 [Pl. 5W; samples OST6, 8]
<i>Bairdia</i> sp. 2 [Pl. 2Y-AA; samples WH227, 234, 235]	Superfamily <b>Sigillioidea</b> Mandelstam, 1960
<i>Bairdia</i> sp. 3 [Pl. 2AB; sample OST7]	Family <b>Sigillidae</b> Mandelstam, 1960
<i>Bairdia</i> sp. 4 [Pl. 2AC; samples OST7, 8]	<i>Cardobairdia?</i> sp. 1 [Pl. 5X; samples OST10, 13]
<i>Bairdia?</i> sp. 6 [Pl. 2AD, AE; sample OST6]	<i>Cardobairdia?</i> sp. 2 [Pl. 5Y; sample WH227]
<i>Bairdia</i> sp. 7 [Pl. 3A; sample OST10]	<i>Cardobairdia?</i> sp. 3 [Pl. 5Z; samples OST6, 12]
<i>Bairdia</i> sp. 8 [Pl. 3B; sample WH227]	<i>Cardobairdia?</i> sp. 4 [Pl. 5AA; sample OST6]
<i>Bairdia</i> sp. 9 [Pl. 3C; sample WH227]	Suborder <b>Metacopina</b> Sylvester-Bradley, 1961
<i>Bairdia</i> sp. 10 [Pl. 3D; samples OST7, WH235]	Superfamily <b>Healdioidea</b> Harlton, 1933
<i>Bairdia</i> sp. 11 [Pl. 3E; samples OST6, 7, 10]	Family <b>Healdiidae</b> Harlton, 1933
<i>Bairdia</i> sp. 12 [Pl. 3F; samples OST3, 10, WH227]	<i>Hungarella limella</i> Forel n. sp. [Pl. 5AB-AE, 6A-C; samples WH227, 232, 234-236, 259]
<i>Bairdia</i> sp. 13 [Pl. 3G, H; samples OST4, 7, WH227, 234, 235, 236]	<i>Hungarella</i> sp. [Pl. 6D, E; samples OST4, 6, 7, 12]
<i>Bairdia</i> sp. 14 [Pl. 3I; sample OST9]	Order <b>Platycopida</b> Sars, 1866
<i>Bairdiacypris sorgunensis</i> Forel in Forel et al. 2018 [Pl. 3J, K; samples OST6, 12]	Suborder <b>Platycopina</b> Sars, 1866
<i>Bairdiacypris</i> cf. <i>triassica</i> Kozur, 1971c [Pl. 3L-N; samples OST4, 6, 7]	Superfamily <b>Cavellinoidea</b> Egorov, 1950
<i>Bairdiacypris</i> sp. 1 [Pl. 3O; sample OST7]	Family <b>Cavellinidae</b> Egorov, 1950
<i>Bairdiacypris</i> sp. 2 [Pl. 3P; sample OST6]	<i>Bektasia</i> sp. 1 [Pl. 6F; samples OST7, WH234]
<i>Bairdiacypris?</i> sp. 3 [Pl. 3Q, R; samples OST3, 10]	<i>Bektasia</i> sp. 2 [Pl. 6G, H; samples WH227, 232, 234, 236, 259]
<i>Carinobairdia?</i> sp. [Pl. 3S; sample WH235]	<i>Bektasia</i> sp. 3 [Pl. 6I; sample OST8]
<i>Cornutobairdia yukonella</i> Forel n. sp. [Pl. 3T-AF; samples OST6, 12, 13]	Superfamily <b>Cytherelloidea</b> Sars, 1866
<i>Cornutobairdia</i> sp. [Pl. 4A, B; samples OST6, 13]	Family <b>Cytherellidae</b> Sars, 1866
<i>Hiatobairdia subsymetrica</i> Kristan-Tollmann, 1970 [Pl. 4C, D; samples OST6, 13]	<i>Cytherella</i> sp. 1 [Pl. 6J; samples WH227, 234-236]
<i>Hiatobairdia</i> cf. <i>senegasi</i> Forel in Forel et al., 2019a [Pl. 4E; sample WH235]	<i>Cytherella</i> sp. 2 [Pl. 6K; samples WH232, 234, 235, 259]
<i>Hiatobairdia</i> sp. [Pl. 4F; samples OST12, WH236]	<i>Issacherella</i> sp. [Pl. 6L; samples OST4, 7]
<i>Isobithocypris</i> sp. 1 [Pl. 4G; samples OST6, WH227, 234, 236]	<i>Leviella riedeli</i> Forel n. sp. [Pl. 6M-Q; sample OST6]
<i>Isobithocypris?</i> sp. 2 [Pl. 4H; sample WH227]	<i>Leviella sohni</i> Kozur in Kozur et al., 1974 [Pl. 6R; sample OST13]
<i>Lobobairdia whitella</i> Forel n. sp. [Pl. 4I-R; samples OST4, 6, 7, 13, WH227, 236, 259]	<i>Leviella unicostata</i> (Bolz, 1970) [Pl. 6S, T; samples WH227, 232, 234-236, 259]
? <i>Lobobairdia whitella</i> Forel n. sp. [Pl. 4S; sample OST6]	<i>Leviella</i> cf. <i>brevicostata</i> Kristan-Tollmann, 1973 [Pl. 6U; sample OST6]
<i>Lobobairdia</i> sp. 1 [Pl. 4T; sample OST13]	<i>Leviella</i> sp. 1 [Pl. 6V; samples WH227, 234]
<i>Lobobairdia</i> sp. 2 [Pl. 4U; sample OST13]	<i>Leviella</i> sp. 2 [Pl. 6W; sample OST6]
<i>Mirabairdia canadia</i> Forel n. sp. [Pl. 4V-AA; samples OST6, 13]	<i>Leviella</i> sp. 3 [Pl. 6X; sample OST13]
<i>Petasobairdia?</i> sp. [Pl. 4AB; sample OST10]	<i>Leviella</i> sp. 4 [Pl. 6Y; sample OST7]
<i>Ptychobairdia?</i> sp. in Arias & Lord, 2000 [Pl. 4AC; samples WH234, 235]	Subclass <b>Myodocopa</b> Sars, 1866
<i>Ptychobairdia</i> cf. <i>veghae</i> (Kozur, 1971b) [Pl. 4AD; sample WH235]	Order <b>Myodocopida</b> Sars, 1866
<i>Ptychobairdia</i> sp. [Pl. 4AE; samples OST6, 13]	Suborder <b>Myodocopina</b> Sars, 1866
Superfamily <b>Cypridoidea</b> Baird, 1845	Superfamily <b>Polycopoidea</b> Sars, 1866
Family <b>Paracyprididae</b> Sars, 1866	Family <b>Polycopidae</b> Sars, 1866
<i>'Aglaiocypris'</i> sp. [Pl. 5A; samples OST7, 8]	<i>Polycope pumicosa schleiferiae</i> Kozur in Bunza & Kozur, 1971 [Pl. 6Z, AA; sample OST6]
<i>Paracypris</i> cf. <i>ovidi</i> Forel in Forel & Grädinaru, 2020 [Pl. 5B; sample OST6]	<i>Polycope</i> sp. 1 [Pl. 6AB, AC; samples OST3, 4, 7, 8, 10]
<i>Paracypris?</i> sp. 1 [Pl. 5C; samples OST3, 4, 7-10]	<i>Polycope</i> sp. 2 [Pl. 6AD; sample OST9]
<i>Paracypris?</i> sp. 2 [Pl. 5D; sample WH227]	Podocopida indet. [Pl. 6AE, AF; sample OST10]
<i>Paracypris?</i> sp. 3 [Pl. 5E; samples WH232, 236]	
<i>Paracypris</i> sp. 4 [Pl. 5F; sample WH227]	
<i>Paracypris</i> sp. 6 [Pl. 5G; samples OST7, 8]	
<i>Paracypris</i> sp. 7 [Pl. 5H; sample OST9]	
<i>Spinocypris</i> sp. [Pl. 5I, J; samples OST6, 9]	
<i>Triassocypris</i> sp. [Pl. 5K; sample OST9]	
Family <b>Pontocyprididae</b> Müller, 1894	
<i>Pontocypris</i> sp. [Pl. 5L; samples OST8, 9]	
<i>Pseudomacrocypris</i> sp. 1 [Pl. 5M; samples OST9, WH227]	
<i>Pseudomacrocypris?</i> sp. 3 [Pl. 5O; sample OST10]	
<i>Pseudomacrocypris</i> sp. 2 [Pl. 5N; samples OST8, WH227, 236]	

Tab. 1 - Taxonomic list of all ostracod species identified from Lime Peak, Yukon Territory, Canada, Norian, Late Triassic.

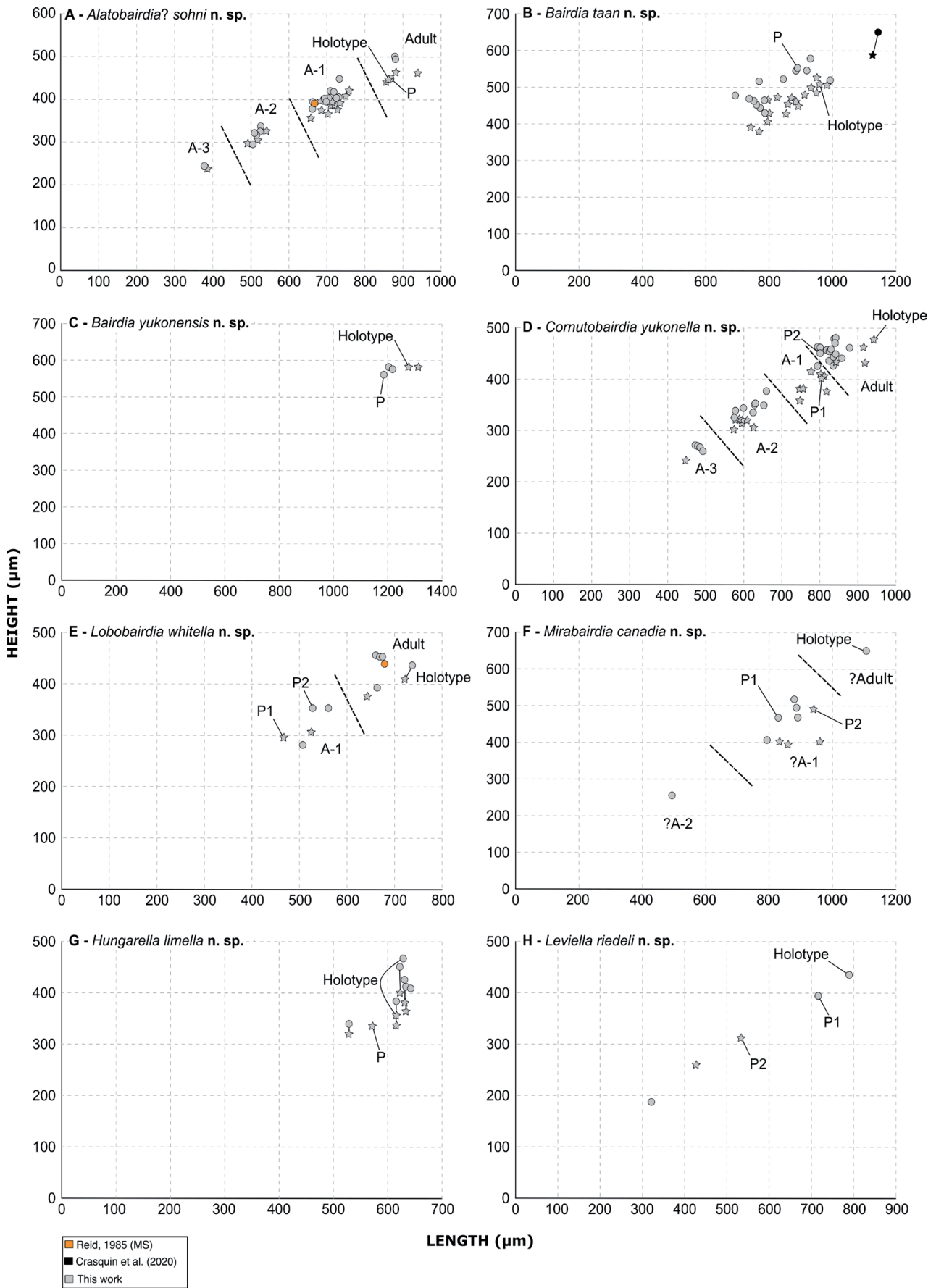


Fig. 2 - Height/Length scatter plots of species from Lime Peak, Yukon Territory, Canada, Norian, Late Triassic. In all diagrams, the dimensions of right (stars) and left (circles) valves of complete carapaces are shown separately and linked by a black line.

is as follows: <400 µm very small, 400-500 µm small, 500-700 µm medium, 700-1000 µm large, >1000 µm very large. In height/length diagrams (Fig. 2), all right and left valves are distinguished, following for instance Urlichs (1971), Harloff (1993) and Forel et al. (2020). When possible, Kernel density maps (PAST software version 4.04; Hammer et al. 2001; Hammer & Harper 2005) have been used to discriminate density patterns of individuals that correspond to different ontogenetical stages, with the heuristic hypothesis that largest specimens are adults.

The classification of Triassic Bairdiidae and Healdiidae is still problematic but a revision of these major ostracod families is beyond the scope of this paper. The present material yielded very typical Triassic ornate bairdiids such as *Alatobairdia* Kristan-Tollmann, 1971 and *Mirabairdia* Kollmann, 1963. A major challenge of modern ostracodology is the clarification of the systematics of ornate Bairdiidae that went through an important period of radiation in the Triassic (see Forel & Crasquin 2020 and references therein). Their current classification mainly relies on ornamentation patterns on the lateral surface of the valves, the importance of which has been highly disputed since the 70's. Ornate Bairdiidae have never been as abundant and morphologically diverse as in the Triassic and the issue of this "Bermuda Triangle of Taxonomy" can only be solved and new paradigms established by the addition of new characters to the traditional descriptions. The present material is exceptional in this matter as it provides material transitional between already known genera to discuss the current classification scheme, as well as material with preserved inner structures and normal pores. In this context, Bairdiidae are here described with a wealth of details and the pores visible on several specimens will be fully addressed in a forthcoming analysis. To avoid bringing a new point of view in an issue that requires new data and new facts rather than new opinions, the original classification of Triassic ornate bairdiids proposed by Kollmann (1960, 1963) is here used.

The possible synonymy of Jurassic *Ogmoconcha* Triebel, 1941 and Triassic *Hungarella* Méhes, 1911 has long been debated but material from the type locality of *Hungarella* has yet to be observed to clarify this issue (e.g. Lord 1972, 1982). We consider the synonymy of *Ogmoconcha* Triebel, 1941 and *Hungarella* Méhes, 1911 as unlikely given the distinct central muscle scar field patterns observed in these genera (e.g. Kristan-Tollmann 1977a, b; Lord 1982; Boomer & Jellinek 1996). Here we agree that "it is preferable to call Lower Jurassic species which are congeneric with *Ogmoconcha contractula* Triebel, 1941 (type species of *Ogmoconcha*) by the generic name *Ogmoconcha* rather than *Hungarella* since the synonymy of the two genera is unproved" (p. 332 in Lord 1972), and consider that as a consequence, the use of *Hungarella* should be restricted to Triassic species. Until the relationship of *Ogmoconcha* and *Hungarella* is clarified, we use *Hungarella* for Triassic species to avoid artificially rooting *Ogmoconcha* down to the Triassic (e.g. Lord 1972), and biasing diversity patterns at the end of the Triassic (Forel & Crasquin 2020). In the absence of observable central muscle scars, all Healdiidae identified in this work are attributed to *Hungarella*.

**Abbreviations used in the text:** L - length; H, height; W - width; LV - left valve; RV - right valve; AB - anterior border; PB - posterior border; DB - dorsal border; VB - ventral border; ADB - anterodorsal border; PDB - posterodorsal border; AVB - anteroventral border; PVB - posteroventral border; AMS - adductor muscle scars; A-1, A-2, A-3, A-4, Ad - estimated growth stages.

**Repository:** All type and figured specimens are deposited in the collections of the Natural History Museum of Geneva (Switzerland), under catalogue numbers MHNG-GEPI-2021-7011 to MHNG-GEPI-2021-7186.

## SYSTEMATIC PALAEOLOGY

(by Marie-Béatrice Forel)

Class **OSTRACODA** Latreille, 1806  
 Subclass **PODOCOPA** Müller, 1894  
 Superfamily Bairdioidea Sars, 1887  
 Family Bairdiidae Sars, 1887  
 Subfamily Bairdiinae Sars, 1923  
 Genus *Alatobairdia* Kristan-Tollmann, 1971

**Type species:** *Alatobairdia foveolata* Kristan-Tollmann, 1971 by original designation

### *Alatobairdia?* *sobni* Forel n. sp.

Pl. 1C-P, Pl. 7A-C

v1985 *Alatobairdia* sp. in Reid, fig. A33a.

**Derivatio nominis:** In reference to I.G. Sohn (U.S. Geological Survey, Washington) who first attributed this species to *Alatobairdia*.

**Holotype:** MHNG-GEPI-2021-7016, one right valve, adult (Pl. 1E).

**Paratype:** MHNG-GEPI-2021-7013, one left valve, adult (Pl. 1C).

**Additional material:** 19 left valves, 19 right valves, numerous fragments.

**Type locality:** Lime Peak, Whitehorse area, Yukon Territory, Canada.

**Type horizon:** Sample OST13, Aksala Formation, Lewes River Group; Upper Norian, Late Triassic.

**Diagnosis:** A species questionably attributed to *Alatobairdia* with antero-ventral and postero-ventral triangular extensions, thick anterior and posterior marginal ridges that do not merge and uniformly reticulate surface.

**Description.** Carapace large, auriform to subrectangular with trailing rear end in lateral view, Hmax at the AD cardinal angle and Lmax below mid-H. Dorsal margin divided into 3 distinct parts: DB straight, slightly bent posteriorly with L ranging from about 60% in juveniles to about 30% in adults, ADB relatively long, straight to slightly convex and PDB more steeply sloping posteriorly with terminal concavity more or less pronounced. VB long with oral concavity around mid-L, only slightly raised posteriorly. PB located below mid-H, relatively large and extended by a long, pustulose and thick triangular process that develops along the ventral margin and provides the posterior end a tapered and trailing appearance. Posterior extension with a more-or-less expressed constriction at the transition with the lateral surface of adult valves. AB large, located around mid-H, with a thick triangular process

convex dorsally and concave ventrally, less developed than the posterior one. Lateral surface with thick antero-marginal and postero-marginal ridges that do not meet. Antero-marginal ridge uniformly convex, symmetrical at both valves, with thickness tapering outward. Posterior ridge unbroken and closely following the morphology of PB in adult and A-1 specimens, subvertical and interrupted in the lower third at LV of some younger specimens (e.g. Pl. 1K, L). Lateral surface uniformly reticulate with deep reticulae in the central area, shallower on the antero- and posteromarginal ridges.

In inner view, ventral margin of anterior and posterior extensions tenuously ridged vertically, the tips of these ridges are sometimes visible in external view (e.g. Pl. 1I, K, L). In adults, calcified inner lamella relatively large anteriorly, very narrow at oral concavity and narrow posteriorly; poorly developed in A-1 specimens. Inner lateral surface with numerous simple pores that are mostly obscured by the reticulation in external view. AMS partly visible below mid-H and around mid-L: subcircular oriented along a posterodorsal-anteroventral axis, comprising 6 subrectangular to subovoid individual scars arranged in 3 rows (Pl. 1D). Hinge line straight, composed of a long and thin bar flanked by triangular grooves overhung by selvage at the anterior and posterior extremities at LV, into which fit thin teeth bracketing a long furrow at RV. Bairdoppilate auxiliary dentition absent.

**Dimensions:** (Fig. 2A)

Holotype: L = 864  $\mu\text{m}$ , H = 445  $\mu\text{m}$ .

Paratype: L = 868  $\mu\text{m}$ , H = 447  $\mu\text{m}$ .

**Remarks.** *Alatobairdia? sobni* Forel n. sp. was first figured from the west and north facing slopes of Lime Peak in Reid (1985), where it was identified as *Alatobairdia* sp. by I.G. Sohn. Sohn (1987) later mentioned “undescribed taxa tentatively referred to” several genera including *Alatobairdia* in Lewes River Group (Norian), Yukon Territory, Canada. However, no discussion was provided regarding this *Alatobairdia* identification. *Alatobairdia* Kristan-Tollmann, 1971 was described from the Rhaetian of Austria to accommodate ornate bairdiids with antero- and posteroventral wings, dorsal thorns/spines/knots at LV, orange peel-like dimpled sculpture in the central area of the valves and accessory bairdoppilate dentition (Kristan-Tollmann 1971b). This

genus was erected on a unique species, type species *Alatobairdia foveolata* Kristan-Tollmann, 1971, and is still currently monotypic. This situation makes it challenging to evaluate and discuss which characters/state of characters are of generic significance as well as their degree of specific variations. *Alatobairdia? sobni* Forel n. sp. questions the relative significance of ornamentation features in the generic classification of *Alatobairdia* Kristan-Tollmann, 1971 and of ornate bairdiids more generally. The antero- and posteromarginal ridges of *Alatobairdia? sobni* and the lack of dorsal structures on LV do not match the original diagnosis of *Alatobairdia* and either implies that the diagnosis of *Alatobairdia* should be emended (to give generic value to the anteroventral and posteroventral structures and specific significance to the lateral ornamentation) or that *Alatobairdia? sobni* should be assigned to a different genus. Kristan-Tollmann (1971b) was already foreseeing the necessity of modifying the diagnosis of *Alatobairdia*. Kristan-Tollmann (1971b) also mentioned the presence of bairdoppilate dentition in *Alatobairdia*, which is absent from *Alatobairdia? sobni*. Here we follow Bolz (1969, 1971a, b) and subsequent authors (e.g. Maddocks, 2015) in considering that this character may be subject to convergence and would have a functional significance only. The subfamily Bairdoppilatae Kristan-Tollmann, 1969 erected to accommodate Bairdiidae with accessory bairdoppilate dentition is therefore considered as invalid (Bolz 1969, 1971a, b; Maddocks 1969, 2015). In modern Bairdiidae, supplemental dentition is found in *Bairdoppilata* and *Glyptobairdia* (e.g. Maddocks 1969, 2015) and may show some degree of intraspecific variation (e.g. Warne 1988). The absence of supplemental dentition in *Alatobairdia? sobni* may point to the necessity of creating a new genus.

Given the possible absence of bairdoppilate dentition for *Bairdiolites*, an emendation of the genus would allow the winged extensions observed in *Alatobairdia? sobni* to be accommodated. *Bairdiolites* Croneis & Gale, 1939, with which *Neobairdiolites* Kollmann, 1963 has been synonymized (Kristan-Tollmann 1970), is diagnosed by “two curved parentheses-like ridges on the anteroventral and posteroventral parts of each valve” (p. 69 in Sohn 1960). However, ridged ornamentation is relatively more common in ornate bairdiids, e.g. *Carinobairdia*, than winged extensions that have been only doc-

umented for *Alatobairdia*. In the absence of information on supplemental dentition in *Bairdiolites* and on AMS in *Alatobairdia* and *Bairdiolites*, we therefore consider that the present new species is closer to *Alatobairdia*. The characters of the lateral ornamentation combined with the absence of bairdoppilate auxiliary dentition of *Alatobairdia? sobni* may require the creation of a new genus that would be diagnosed by the co-occurrence of wings and anterior and posterior marginal ridges and by the lack of bairdoppilate dentition.

All specimens of *Alatobairdia? sobni* have been measured (wings not included) and the H/L diagram of all LV and RV, including the LV illustrated in Reid (1985), is shown in Fig. 2A. All valves are distributed into 4 very distinct scatter plots considered here as successive ontogenetic stages. The largest specimens being considered as adults, the 4 scatter plots are identified as A-3 to Adults in ascending order. All ontogenetic stages are illustrated by LV and RV, the most abundant being A-1. According to this reconstruction, the LV in Reid (1985) may correspond to an A-1 stage. In all ontogenetic stages identified here, LV are relatively larger than RV. From A-3 to adult stage, the development of *Alatobairdia? sobni* is marked by the general increase of the dimensions of the valves (not considering the ventral extensions), the shortening of DB and the enforcement of marginal ridges and reticulation.

**Occurrence.** Sample R-81-39-8, Aksala Formation, Lewes River Group, Norian, Upper Triassic (Reid 1985; Sohn 1987). Samples OST6, 13, Aksala Formation, Lewes River Group, Upper Norian, Upper Triassic (this work).

#### Genus *Bairdia* McCoy, 1844

**Type species:** *Bairdia curta* McCoy, 1844 subsequently designated by Ulrich & Bassler (1923)

**Preliminary remarks.** The studied samples yielded numerous *Bairdia* species represented by specimens that most of the time were not sufficiently well-preserved and/or abundant enough to describe their diagnostic characters in detail. Most of them are thus kept in open nomenclature and only figured in Pl. 2, 3. The good preservation of some of the specimens allows for the observation of characters that may shed new light on the taxonomy of Triassic Bairdiidae as they are used to distinguish between modern genera. For instance, the

frilled anterior margin visible on the RV of *Bairdia? sp. 6* (Pl. 2AD, AE) is an important character that distinguishes *Paranesidea* and *Bairdoppilata* from other bairdiids (e.g. Maddocks 1969).

#### *Bairdia aksala* Forel n. sp.

Pl. 1Q-T, 2A-D, Pl. 7D

**Derivatio nominis:** In reference to the Aksala Formation that yielded this species.

**Holotype:** MHNG-GEPI-2021-7026, one carapace (Pl. 1Q).

**Paratypes:** MHNG-GEPI-2021-7028, one carapace (Pl. 1S), MHNG-GEPI-2021-7029, one carapace (Pl. 1T).

**Additional material:** 37 carapaces, 4 left valves, 1 right valve, numerous fragments.

**Type locality:** Lime Peak, Whitehorse area, Yukon Territory, Canada.

**Type horizon:** Sample WH235, Aksala Formation, Lewes River Group; Upper Norian, Upper Triassic.

**Diagnosis:** *Bairdia* with very tapered and trailing posterior end, posterior border located only slightly above ventral margin.

---

#### PLATE 1

SEM micrographs of ostracods from Lime Peak, Yukon Territory, Canada, Norian, Late Triassic. All specimens are housed in the collections of the Natural History Museum of Geneva (Switzerland). A) *Acratia* sp. 1, left view of a complete carapace, sample OST6, MHNG-GEPI-2021-7011. B) *Acratia* sp. 2, external view of a left valve, sample OST6, MHNG-GEPI-2021-7012. C-P) *Alatobairdia? sobni* Forel n. sp. C. paratype, external view of a left valve, adult, sample OST6, MHNG-GEPI-2021-7013. D. internal view of a left valve, adult, sample OST6, MHNG-GEPI-2021-7014. E. holotype, external view of a right valve, adult, sample OST13, MHNG-GEPI-2021-7015. F. internal view of a right valve, adult, sample OST6, MHNG-GEPI-2021-7016. G. external view of a left valve, A-1, sample OST6, MHNG-GEPI-2021-7017. H. internal view of a left valve, A-1, sample OST6, MHNG-GEPI-2021-7018. I. external view of a right valve, A-1, sample OST6, MHNG-GEPI-2021-7019. J. same specimen, internal view. K. external view of a left valve, A-2, sample OST6, MHNG-GEPI-2021-7020. L. external view of a left valve, A-2, sample OST6, MHNG-GEPI-2021-7021. M. external view of a right valve, A-2, sample OST6, MHNG-GEPI-2021-7022. N. external view of a right valve, A-2, sample OST6, MHNG-GEPI-2021-7023. O. external view of a left valve, A-3, sample OST6, MHNG-GEPI-2021-7024. P. external view of a right valve, A-3, sample OST6, MHNG-GEPI-2021-7025. Q-T) *Bairdia aksala* Forel n. sp. Q. holotype, right view of a complete carapace, sample WH235, MHNG-GEPI-2021-7026. R. right view of a complete carapace, sample WH235, MHNG-GEPI-2021-7027. S. paratype, right view of a complete carapace, sample WH235, MHNG-GEPI-2021-7028. T. paratype, right view of a complete carapace, sample WH227, MHNG-GEPI-2021-7029.

All scale bars are 100 µm.

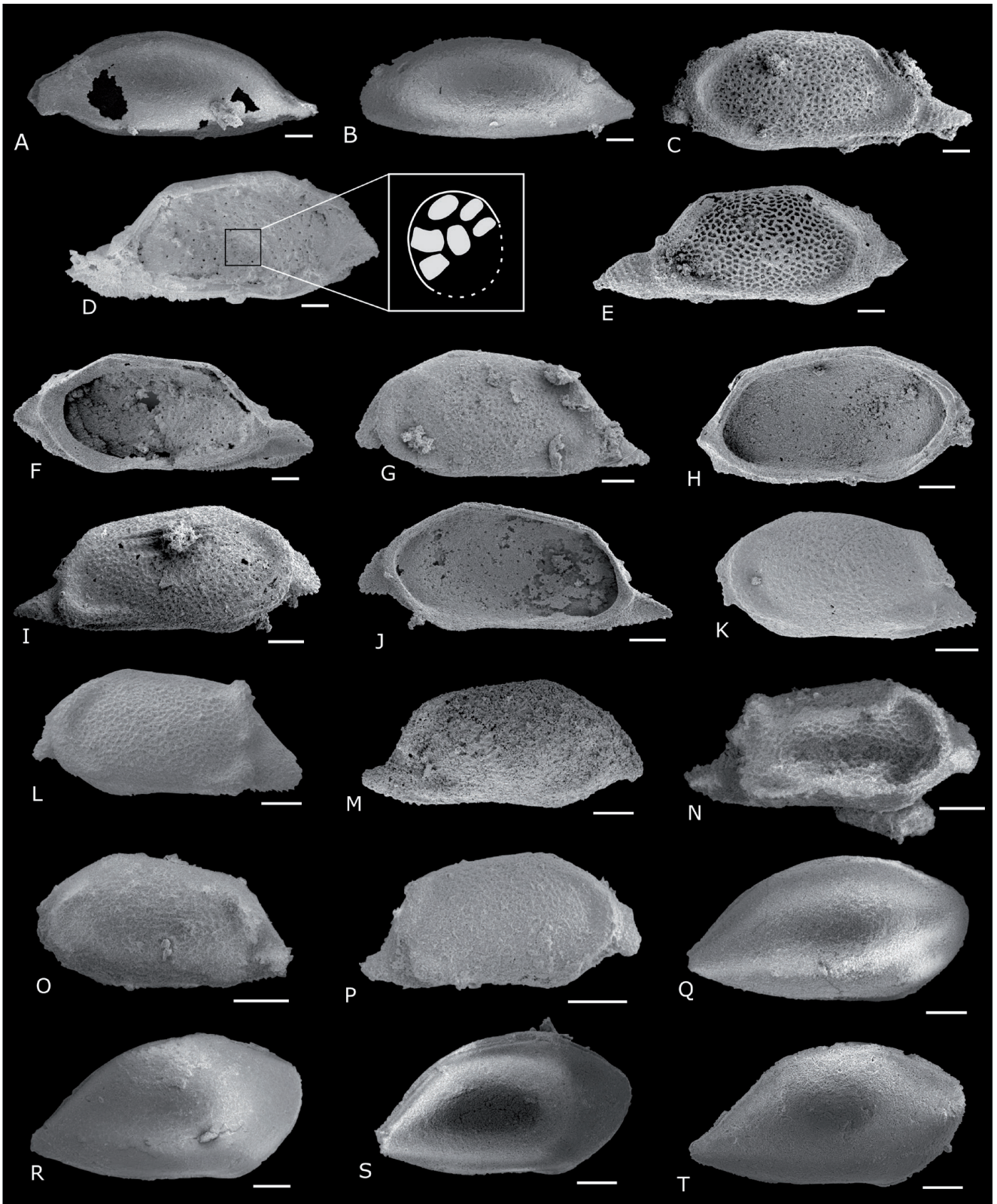


PLATE 1

**Description.** Carapace relatively small, elongate and very tapered posteriorly in lateral view, with Hmax in the anterior third and Lmax close to ventral margin. LV overlaps RV along the entire margin with maximum at DB and very thinly along ventral margin. Dorsal margin uniformly convex at both valves with posterior slope much steeper than anterior one. Ventral margin long with oral concavity in front of mid-L and PVB only slightly bent upward. AB relatively large located in the upper third of H, AVB steeply raised, only gently convex with tenuous concavity in its lower portion at some specimens. PB narrow, located just above ventral margin, resulting in a strongly tapered posterior end. Lateral surface smooth. AMS partly visible on a steinkern, located slightly below mid-H and in front of mid-L, ovoid in outline, inclined along a posterodorsal-anteroventral axis with six small and subovoid individual scars, arranged in three loose rows (Pl. 2C). Hinge not observed.

#### Dimensions:

L = 459-745  $\mu\text{m}$ , H = 240-403  $\mu\text{m}$  (illustrated, sub-complete specimens).

Holotype: L = 691  $\mu\text{m}$ , H = 353  $\mu\text{m}$ .

Paratypes: L = 660  $\mu\text{m}$ , H = 370  $\mu\text{m}$  (Pl. 1S),  
L = 674  $\mu\text{m}$ , H = 368  $\mu\text{m}$  (Pl. 1T).

**Remarks.** Because of their very tapered and narrow PB, most specimens of *Bairdia aksala* n. sp. are broken posteriorly and no reliable measurements of the specimens have been possible. *Bairdia aksala* n. sp. belongs to the group of *Bairdia* species with slender valves, posterior end very tapered and trailing with maximum of convexity located very low (e.g. *Bairdia urodeiformis* Chen in Shi & Chen, 1987 from the Changhsingian, Upper Permian of South China; Shi & Chen, 1987). This morphology may reflect environmental influence rather than phylogeny and taxonomic signals are to be found in the degree of dorsal cardinal angles, overlap, position of AB and PB. Although very close, *Bairdia aksala* n. sp. differs from the Permian *Bairdia urodeiformis* Chen, 1987 by cardinal angles being much less expressed to quasi indistinct depending on the specimens and by the lack of the pronounced AD concavity. *Bairdia* n. sp. cf. *B. cassiana* Reuss (1868) from the Norian-Rhaetian of Australia (Dépêche & Crasquin 1992) is also very close to *Bairdia aksala* but its posterior end is shorter with a more concave PD border and AVB

and PVB seem slightly compressed laterally. It is very close to *Bairdia* cf. *urodeiformis* Chen, 1987 in Forel et al., 2019b from the Carnian of Southern Turkey (Forel et al. 2019b) but the Carnian species has more expressed cardinal angles, ADB slightly concave and PB with maximum of curvature located higher.

**Occurrence.** Samples OST6, 12, WH227, 234, 235, Aksala Formation, Lewes River Group; Stikinia terrane, Whitehorse area, Yukon Territory, Canada, Upper Norian, Upper Triassic (this work).

### *Bairdia taan* Forel n. sp.

Pl. 2E-L, Pl. 7E, F

v2020 *Bairdia* sp. C in Crasquin et al., p. 15, pl. 1N.

**Derivatio nominis:** By apposition, in reference to the Ta'an Kwäch'än (= people from Lake Laberge) First Nation who own the rights of the settlement land where the samples were collected.

**Holotype:** MHNG-GEPI-2021-7034, one right valve, (Pl. 2E).

**Paratype:** MHNG-GEPI-2021-7038, one left valve, (Pl. 2I).

**Additional material:** 4 carapaces, 21 left valves, 15 right valves, numerous fragments.

**Type locality:** Lime Peak, Stikinia terrane, Whitehorse area, Yukon Territory, Canada.

**Type horizon:** Sample OST6, Aksala Formation, Lewes River Group; Upper Norian, Upper Triassic.

**Diagnosis:** Large *Bairdia* with AVB and PVB laterally compressed, lateral surface tenuously pitted and abundant normal pore canals mainly in the anterior half.

**Description.** Carapace large, subtriangular in lateral view, with Lmax below mid-H and Hmax at anterodorsal angle in RV, at mid-L in LV. At RV, dorsal margin tripartite with straight DB sloping posteriorly (around 15°), PDB steeply inclined towards PB (from 42° in Pl. 2H to 55° in Pl. 1E, F), slightly convex with a major terminal concavity, ADB about the same L as DB, slightly concave. At LV, dorsal margin subtriangular with apex at mid-L, PDB uniformly convex, ADB straight and gently sloping anteriorly (20-23°). Ventral margin long at both valves, uniformly convex at LV, with marked oral concavity slightly in front of mid-L, only slightly raised posteriorly to PB and AVB very inclined to AB with a small concavity ventrally at RV. AB large, located in the upper 1/3<sup>rd</sup> to 1/4<sup>th</sup> of H, laterally compressed above the ventral concavity of AVB. PB caudate, in the lower 1/4<sup>th</sup> of H, PVB laterally compressed. Lateral surface uniformly and densely pitted. Numerous and relatively large, rounded normal pore canals dispersed all over the lateral surface; more densely

distributed in the anterior area and sparse to absent in the central area of the valves. A series of large pores are evenly distributed along the posteroventral margin, the last of which occurs on the apex of PB. Possible radial pore canals along the anterior margin of some specimens (e.g. Pl. 2F).

**Dimensions:** (Fig. 2B)

Holotype: L = 960  $\mu\text{m}$ , H = 508  $\mu\text{m}$ .

Paratype: L = 890  $\mu\text{m}$ , H = 551  $\mu\text{m}$ .

**Remarks.** *Bairdia taan* Forel n. sp. is very close to *Bairdia cassiana* (Reuss, 1868), which is typical of the Middle and lower Upper Triassic marine deposits of Europe (e.g. Reuss 1868; Gümbel 1869; Ulrichs 1971; Kristan-Tollmann 1978; Monostori & Tóth 2013, 2014; Mette et al. 2015; Crasquin et al. 2018; Forel et al. 2019b). *Bairdia taan* is however distinguished by the position of Hmax around mid-L while the very first drawings of *Bairdia cassiana* Gümbel (1869) document a very preplete LV. The numerous pores observed on *Bairdia taan* Forel n. sp. are furthermore unique and have never been observed on *Bairdia cassiana*. *Bairdia* sp. B in Bolz, 1971 from the Upper Triassic of Austria (Bolz 1971b) differs by its AB located more ventrally, AVB more rounded and in continuity with VB, while an angulation is visible in *Bairdia taan*. *Bairdia* n. sp. cf. *B. cassiana* Reuss (1868) in Dépêche & Crasquin (1992) from the Norian-Rhaetian interval of Australia (Dépêche & Crasquin 1992) is very close to *Bairdia taan* with rows of pores mainly visible posterodorsally but the quality of the pictures and preservation of the material do not allow us to distinguish pores along the PB. The PB of the Australian species is furthermore much less caudate with a less pronounced terminal posterodorsal concavity than in *Bairdia taan*. The lateral outline of *Bairdia taan* is reminiscent of *Bairdia* sp. 7 in Mette & Mohtat-Aghai, 1999 from the Rhaetian of Austria (Mette & Mohtat-Aghai 1999). However, *Bairdia* sp. 7 in Mette & Mohtat-Aghai, 1999 lacks the characteristic pores and anterior lateral compression. *Bairdia taan* has first been documented from the Tuvolian, Upper Carnian, of Sicily (Crasquin et al. 2020). The complete carapace shown in Crasquin et al. (2020), identified as *Bairdia* sp. C, is slightly larger than the present material but displays all diagnostic characters of *Bairdia taan*. *Bairdia* sp. 2 from Lime Peak (Pl. 2Y-AA) also differs from *Bairdia taan* by its uniformly convex dorsal margin at LV

as well as longer and straighter ventral margin. Finally, *Bairdia jiangyouensis* Xie in Wei et al., 1983 from the Norian of South China (Wei et al. 1983) could be conspecific to *Bairdia taan* as shown by their extremely similar lateral outline and dimensions, with the exception of PB which is located more ventrally in *Bairdia taan*. However, a single carapace is shown in Wei et al. (1983) and close observation of specimens from the Carnian of South China (Forel et al. 2019a) did not confirm this hypothesis because no complete carapace from Lime Peak material allowed the overlap to be observed, the observability of pores being dependent on the quality of preservation.

The H/L diagram documents the large size range of LV and RV of *Bairdia taan* (Fig. 2B). All LV are larger than RV, illustrating the relatively large overlap of LV over RV. The size distribution of all specimens is relatively continuous, especially for RV, and no clusters can be distinguished.

**Occurrence.** Monte Gambanera, Central-Eastern Sicily, Italy, *Tropites subbullatus*/*Anatropites spinosus* zones, Tuvolian, Carnian, Upper Triassic (Crasquin et al. 2020). Samples OST6, WH227, 232, 235, Aksala Formation, Lewes River Group; Stikinia terrane, Whitehorse area, Yukon Territory, Canada, Upper Norian, Upper Triassic (this work).

***Bairdia yukonensis* Forel n. sp.**

Pl. 2M-Q, Pl. 7G, H

**Derivatio nominis:** In reference to the Yukon Territory where the species was found.

**Holotype:** MHNG-GEPI-2021-7045, one right valve (Pl. 2P).

**Paratype:** MHNG-GEPI-2021-7044, one left valve (Pl. 2O).

**Additional material:** 2 left valves, 1 right valve.

**Type locality:** Lime Peak, Whitehorse area, Yukon Territory, Canada.

**Type horizon:** Sample OST6, Aksala Formation, Lewes River Group; Upper Norian, Upper Triassic.

**Diagnosis:** *Bairdia* species with anterior border close to dorsal margin, very upturned and caudate posterior border and large 'openings' distributed along the dorsal and ventrolateral margin with two near the centre of the valve.

**Description.** Carapace very large and elongate in lateral view, with Hmax at ADB and Lmax below mid-H. Dorsal margin tripartite at RV with straight and short DB (around 27%), AD cardinal angle poorly expressed, ADB straight with terminal concavity, nearly in continuity with DB, PDB steeper and very concave. At LV, dorsal margin

uniformly convex with DB and ADB in continuity. Ventral margin long at both valves, with oral concavity in the anterior half of L more pronounced at RV, PVB long and gently raised to PB, AVB steep, long and straight with a tenuous concavity in the lower part. AB roundly acute with maximum located only slightly below dorsal margin. PB located below mid-H, narrow, pointed and very upturned. PB, PVB and VB laterally compressed, lateral compression marked by a tenuous ridge at LV. Antero-ventral and posteroventral margins bordered by a series of possible very small radial pore canals. Lateral surface of the valves smooth except for a series of aligned relatively wide “openings”:

Two at the centre of each valve;

A dorsal series: at least 5 from the anterior to the dorsal borders, positioned on tiny promontories on the LV;

A subventral series of at least four “openings” extending diagonally from mid-anterior to posteroventral margin.

The number of “openings” of the dorsal and subventral series is unclear due to the preservation of specimens.

**Dimensions:** (Fig. 2C)

Holotype: L = 1281 µm, H = 577 µm.

Paratype: L = 1190 µm, H = 557 µm.

**Remarks.** Because of their distribution and large size and location on the lateral surface, we refer to “openings” rather than pores. Although not abundant in the studied material, *Bairdia yukonensis* n. sp. is unique among the known *Bairdia* species by its general morphology and by the dimensions and distribution of the ‘openings’ on its lateral surface.

**Occurrence.** Sample OST6, Aksala Formation, Lewes River Group; Stikinia terrane, Whitehorse area, Yukon Territory, Canada, Upper Norian, Upper Triassic (this work).

***Bairdia* sp. 7** in Forel et al., 2019b

Pl. 2R, S

v2019b *Bairdia* sp. 7 in Forel et al., fig. 8, O, Q.

**Occurrence.** Huğlu Tuffite, Mersin Mélange, southern Turkey, *Tetraporobrachia haeckeli* radiolarian Zone, Julian, Middle Carnian, Upper Triassic (Forel et al. 2019b). Samples OST7, WH227, 234, 235,

236, Aksala Formation, Lewes River Group; Stikinia terrane, Whitehorse area, Yukon Territory, Canada, Upper Norian, Upper Triassic (this work).

PLATE 2

SEM micrographs of ostracods from Lime Peak, Yukon Territory, Canada, Norian, Late Triassic. All specimens are housed in the collections of the Natural History Museum of Geneva (Switzerland). A-D) *Bairdia aksala* Forel n. sp. A. left view of a complete carapace, sample OST6, MHNG-GEPI-2021-7030. B. left view of a complete carapace, sample OST6, MHNG-GEPI-2021-7031. C. right view of a complete carapace, sample WH227, MHNG-GEPI-2021-7032. D. right view of a complete carapace, sample WH227, MHNG-GEPI-2021-7033. E-I) *Bairdia taan* Forel n. sp. E. holotype, external view of a right valve, sample OST6, MHNG-GEPI-2021-7034. F. external view of a right valve, sample OST6, MHNG-GEPI-2021-7035. G. external view of a right valve, sample OST6, MHNG-GEPI-2021-7036. H. external view of a right valve, sample OST6, MHNG-GEPI-2021-7037. I. paratype, external view of a left valve, sample OST6, MHNG-GEPI-2021-7038. J. external view of a left valve, sample OST6, MHNG-GEPI-2021-7039. K. external view of a left valve, sample OST6, MHNG-GEPI-2021-7040. L. external view of a left valve, sample OST6, MHNG-GEPI-2021-7041. M-Q) *Bairdia yukonensis* Forel n. sp. M. external view of a left valve, sample OST6, MHNG-GEPI-2021-7042. N. external view of a left valve, sample OST6, MHNG-GEPI-2021-7043. O. paratype, external view of a left valve, sample OST6, MHNG-GEPI-2021-7044. P. holotype, external of a right valve, sample OST6, MHNG-GEPI-2021-7045. Q. external view of a right valve, sample OST6, MHNG-GEPI-2021-7046. R, S) *Bairdia* sp. 7 in Forel et al., 2019b. R. right view of a complete carapace, sample WH235, MHNG-GEPI-2021-7047. S. right view of a complete carapace, sample WH235, MHNG-GEPI-2021-7048. T, U) *Bairdia* sp. A in Dépêche & Crasquin-Soleau, 1992. T. left view of a complete carapace, sample OST7, MHNG-GEPI-2021-7049. U. right view of a complete carapace, sample OST10, MHNG-GEPI-2021-7050. V, W) *Bairdia* cf. *balatonica* Mehes, 1911. V. right view of a complete carapace, sample WH235, MHNG-GEPI-2021-7051. W. right view of a complete carapace, sample WH235, MHNG-GEPI-2021-7052. X) *Bairdia* sp. 1, right view of a complete carapace, sample OST4, MHNG-GEPI-2021-7053. Y-AA) *Bairdia* sp. 2. Y. left view of a complete carapace, sample WH235, MHNG-GEPI-2021-7054. Z. left view of a complete carapace, sample WH235, MHNG-GEPI-2021-7055. AA. right view of a complete carapace, sample WH235, MHNG-GEPI-2021-7056. AB) *Bairdia* sp. 3, left view of a complete carapace, sample OST7, MHNG-GEPI-2021-7057. AC) *Bairdia* sp. 4, left view of a complete carapace, sample OST7, MHNG-GEPI-2021-7058. AD, AE) *Bairdia?* sp. 6. AD. right view of a complete carapace and enlargement of anterior margin, sample OST6, MHNG-GEPI-2021-7059. AE. right view of a complete carapace, sample OST6, MHNG-GEPI-2021-7060.

All scale bars are 100 µm.

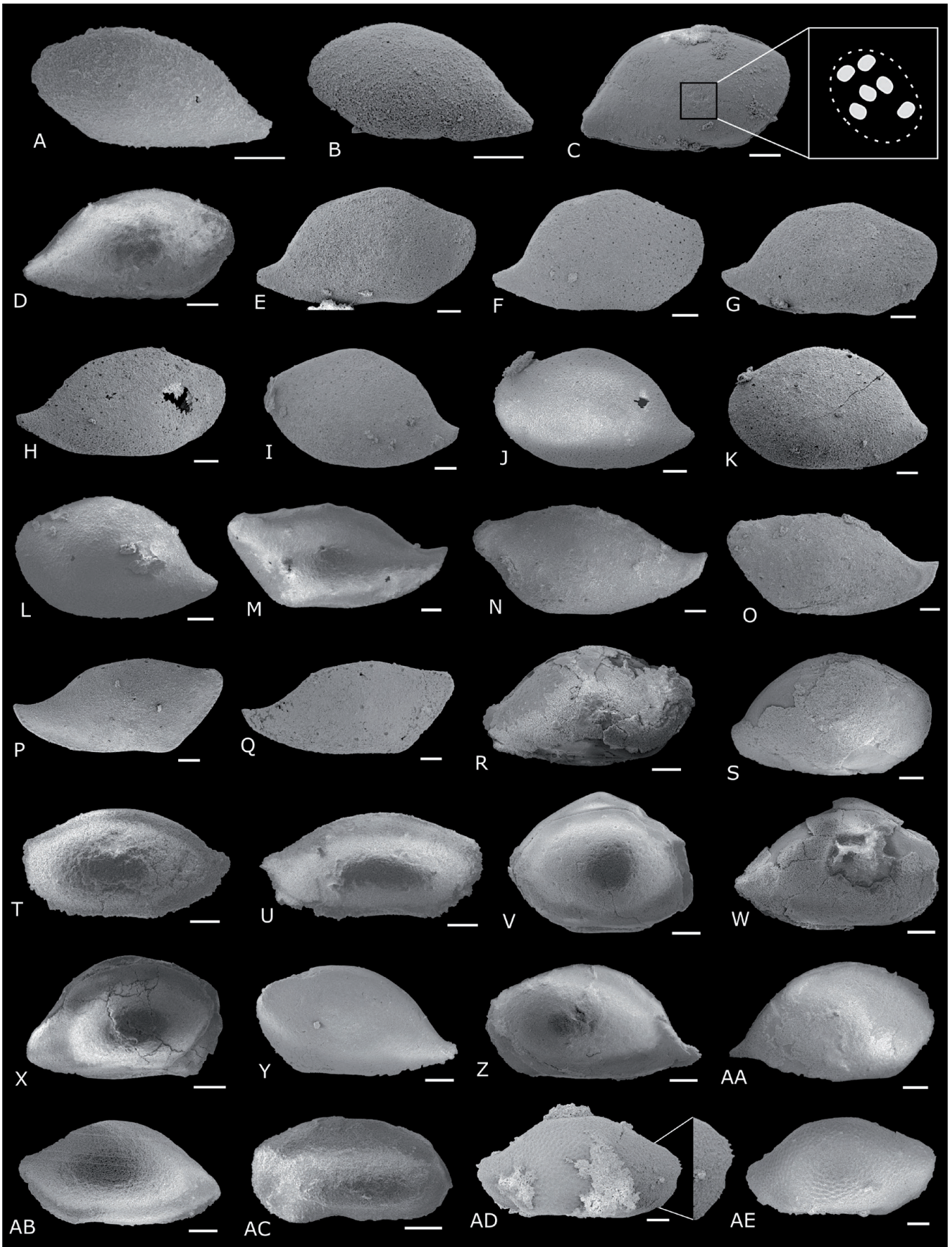


PLATE 2

***Bairdia* sp. A** in Dépêche & Crasquin-Soleau,  
1992  
Pl. 2T, U

v1992 *Bairdia* sp. A in Dépêche & Crasquin-Soleau, pl. 1, fig. 8.

**Occurrence.** Exmouth Plateau, northwestern margin of Australia, Rhaetian, Upper Triassic (Dépêche & Crasquin-Soleau 1992). Samples OST3, 6, 7, 10, WH227, 235, 236, Aksala Formation, Lewes River Group; Stikinia terrane, Whitehorse area, Yukon Territory, Canada, Upper Norian, Upper Triassic (this work).

Genus *Bairdiacypris* Bradfield, 1935

**Type species:** *Bairdiacypris deloi* Bradfield, 1935 by original designation.

***Bairdiacypris sorgunensis*** Forel in Forel et al.,  
2018  
Pl. 3J, K

v2018 *Bairdiacypris sorgunensis* Forel et al., p. 8, figs 4.14, 4.15.

v2019b *Bairdiacypris aequisymmetrica* Mette et al. 2015; Forel et al., p. 11, figs 10R–T.

**Occurrence.** Killik Formation, Tavuşçayırı Block, Sorgun Ophiolitic Mélange, Huğlu Tuffite, southern Turkey; *Spongortilispinus moixi* radiolarian Zone, lower Tuvalian, Upper Carnian (Forel et al. 2018). Huğlu Tuffite, Mersin Mélange, southern Turkey, *Tetraporobrachia haeckeli* radiolarian Zone, Julian, Middle Carnian (Forel et al. 2019b). Samples OST6, 12, Aksala Formation, Lewes River Group; Stikinia terrane, Whitehorse area, Yukon Territory, Canada, Upper Norian, Upper Triassic (this work).

Genus *Cornutobairdia* Kristan-Tollmann, 1970

**Type species:** *Cornutobairdia reticulata* Kristan-Tollmann, 1970 by original designation.

***Cornutobairdia yukonella*** Forel n. sp.  
Pl. 3T-AF, Pl. 7I

**Derivatio nominis:** In reference to the Yukon Territory where the specimens have been recovered.

**Holotype:** MHNG-GEPI-2021-7081, one right valve, adult (Pl. 3U).

**Paratypes:** MHNG-GEPI-2021-7082, one right valve, A-1 (Pl. 3V); MHNG-GEPI-2021-7087, one left valve, adult (Pl. 3AA).

**Additional material:** 45 left valves, 21 right valves, numerous fragments.

**Type locality:** Lime Peak, Whitehorse area, Yukon Territory, Canada.

**Type horizon:** Sample OST6, Aksala Formation, Lewes River Group; Upper Norian, Upper Triassic.

**Diagnosis:** *Cornutobairdia* with three separated subcentral nodes, posterior one being transformed into a horn, postero-dorsolateral spine at left valve, spines along anteroventral and posteroventral margins.

PLATE 3

SEM micrographs of ostracods from Lime Peak, Yukon Territory, Canada, Norian, Late Triassic. All specimens are housed in the collections of the Natural History Museum of Geneva (Switzerland). A) *Bairdia* sp. 7, right view of a complete carapace, sample OST10, MHNG-GEPI-2021-7061. B) *Bairdia* sp. 8, right view of a complete carapace, sample WH227, MHNG-GEPI-2021-7062. C) *Bairdia* sp. 9, right view of a complete carapace, sample WH227, MHNG-GEPI-2021-7063. D) *Bairdia* sp. 10, right view of a complete carapace, sample OST7, MHNG-GEPI-2021-7064. E) *Bairdia* sp. 11, right view of a complete carapace, sample OST10, MHNG-GEPI-2021-7065. F) *Bairdia* sp. 12, left view of a complete carapace, sample OST3, MHNG-GEPI-2021-7066. G, H) *Bairdia* sp. 13. G. right view of a complete carapace, sample WH227, MHNG-GEPI-2021-7067. H. left view of a complete carapace, sample WH227, MHNG-GEPI-2021-7068. I) *Bairdia* sp. 14, right view of a complete carapace, sample OST9, MHNG-GEPI-2021-7069. J, K) *Bairdiacypris sorgunensis* Forel in Forel et al., 2018. J. external view of a broken right valve, sample OST6, MHNG-GEPI-2021-7070. K. external view of a right valve, sample OST12, MHNG-GEPI-2021-7071. L–N) *Bairdiacypris* cf. *triassica* Kozur, 1971c. L. right view of a complete carapace, sample OST6, MHNG-GEPI-2021-7072. M. external view of a right valve, sample OST6, MHNG-GEPI-2021-7073. N. external view of a right valve, sample OST6, MHNG-GEPI-2021-7074. O) *Bairdiacypris* sp. 1, left view of a complete carapace, sample OST7, MHNG-GEPI-2021-7075. P) *Bairdiacypris* sp. 2, external view of a left valve, sample OST6, MHNG-GEPI-2021-7076. Q, R) *Bairdiacypris?* sp. 3. Q. external view of a left valve, sample OST10, MHNG-GEPI-2021-7077. R. external view of a left valve, sample OST10, MHNG-GEPI-2021-7078. S) *Carinobairdia?* sp., left view of a complete carapace, sample WH235, MHNG-GEPI-2021-7079. T–AF) *Cornutobairdia yukonella* Forel n. sp. T. external view of a right valve, adult, sample OST6, MHNG-GEPI-2021-7080. U. holotype, external view of a right valve, adult, sample OST6, MHNG-GEPI-2021-7081. V. paratype 1, external view of a right valve, A-1, sample OST6, MHNG-GEPI-2021-7082. W. external view of a right valve, adult, sample OST6, MHNG-GEPI-2021-7083. X. external view of a right valve, A-2, sample OST6, MHNG-GEPI-2021-7084. Y. external view of a right valve, A-2, sample OST6, MHNG-GEPI-2021-7085. Z. external view of a left valve, adult, sample OST6, MHNG-GEPI-2021-7086. AA. paratype 2, external view of a left valve, A-1, sample OST6, MHNG-GEPI-2021-7087. AB. external view of a left valve, adult, sample OST6, MHNG-GEPI-2021-7088. AC. same specimen, internal view. AD. external view of a left valve, A-2, sample OST6, MHNG-GEPI-2021-7089. AE. external view of a left valve, A-2, sample OST6, MHNG-GEPI-2021-7090. AF. external view of a left valve, A-3, sample OST6, MHNG-GEPI-2021-7091.

All scale bars are 100 µm.

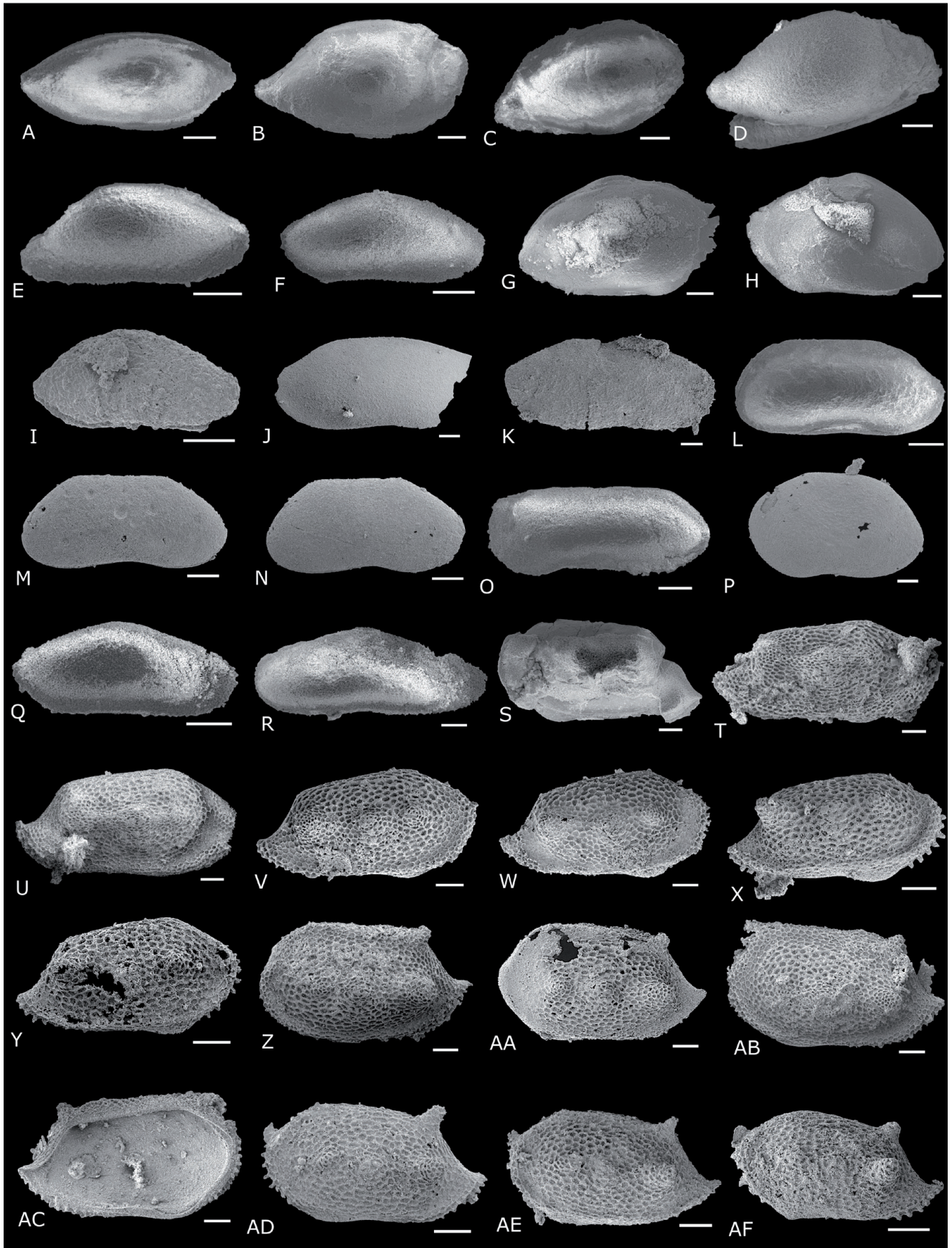


PLATE 3

**Description.** Carapace large, heavily calcified, subrectangular in lateral view with Hmax at AD cardinal angle and Lmax around mid-H. At both valves, dorsal margin divided into three parts: ADB short and straight, DB long, straight and with a slope from 7 to 10° in adults (e.g. Pl. 3), 15° in the smallest specimen, PDB short, concave and steeply sloping posteriorly (50-60°). Ventral margin long at both valves, with oral concavity located around mid-L, more expressed at RV than LV; PB narrow, located in the lower 1/3<sup>rd</sup> of H in young specimens (e.g. Pl. 3X, Y, AF) and only slightly below mid-H in adults (e.g. Pl. 3T, U, Z, AA); PB prolonged by a narrow spine at LV of well-preserved specimens; AB large, located above mid-H; AVB with small concavity in its ventral extremity; AB and PB bordered by a series of minute and relatively thick spines, the number of which increases through the development; valves laterally compressed along the entire free margins; lateral surface uniformly reticulate with reticulation barely visible along the anterior and posterior margin of some specimens (e.g. Pl. 3AA); lateral ornamentation of the valves asymmetric:

Three individual nodes in the median part of each valve, aligned slightly upward anteriorly, the posterior being horn-shaped and the most massive. The three elements are separated in juveniles (e.g. Pl. 3AD, AA) but linked by a very narrow ridge in adults (e.g. Pl. 3T, U).

A posterodorsal spine at LV, straight, oriented upward and backward, obscuring the PD cardinal angle.

A relatively narrow reticulate ridge extends all along the ventral margin, more pronounced at RV;

Internal structures not observed.

**Dimensions:** (Fig. 2D)

Holotype: L = 943 µm, H = 478 µm.

Paratypes: L = 806 µm, H = 401 µm (Pl. 3V), L = 804 µm, H = 451 µm (Pl. 3AA).

**Remarks.** *Cornutobairdia yukonella* Forel n. sp. differs from *C. bicornuta* Kristan-Tollmann, 1979 from the Rhaetian of Iran (Kristan-Tollmann et al. 1979) by the absence of a second posterodorsal horn, the very weakly developed marginal bulge in small specimens and by the central sculpture composed of 3 distinct nodes rather than an elongate bar. It also differs from *C. reticulata* Kristan-Toll-

mann, 1970 from the Norian of Austria (Kristan-Tollmann 1970) by the 3 central nodes and the relatively weak development of the marginal ridge. *C. reidae* Sohn, 1987 was described from the Lewes River Group and considered as “representative of an abundant and varied silicified ostracode assemblage” (p. C1 in Sohn 1987). However, it possesses two subcentral nodes and an anterodorsal spine on LV. Sohn (1987) also noticed that *C. reidae* “is associated with specimens on which the subcentral nodes coalesce to form a ridge [...]”. A few specimens have three distinct nodes in a straight line, with or without the posterior node extending into a lateral spine. They are, however, distinct from *C. reidae* because the posterior node in the new species is located higher on the lateral surface than the subcentral node, and, on the variants, more than two nodes occur in a straight line.” (p. C9 in Sohn 1987). In the present material, no specimen displays the anterodorsal spine diagnostic of *C. reidae* and the posterior horn never occurs above the central one. The morphological variations observed by Sohn (1987) are not recognized here as no specimen displays coalescing subcentral nodes. Changes in the organisation of the 3 central nodes are also observed for *C. yukonella* but may relate to ontogeny as the nodes are separated in all juveniles and linked by a narrow ridge only in the largest specimens. *C. yukonella* shares the highest resemblance with *C. trinodosa* Kristan-Tollmann, 1971 from the Norian of Austria (Kristan-Tollmann 1971a), which is diagnosed by a posterodorsal horn on LV not connected to the anterior marginal ridge and by the laterocentral ornamentation subdivided into 3 parts, the posterior one being transformed into a spine. Although extremely close, *C. yukonella* primarily differs from *C. trinodosa* by the morphology of the three central features that are separated nodes, the posterior one being also extending into a thorn, while they are of elongate nodules separated by constrictions in *C. trinodosa*. *C. yukonella* furthermore lacks the thick anteromarginal ridge, which is replaced by a laterally compressed area.

The H/L diagram of all specimens is plotted in Fig. 2D and may document the co-occurrence of four stages (A-3 to Adults). Although no complete carapace was found, clusters of LV and RV are grouped with LV always larger than RV, indicating that LV should have been overlapping RV. The

ontogeny of this species is marked by the increase of the number of marginal spines, the enlargement and increase of convexity of antero-ventral margin and migration upward of PB.

**Occurrence.** Samples OST6, 12, 13, Aksala Formation, Lewes River Group; Stikinia terrane, Whitehorse area, Yukon Territory, Canada, Upper Norian, Upper Triassic (this work).

#### Genus *Hiatobairdia* Kristan-Tollmann, 1970

**Type species:** *Hiatobairdia subsymmetrica* Kristan-Tollmann, 1970 by original designation.

#### *Hiatobairdia subsymmetrica* Kristan-Tollmann, 1970

Pl. 4C, D

- v1970 *Hiatobairdia subsymmetrica* Kristan-Tollmann, p. 268, pl. 35, figs 1–3.
- v1976 *Hiatobairdia subsymmetrica* Kristan-Tollmann; Tollmann, p. 276, pl. 163, fig. 14.
- v1978 *Hiatobairdia subsymmetrica deformis* Kristan-Tollmann, p. 83, pl. 4, figs 1–7.
- v1979 *Hiatobairdia subsymmetrica* Kristan-Tollmann; Kristan-Tollmann et al., p. 147, pl. 6, fig. 4.
- v1980 *Hiatobairdia subsymmetrica* Kristan-Tollmann; Kristan-Tollmann et al., pl. 9, fig. 1–3.
- v1988 *Hiatobairdia subsymmetrica* Kristan-Tollmann; Kristan-Tollmann, fig. 6.2.
- v1992 *Hiatobairdia subsymmetrica subsymmetrica* Kristan-Tollmann; Dépêche & Crasquin-Soleau, pl. 1, fig. 1
- v2014 *Hiatobairdia subsymmetrica* Kristan-Tollmann; Monostori & Tóth, pl. 2, figs 4, 5.
- v2018 *Hiatobairdia subsymmetrica* Kristan-Tollmann; Crasquin et al., p. 134, figs 6 F–H;
- v2020 *Hiatobairdia subsymmetrica* Kristan-Tollmann; Crasquin et al., p. 13, pl. 1R.

**Occurrence.** Austria, Rhaetian, Upper Triassic (Kristan-Tollmann 1970). South Tyrol, Italy, Lower Carnian, Upper Triassic (Tollmann 1976; Kristan-Tollmann 1978). Saltspring section, Bagerabad near Isfahan, Iran, Rhaetian, Upper Triassic (Kristan-Tollmann et al. 1979, 1980; Kristan-Tollmann 1988). Exmouth Plateau, northwestern margin of Australia, Rhaetian, Upper Triassic (Dépêche & Crasquin-Soleau 1992). Bakonykúti, eastern Bakony, Hungary, Ladinian, Middle Triassic (Monostori & Tóth 2014). Monte Gambanera, Central-Eastern Sicily, Italy, *Tropites dilleri* and *Tropites subbullatus/Anatropites spinosus* zones, Tuvalian, Carnian, Upper Triassic (Crasquin et al. 2018, 2020). Samples OST6, 13, Aksala Formation, Lewes River Group; Stikinia terrane, Whitehorse area, Yukon Territory, Canada, Upper Norian, Upper Triassic (this work).

#### Genus *Lobobairdia* Kollmann, 1963

**Type species:** *Lobobairdia salinaria* Kollmann, 1963 by original designation.

#### *Lobobairdia whitella* Forel n. sp.

Pl. 4I–R (P4S)

v1985 cf. *Lobobairdia* sp. in Reid, fig. A33b.

**Derivatio nominis:** In reference to the Whitehorse area where the studied area is located.

**Holotype:** MHNG-GEPI-2021-7100, one carapace, adult (Pl. 4I).

**Paratypes:** MHNG-GEPI-2021-7102, one right valve, A-1 (Pl. 4K); MHNG-GEPI-2021-7107, one left valve, A-1 (Pl. 4P).

**Additional material:** 6 carapaces, 15 left valves, 6 right valves, numerous fragments.

**Type locality:** Lime Peak, Whitehorse area, Yukon Territory, Canada.

**Type horizon:** Sample OST6, Aksala Formation, Lewes River Group; Upper Norian, Upper Triassic.

**Diagnosis:** *Lobobairdia* species with reticulate surface and rows of spines on anterior and posterior margins, the uppermost spine being close to vertical at the anterior margin.

**Description.** Carapace medium to large, subtriangular in lateral view, with Hmax at the AD cardinal angle and Lmax below mid-H; LV overlaps RV along the dorsal margin with a nearly uniform strength; dorsal margin divided into three parts of similar length with cardinal angles more distinct at RV; DB straight and gently inclined posteriorly (about 10–20°), PDB convex with terminal concavity with relatively steep slope (50–60°), ADB (10–20°) straight with terminal concavity at RV, gently concave at LV; VB with oral concavity slightly in front of mid-L; PVB laterally compressed, short and slightly convex to straight, bordered by relatively thick and long spines, the terminal one being horizontal to pointing upward; AVB laterally compressed, long and steeply raised, bordered by spines oriented downward in the lower part, horizontal in the middle part and upward in the upper part, the most dorsal spine being nearly vertical; AB located in the upper 1/3<sup>rd</sup> of Hmax, large; PB narrow, in the lower 1/4<sup>th</sup> of Hmax.

**Dimensions:** (Fig. 2E)

Holotype: L = 741 µm, H = 433 µm.

Paratypes: L = 470 µm, H = 291 µm (Pl. 4K), L = 532 µm, H = 349 µm (Pl. 4P).

**Remarks.** *Lobobairdia whitella* Forel n. sp. differs from *Lobobairdia impressa* Kristan-Tollmann in

Kristan-Tollmann *et al.*, 1979 from the Rhaetian of Iran (Kristan-Tollmann *et al.* 1979) in lacking the compressed areas on the lateral surface of the valves and in having a much higher AB with spinose extremities. *Lobobairdia whitella* also differs from *Lobobairdia rotundata* Monostori, 1996 from the Pliensbachian, Early Jurassic, of the Transdanubian Central Range, Hungary (Monostori 1996) by its more elongate outline, posterior end lower and narrower, higher anterior end and lack of ventral overlap. The new species also strongly differs from the typical Triassic *Lobobairdia salinaria* Kollmann, 1963 by the anterior margin outline, higher position of AB, lower and narrower PB and lack of ventral overlap.

The H/L diagram of all specimens of *Lobobairdia whitella* shows a relatively large distribution of the dimensions of the specimens, identified as A-1 and Adult stages (Fig. 2E). The holotype is the only known complete carapace to date and is attributed to the Adult stage, the two paratypes correspond to submature specimens of the A-1 stage.

**Occurrence.** Sample R-81-39-8, locality Lewes River Group, Norian, Upper Triassic (Reid 1985; Sohn 1987). Samples OST4, 6, 7, 13, WH227, 236, 259, Aksala Formation, Lewes River Group; Stikinia terrane, Whitehorse area, Yukon Territory, Canada, Upper Norian, Upper Triassic (this work).

#### Genus *Mirabairdia* Kollmann, 1963

**Type species:** *Mirabairdia pernodosa* Kollmann, 1963 by original designation.

1973a *Vavilovella* Kozur, p. 21–24, pl. 3, figs 4, 5.

#### *Mirabairdia canadia* Forel n. sp.

Pl. 4V-AA, Pl. 7J, K

v1985 *Vavilovella?* sp. in Reid, fig. A33d.

**Derivatio nominis:** Of Canada.

**Holotype:** MHNG-GEPI-2021-7114, one left valve, ?Ad (Pl. 4W).

**Paratypes:** MHNG-GEPI-2021-7113, one left valve, ?A-1 (Pl. 4V); MHNG-GEPI-2021-7116, one right valve, ?A-1 (Pl. 4Y).

**Additional material:** 5 left valves, 4 right valves, numerous fragments.

**Type locality:** Lime Peak, Whitehorse area, Yukon Territory, Canada.

**Type horizon:** Sample OST6, Aksala Formation, Lewes River Group; Upper Norian, Upper Triassic.

**Diagnosis:** A species of *Mirabairdia* with anterior and posterior subdorsal horns inclined posteriorly at LV, subcentral massive node at both valves and posterior end caudate.

**Description.** Carapace large to very large, subrectangular in lateral view with Hmax at AD cardinal angle at both valves and Lmax below mid-H; dorsal margin subdivided into three distinct parts

#### PLATE 4

SEM micrographs of ostracods from Lime Peak, Yukon Territory, Canada, Norian, Late Triassic. All specimens are housed in the collections of the Natural History Museum of Geneva (Switzerland). A, B) *Cornutobairdia* sp. A. external view of a left valve, sample OST6, MHNG-GEPI-2021-7092. B. external view of a left valve, sample OST6, MHNG-GEPI-2021-7093. C, D) *Hiatobairdia subsymmetrica* Kristan-Tollmann, 1970. C. external view of a right valve, sample OST6, MHNG-GEPI-2021-7094. D. external view of a left valve, sample OST6, MHNG-GEPI-2021-7095. E) *Hiatobairdia* cf. *senegasi* Forel in Forel *et al.*, 2019a, right view of a complete carapace, sample WH235, MHNG-GEPI-2021-7096. F) *Hiatobairdia* sp., external view of a left valve, sample OST12, MHNG-GEPI-2021-7097. G) *Isobytocypris* sp. 1, external view of a left valve, sample OST6, MHNG-GEPI-2021-7098. H) *Isobytocypris?* sp. 2, right view of a complete carapace, sample WH227, MHNG-GEPI-2021-7099. I-R) *Lobobairdia whitella* Forel n. sp. I. holotype, right view of a complete carapace, adult, sample OST6, MHNG-GEPI-2021-7100. J. external view of a right valve, adult, sample OST6, MHNG-GEPI-2021-7101. K. paratype 1, external view of a right valve, A-1, sample OST6, MHNG-GEPI-2021-7102. L. external view of a right valve, A-1, sample OST6, MHNG-GEPI-2021-7103. M. external view of a left valve, adult, sample OST6, MHNG-GEPI-2021-7104. N. external view of a left valve, adult, sample OST13, MHNG-GEPI-2021-7105. O. external view of a left valve, adult, sample OST13, MHNG-GEPI-2021-7106. P. paratype 2, external view of a left valve, A-1, sample OST6, MHNG-GEPI-2021-7107. Q. external view of a left valve, A-1, sample OST6, MHNG-GEPI-2021-7108. R. inner view of a broken left valve showing the anterior margin, sample OST6, MHNG-GEPI-2021-7109. S) ?*Lobobairdia whitella* Forel n. sp., external view of a right valve, sample OST6, MHNG-GEPI-2021-7110. T) *Lobobairdia* sp. 1, external view of a right valve, sample OST13, MHNG-GEPI-2021-7111. U) *Lobobairdia* sp. 2, external view of a right valve, sample OST13, MHNG-GEPI-2021-7112. V-AA) *Mirabairdia canadia* Forel n. sp. V. paratype 2, external view of a left valve, A-1, sample OST6, MHNG-GEPI-2021-7113. W. holotype, external view of a left valve, adult, sample OST6, MHNG-GEPI-2021-7114. X. external view of a left valve, A-1, sample OST6, MHNG-GEPI-2021-7115. Y. paratype 1, external view of a right valve, A-1, sample OST6, MHNG-GEPI-2021-7116. Z. external view of a right valve, A-1, sample OST13, MHNG-GEPI-2021-7117. AA. external view of a left valve, A-2, sample OST6, MHNG-GEPI-2021-7118. AB) *Petasobairdia?* sp., right view of a broken carapace, sample OST10, MHNG-GEPI-2021-7119. AC) *Ptychobairdia?* sp. in Arias & Lord, 2000, external view of a left valve, sample WH235, MHNG-GEPI-2021-7120. AD) *Ptychobairdia* cf. *veghae* (Kozur, 1971b), right view of a broken carapace, sample WH235, MHNG-GEPI-2021-7121. AE) *Ptychobairdia* sp., external view of a left valve, sample OST13, MHNG-GEPI-2021-7122. AF) Cytheroidea gen. et sp. indet., right view of a broken carapace, sample WH234, MHNG-GEPI-2021-7123.

All scale bars are 100  $\mu$ m.

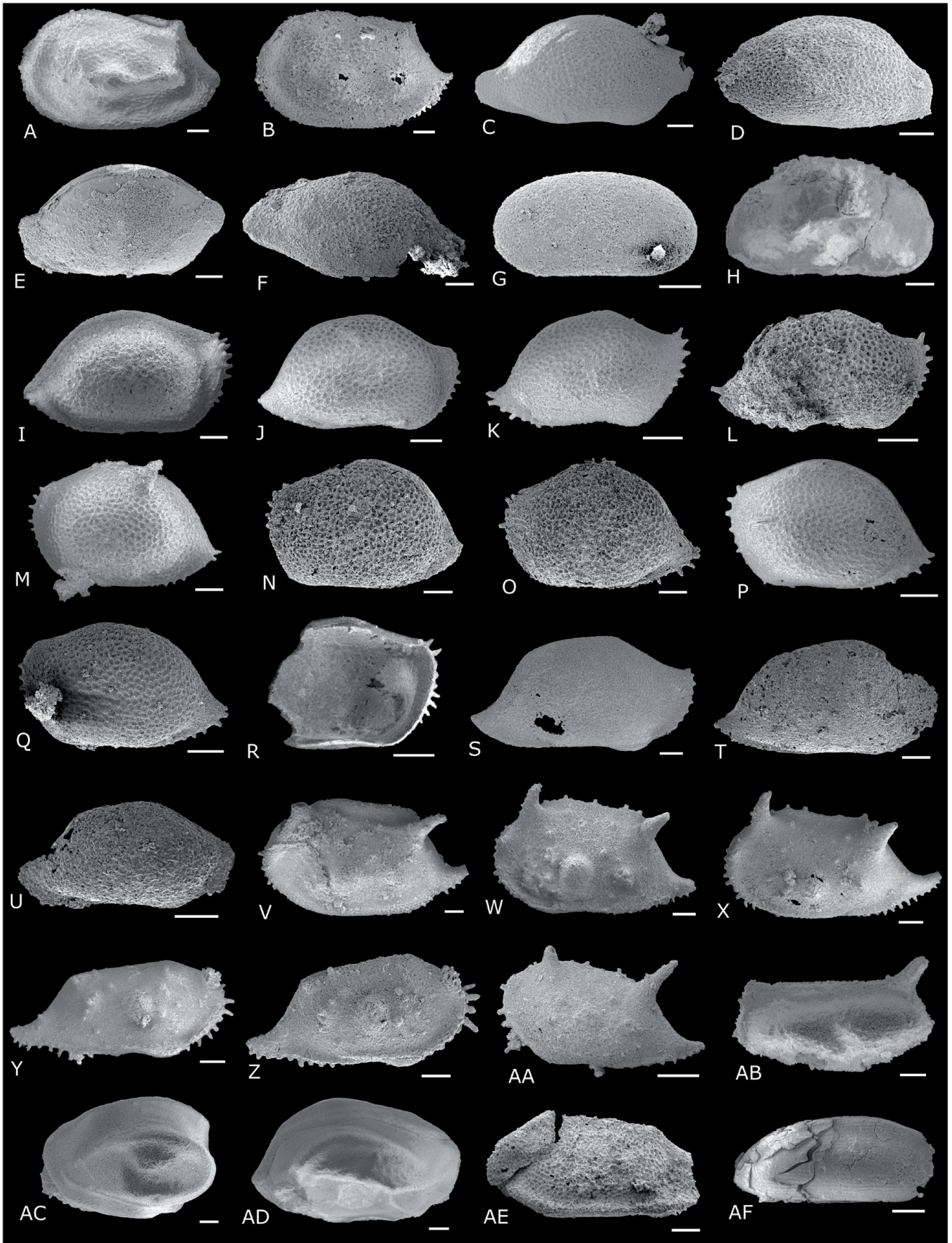


PLATE 4

at both valves with ADB straight and short, DB straight and long, PDB steep (55–65°) and straight until a prominent terminal concavity; ventral margin long and straight to slightly concave at LV, oral concavity more expressed at RV; AVB steeply raised, more rounded at LV than RV, laterally compressed; at RV and LV of juveniles (Pl. 4AA) PVB relatively in line with VB with a tenuous mid-concavity, more strongly raised at LV; AB located in the upper 1/3<sup>rd</sup> of Hmax; PB elongate, caudate and located very ventrally at RV, developed into a thick spine at large specimens (Pl. 4V, W, X) located around lower 1/3<sup>rd</sup> of Hmax at LV. Ornamentation pattern complex with AVB and PVB flanked by thick and long marginal spines oriented downward along AVB at both valves; at RV, a submarginal ridge extends from AB to posterior end of oral concavity, covered with loose reticulation at well preserved specimens (Pl. 4Y, Z), at LV, ridge replaced by a more or less pronounced reticulate bulge developing as a prolongation of the anterior sub-dorsal horn running to the posterior of oral concavity (e.g. Pl. 4V, W); at LV, two sub-dorsal hollow horns developed below AD and PD cardinal angles, orientated backward, reticulate at well preserved specimens (Pl. 4V); at both valves, one massive ovoid node, oriented dorsoventrally, reticulate on well preserved specimens (Pl. 4VU), located around mid-L and slightly below mid-H at LV, at mid-H at RV; at LV, it is posteriorly flanked by a smaller node covered with nodes, which is replaced by a series of 4 small nodes at RV; RV displays two subdorsal structures: one group of nodules below PD cardinal angle, one thick tubercle terminated by bulbous hollow structures in front of AB; lateral surface scattered with small nodules.

**Dimensions:** (Fig. 2F)

Holotype: L = 885 µm, H = 514 µm.

Paratypes: L = 1112 µm, H = 643 µm (Pl. 4V), L = 863 µm, H = 389 µm (Pl. 4Y).

**Remarks.** *Mirabairdia canadia* Forel n. sp. is reminiscent of *Mirabairdia longispinosa* Kristan-Tollmann, 1978 from the Cordevolian, early Carnian of Ruones-Wiesen, Dolomites, Italy (Kristan-Tollmann 1978) from which it differs by the ventromarginal ridge, subcentral node, lack of a third spine and less abundant bulbous tubercles. The H/L diagram of all specimens documents LV larger than RV (Fig. 2F) indicating that although no complete carapace

was recovered, an overlap may have occurred for at least A-1. Noteworthy, the specimen shown in Reid (1985) was not measured because it is broken in its median part. On Fig. 2F, three main scatter plots are observed with important gaps that may correspond to an incomplete reconstitution related to the loss of intervening moults. For this reason, the successive ontogenetic stages are here referred to ?Adult, ?A-1, ?A-2. The holotype is the only ?Adult and the 2 paratypes correspond to ?A-1. The development of this species is marked by the increase of its dimensions and the reinforcement of its lateral ornamentation, as shown by the poorly expressed elements of the unique ?A-2 shown in Pl. 4AA.

**Occurrence.** Sample R-81-39-8, locality Lewes River Formation, Norian, Upper Triassic (Reid 1985; Sohn 1987). Samples OST6, 13, Aksala Formation, Lewes River Group; Stikinia terrane, Whitehorse area, Yukon Territory, Canada, Upper Norian, Upper Triassic (this work).

Genus *Ptychobairdia* Kollmann, 1960

**Type species:** *Ptychobairdia kuepperi* Kollmann, 1960 by original designation.

*Ptychobairdia?* sp. in Arias & Lord, 2000

Pl. 4AC

v2000 *Ptychobairdia?* sp. in Arias & Lord, p. 183, pl. 1, figs 9, 10.

**Occurrence.** Yakoun Lake area, Graham Island, Queen Charlotte Islands, Upper Norian, Upper Triassic (Arias & Lord 2000). Samples WH234, 235, Aksala Formation, Lewes River Group; Stikinia terrane, Whitehorse area, Yukon Territory, Canada, Upper Norian, Upper Triassic (this work).

Superfamily Cytheroidea Baird, 1850

Family Cytheruridae Müller, 1894

Genus *Judabella* Sohn, 1968

Type species: *Judabella tsorfatia* Sohn, 1968 by original designation.

*Judabella dizluense* Kristan-Tollmann in Kristan-Tollmann et al., 1980

Pl. 5P

v1980 *Judabella (Judabella) dizluense* Kristan-Tollmann in Kristan-Tollmann et al., p. 190–192, pl. 9, fig. 16.

v2019b *Judabella (Judabella) dizluense* Kristan-Tollmann; Forel et al., p. 35, fig. 181.

**Occurrences.** Saltspring section, Bagerabad, Iran, Rhaetian, Upper Triassic (Kristan-Tollmann et al. 1980). Mersin Mélange, Huğlu Tuffite, southern Turkey, *Tetraporobrachia haeckeli* radiolarian Zone, Julian, Middle Carnian, Upper Triassic (Forel et al. 2019b). Samples OST6, 13, Aksala Formation, Lewes River Group, Stikinia terrane, Whitehorse area, Yukon Territory, Canada, Upper Norian, Upper Triassic (this work).

***Judabella nodosa nodosa*** (Kozur in Bunza & Kozur, 1971 *sensu* Kristan-Tollmann 1989)

Pl. 5Q, R

1989 *Mostlerella nodosa nodosa* Kozur, 1971; Kristan-Tollmann, pl. 4, figs 6, 7.

**Occurrences.** Lower Austria; Rhaetian, Upper Triassic (Kristan-Tollmann 1989). Sample OST6, Aksala Formation, Lewes River Group, Stikinia terrane, Whitehorse area, Yukon Territory, Canada, Upper Norian, Upper Triassic (this work).

Suborder **Metacopina** Sylvester-Bradley, 1961  
Superfamily Healdioidea Harlton, 1933  
Family Healdiidae Harlton, 1933  
Genus *Hungarella* Méhes, 1911

**Type species:** *Hungarella problematica* Méhes, 1911 by original designation.

***Hungarella limella*** Forel n. sp.

Pl. 5AB-AE, 6A-C

**Derivatio nominis:** In reference to the Lime Peak where the studied area is located.

**Holotype:** MHNG-GEPI-2021-7155, one complete carapace, Ad (Pl. 6A).

**Paratype:** MHNG-GEPI-2021-7151, one broken carapace, Ad (Pl. 5AB; only RV measured in Fig. 2G).

**Additional material:** 4 left valves, 2 right valves, numerous carapaces often broken.

**Type locality:** Lime Peak, Whitehorse area, Yukon Territory, Canada.

**Type horizon:** Sample WH259, Aksala Formation, Lewes River Group; Upper Norian, Upper Triassic.

**Diagnosis:** Triangular *Hungarella* species with LV strongly overlapping RV all around the carapace, triangular overlap at dorsal margin and DB concave at RV.

**Description.** Carapace of medium size with Hmax in front of mid-L at both valves, Lmax slightly below mid-H; LV overlaps RV all around with maximum of triangular shape at in front of mid-L; surface smooth. Internal features not known.

LV: subtriangular in lateral view; dorsal margin bipartite with straight PDB and ADB, PDB longer than ADB; AB and PB uniformly rounded, AB slightly larger than PB, anterior maximum of curvature located around mid-H and posterior one located around the lower 1/3<sup>rd</sup> of H; ventral margin uniformly convex.

RV: ovoid to subrectangular in lateral view; dorsal margin tripartite with ADB straight and close to horizontal, DB concave and PDB reduced; AB and PB as for LV; ventral margin long with tenuous oral concavity around mid-L.

**Dimensions:** (Fig. 2G)

Holotype: L = 632 µm, H = 462 µm.

Paratype: L = 594 µm, H = 576 µm (only RV meas µred).

**Remarks.** *Hungarella limella* n. sp. is unique among *Hungarella* species by its concave DB at RV. The H/L scatter plots of measurable specimens of *Hungarella limella* are shown in Fig. 2G. The majority of specimens gather into one scatter plot that may correspond to the adult stage. One carapace of smaller dimensions, possibly A-1 stage, documents a weaker overlap, possibly illustrating the increase of the overlap through the ontogeny of *Hungarella limella*.

**Occurrence.** Samples WH227, 232, 234-236, 259, Aksala Formation, Lewes River Group, Stikinia terrane, Whitehorse area, Yukon Territory, Canada, Upper Norian, Upper Triassic (this work).

Order **Platycopida** Sars, 1866

Suborder **Platycopina** Sars, 1866

Superfamily Cytherelloidea Sars, 1866

Family Cytherellidae Sars, 1866

Genus *Leviella* Sohn, 1968

**Type species:** *Leviella bentori* Sohn, 1968 by original designation.

***Leviella riedeli*** Forel n. sp.

Pl. 6M-Q, Pl. 7L

**Derivatio nominis:** In reference to Gunnar Riedel (Senckenberg Forschungsinstitut, Frankfurt-am-Main, Germany) who kindly provided the first author with missing literature of first importance to describe this new species.

**Holotype:** MHNG-GEPI-2021-7170, one left valve (Pl. 6P).

**Paratypes:** MHNG-GEPI-2021-7167, one left valve (Pl. 6M); MHNG-GEPI-2021-7171, one right valve (Pl. 6Q).

**Additional material:** 2 left valves, 1 right valve, numerous fragments.

**Type locality:** Lime Peak, Whitehorse area, Yukon Territory, Canada.

**Type horizon:** Sample OST6, Aksala Formation, Lewes River Group; Upper Norian, Upper Triassic.

**Diagnosis:** *Leviella* species with spinose anterior and posterior margins, lateral surface loosely reticulate with a straight longitudinal rib located below pit.

**Description.** Valves large, subrectangular in lateral view with Lmax around mid-H and Hmax in the anterior half of L. Dorsal margin relatively straight at small specimens (Pl. 6N) and divided into 2 distinct parts in larger ones (Pl. 6M, P, Q), with abrupt change in the slope around mid-L to posteriorly to mid-L marking the transition from PDB overhang by marginal ridge and ADB horizontal and slightly concave. PB larger and close to straight, AB uniformly convex with maximum of curvature around mid-H. Ventral margin long with large median oral concavity expressed at both valves. Anterior and posterior margins bordered by numerous tiny spines, the bases of which are linked by a thin fringe at least along the anterior margin. Pit well visible at mid-L and above mid-H. Lateral surface covered with uniform loose and shallow reticulation with scattered nodes bearing a pore at well preserved specimens (Pl. 6M). A ridge runs all around the margins, flanked by a depressed area stronger along anterior and posterior, changes direction ahead of the dorsal break of slope to run parallel to the dorsal margin before it interrupts in anterior third. One straight longitudinal rib located below the pit runs from posterior third to anterior third, inclined antero-ventrally. Anterior extremity of the longitudinal rib aligned with the 2 extremities of the marginal ridge.

**Dimensions:** (Fig. 2H)

Holotype: L = 793  $\mu$ m, H = 432  $\mu$ m.

Paratypes: L = 722  $\mu$ m, H = 391  $\mu$ m (Pl. 6M), L = 539  $\mu$ m, H = 308  $\mu$ m (Pl. 6Q).

**Remarks.** *Leviella riedeli* Forel n. sp. is currently only known by isolated valves and although only 5 have been found to date, the diagnostic characters are well recognizable to differentiate it from all previously known species. It is very close to *Leviella fraterna fraterna* and *Leviella fraterna vali-*

*da* (Bolz, 1970) from the Norian-Rhaetian interval of Austria (Bolz 1970). However, *Leviella riedeli* has only one longitudinal rib below the pit. *Leviella riedeli* Forel differs from *Leviella unicastata* (Bolz, 1970)

---

PLATE 5

SEM micrographs of ostracods from Lime Peak, Yukon Territory, Canada, Norian, Late Triassic. All specimens are housed in the collections of the Natural History Museum of Geneva (Switzerland). A) '*Aglaiocypris*' sp., right view of a carapace, sample OST7, MHNG-GEPI-2021-7124. B) *Paracypris* cf. *ovidi* Forel in Forel & Grădinaru, 2020, left view of a carapace, sample OST6, MHNG-GEPI-2021-7125. C) *Paracypris*? sp. 1, left view of a carapace, sample OST3, MHNG-GEPI-2021-7126. D) *Paracypris*? sp. 2, right view of a carapace, sample WH227, MHNG-GEPI-2021-7127. E) *Paracypris*? sp. 3, external view of an encrusted left valve, sample WH236, MHNG-GEPI-2021-7128. F) *Paracypris* sp. 4, left view of a broken carapace, sample WH227, MHNG-GEPI-2021-7129. G) *Paracypris* sp. 6, right view of a broken carapace, sample OST7, MHNG-GEPI-2021-7130. H) *Paracypris* sp. 7, right view of a carapace, sample OST9, MHNG-GEPI-2021-7131. I, J) *Spinocypris* sp. I. right view of a carapace, sample OST6, MHNG-GEPI-2021-7132. J. right view of a carapace, sample OST6, MHNG-GEPI-2021-7133. K) *Triassocypris* sp., left view of a carapace, sample OST9, MHNG-GEPI-2021-7134. L) *Pontocypris* sp., right view of a carapace, sample OST9, MHNG-GEPI-2021-7135. M) *Pseudomacrocypris* sp. 1, left view of a carapace, sample WH227, MHNG-GEPI-2021-7136. N) *Pseudomacrocypris* sp. 2, left view of a carapace, sample WH227, MHNG-GEPI-2021-7137. O) *Pseudomacrocypris*? sp. 3, right view of a carapace, sample OST10, MHNG-GEPI-2021-7138. P) *Judabella dizhuense* Kristan-Tollmann in Kristan-Tollmann et al., 1980, right view of a carapace, sample OST6, MHNG-GEPI-2021-7139. Q, R) *Judabella nodosa nodosa* (Kozur in Bunza & Kozur, 1971 sensu Kristan-Tollmann 1989). Q. right view of a carapace, sample OST6, MHNG-GEPI-2021-7140. R. left view of a carapace, sample OST6, MHNG-GEPI-2021-7141. S) *Judabella* sp., left view of a carapace, sample OST6, MHNG-GEPI-2021-7142. T) *Lutkevichinella*? sp., external view of a right valve (on sediment), sample WH236, MHNG-GEPI-2021-7143. U) *Patellacythere*? sp., external view of a right valve, sample WH227, MHNG-GEPI-2021-7144. V) *Praemacrocypris* sp. 1, external view of a broken right valve, sample OST6, MHNG-GEPI-2021-7145. W) *Praemacrocypris*? sp. 2, left view of a carapace, sample OST6, MHNG-GEPI-2021-7146. X) *Cardobairdia*? sp. 1, right view of a carapace, sample OST13, MHNG-GEPI-2021-7147. Y. *Cardobairdia*? sp. 2, right view of a carapace, sample WH227, MHNG-GEPI-2021-7148. Z) *Cardobairdia*? sp. 3, external view of a broken left valve, sample OST6, MHNG-GEPI-2021-7149. AA) *Cardobairdia*? sp. 4, external view of a right valve, sample OST6, MHNG-GEPI-2021-7150. AB-AE) *Hungarella limella* Forel n. sp. AB. Paratype, right view of a broken carapace, sample WH259, MHNG-GEPI-2021-7151. AC. right view of a broken carapace, sample WH227, MHNG-GEPI-2021-7152. AD. right view of a broken carapace, sample WH227, MHNG-GEPI-2021-7153. AE. right view of a broken carapace, sample WH227, MHNG-GEPI-2021-7154.

All scale bars are 100  $\mu$ m.

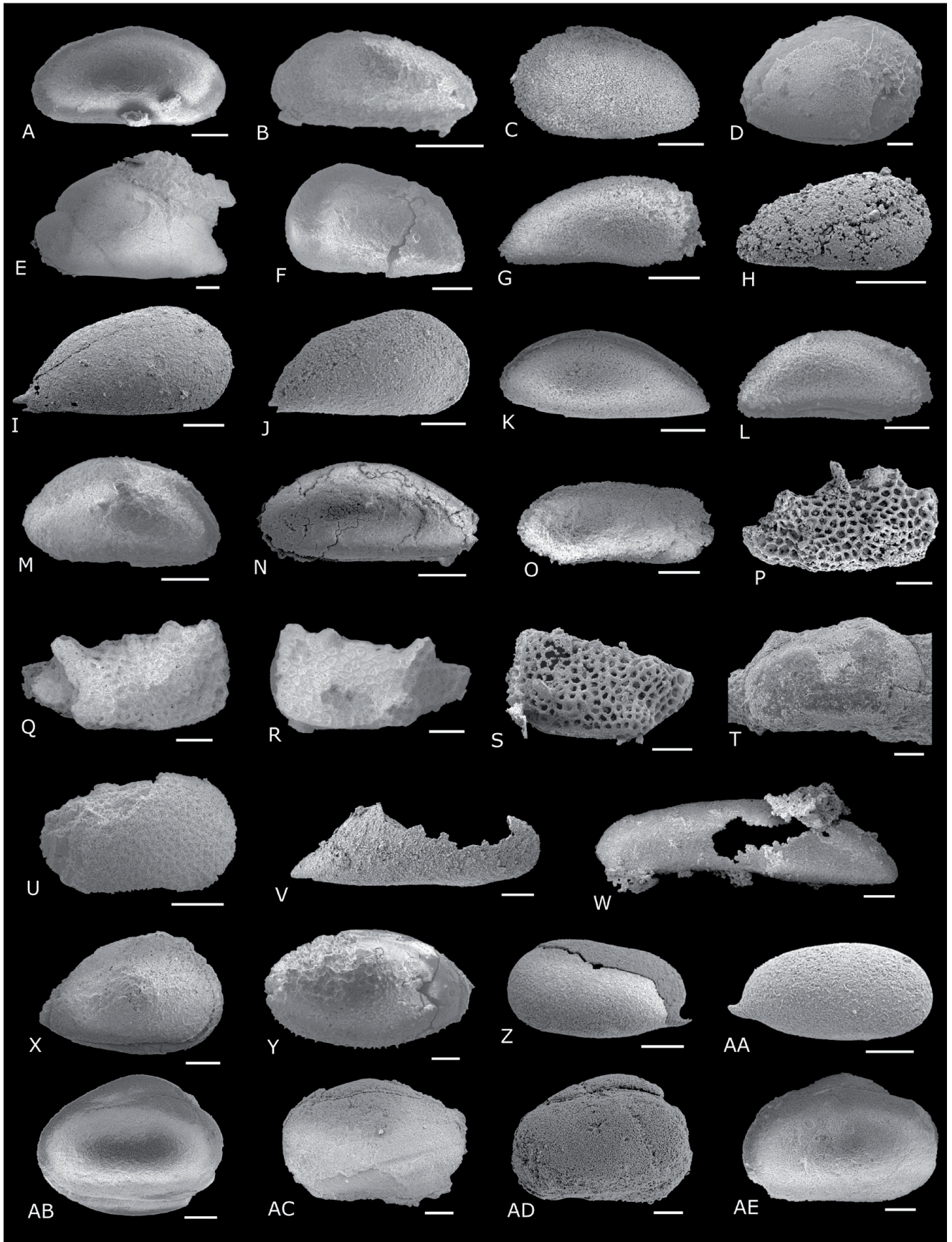


PLATE 5

from the Norian of Austria (Bolz 1970) in being more rectangular in lateral outline, with spinose anterior and posterior margins of well-preserved specimens, and with a straight longitudinal ridge bent anteriorly. *Leviella riedeli* is close to *Leviella simplex* (Bolz, 1970) from the Norian-Rhaetian interval of Austria (Bolz 1970) as shown by its lateral outline and pattern of marginal ridge, *Leviella simplex* however lacks the longitudinal rib on the lateral surface. The H/L diagram of all specimens (Fig. 2H) does not allow to distinguish ontogenetic stages, however, the holotype being the largest one may therefore be an adult.

**Occurrence.** Sample OST6, Aksala Formation, Lewes River Group, Stikinia terrane, Whitehorse area, Yukon Territory, Canada, Upper Norian, Upper Triassic (this work).

### *Leviella sobni* Kozur, 1974

Pl. 6R

v1968 *Leviella* n. sp. Sohn, p. 22, pl. 3, figs 4, 5.

v1974 *Leviella sobni* Kozur in Kozur et al., p. 42, figs 21b–d.

v2000 *Leviella sobni* Kozur; Arias & Lord, p. 186, pl. 2, figs 5–7.

**Occurrence.** Grantsville Formation, Nevada, USA, Ladinian, Middle Triassic (Sohn 1968). Betic Zone, southern Spain, Longobardian, Upper Ladinian, Upper Triassic (Kozur et al. 1974). Frederick Island, British Columbia, Canada, Upper Carnian, Upper Triassic (Arias & Lord 2000). Sample OST13, Aksala Formation, Lewes River Group, Stikinia terrane, Whitehorse area, Yukon Territory, Canada, Upper Norian, Upper Triassic (this work).

### *Leviella unicostata* (Bolz, 1970)

Pl. 6S, T

v1970 *Cytherelloidea? unicostata* Bolz, p. 254–256, pl. 2, fig. 31–33.

v1973 *Cytherelloidea? unicostata* Bolz; Kristan-Tollmann, pl. 5, fig. 9.

v1992 *Cytherelloidea? unicostata* Bolz; Dépêche & Crasquin-Soleau, pl. 3, fig. 1, 2.

**Occurrence.** Zlambach beds, Northern Calcareous Alps, Norian-Rhaetian, Upper Triassic (Bolz 1970). Zlambach beds, Rossmoosalm, north-east Goisern, Austria, Upper Norian, Upper Triassic (Kristan-Tollmann 1973). Exmouth Plateau, northwestern margin of Australia, Rhaetian, Upper Triassic (Dépêche & Crasquin-Soleau 1992). Samples WH227, 232, 234–236, 259, Aksala Formation,

Lewes River Group, Stikinia terrane, Whitehorse area, Yukon Territory, Canada, Upper Norian, Upper Triassic (this work).

## PLATE 6

SEM micrographs of ostracods from Lime Peak, Yukon Territory, Canada, Norian, Late Triassic. All specimens are housed in the collections of the Natural History Museum of Geneva (Switzerland). A–C) *Hungarella limella* Forel n. sp. A. holotype, right view of a carapace, sample WH259, MHNG-GEPI-2021-7155. B. right view of a carapace, sample WH259, MHNG-GEPI-2021-7156. C. external view of a left valve, sample WH235, MHNG-GEPI-2021-7157. D, E) *Hungarella* sp. D. external view of a right valve, sample OST6, MHNG-GEPI-2021-7158. E. external view of a right valve, sample OST6, MHNG-GEPI-2021-7159. F) *Bektasia* sp. 1, right view of a carapace, sample OST7, MHNG-GEPI-2021-7160. G, H) *Bektasia* sp. 2. G. left view of a carapace, sample WH234, MHNG-GEPI-2021-7161. H. left view of a carapace, sample WH232, MHNG-GEPI-2021-7162. I) *Bektasia* sp. 3, left view of a carapace, sample OST8, MHNG-GEPI-2021-7163. J) *Cytherella* sp. 1, right view of a carapace, sample WH235, MHNG-GEPI-2021-7164. K) *Cytherella* sp. 2, right view of a carapace, sample WH234, MHNG-GEPI-2021-7165. L) *Issacharella* sp., left view of a carapace, sample OST7, MHNG-GEPI-2021-7166. M–Q) *Leviella riedeli* Forel n. sp. M. paratype 1, external view of a left valve, sample OST6, MHNG-GEPI-2021-7167. N. external view of a right valve, sample OST6, MHNG-GEPI-2021-7168. O. external view of a left valve, sample OST6, MHNG-GEPI-2021-7169. P. holotype, external view of a left valve, sample OST6, MHNG-GEPI-2021-7170. Q. paratype 2, external view of a right valve, sample OST6, MHNG-GEPI-2021-7171. R) *Leviella sobni* Kozur in Kozur et al., 1974, right view of a carapace, sample OST13, MHNG-GEPI-2021-7172. S, T) *Leviella unicostata* (Bolz, 1970). S, external view of a right valve, sample WH227, MHNG-GEPI-2021-7173. T. right view of a carapace, sample WH236, MHNG-GEPI-2021-7174. U) *Leviella* cf. *brevicostata* Kristan-Tollmann, 1973, external view of a left valve, sample OST6, MHNG-GEPI-2021-7175. V) *Leviella* sp. 1, external view of a right valve, sample WH234, MHNG-GEPI-2021-7176. W) *Leviella* sp. 2, external view of a left valve, sample OST6, MHNG-GEPI-2021-7177. X) *Leviella* sp. 3, left view of a carapace, sample OST13, MHNG-GEPI-2021-7178. Y) *Leviella* sp. 4, left view of a broken carapace, sample OST7, MHNG-GEPI-2021-7179. Z, AA) *Polycope pumicosa schleiferiae* Kozur in Bunza & Kozur, 1971. Z. left view of a carapace, sample OST6, MHNG-GEPI-2021-7180. AA. left view of a carapace, sample OST6, MHNG-GEPI-2021-7181. AB, AC) *Polycope* sp. 1. AB. left view of a carapace, sample OST7, MHNG-GEPI-2021-7182. AC. left view of a carapace, sample OST7, MHNG-GEPI-2021-7183. AD) *Polycope* sp. 2. left view of a carapace, sample OST9, MHNG-GEPI-2021-7184. AE, AF) Podocopida indet. AE. external view of a left valve, sample OST10, MHNG-GEPI-2021-7185. AF. external view of a right valve, sample OST10, MHNG-GEPI-2021-7186.

All scale bars are 100 µm.

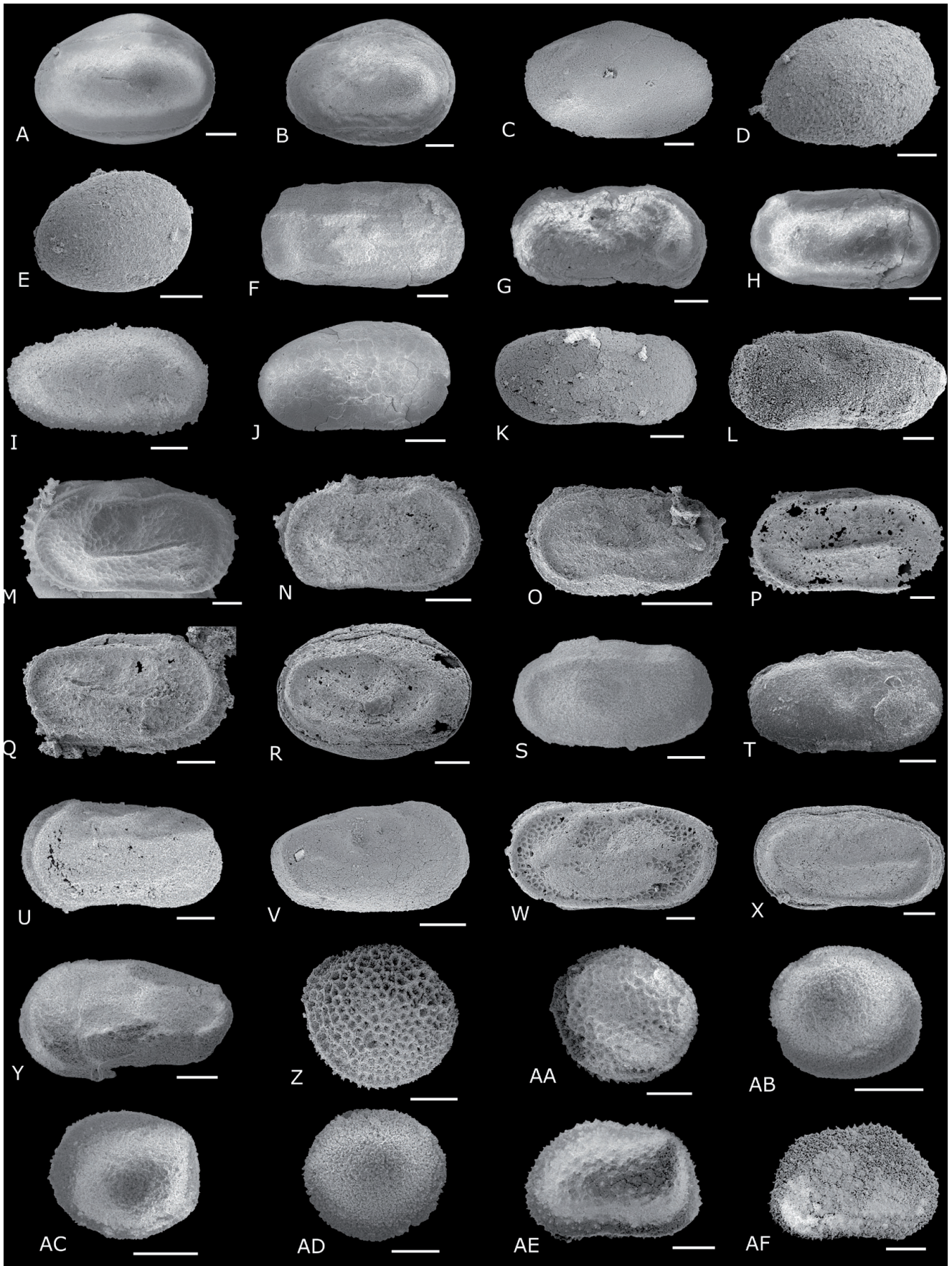


PLATE 6

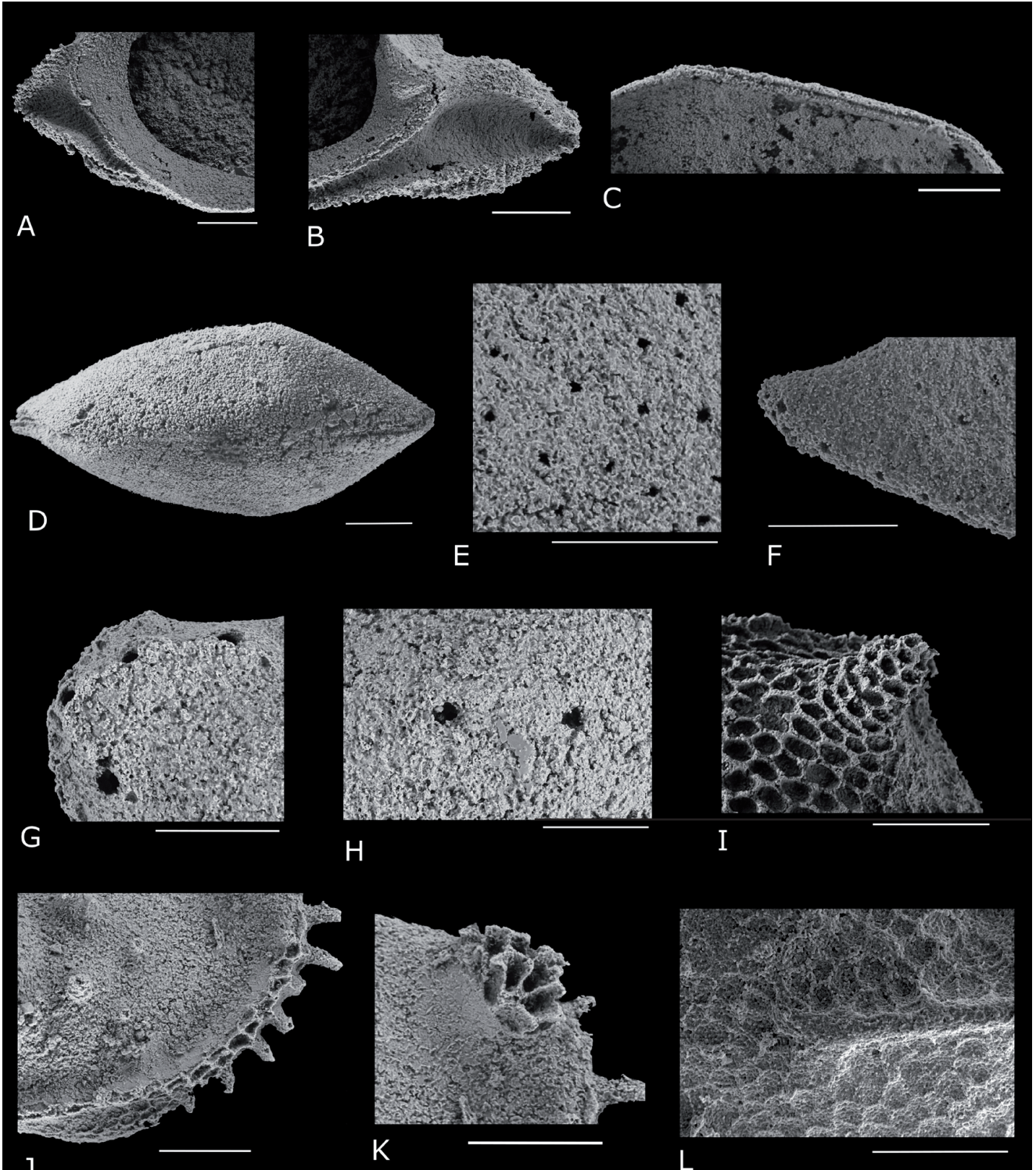


PLATE 7

Close ups on important structures of ostracods from Lime Peak, Yukon Territory, Canada, Norian, Late Triassic. All specimens are housed in the collections of the Natural History Museum of Geneva (Switzerland). A-C) *Alatobairdia? sobni* n. sp. A. Internal view of the anteroventral triangular extension (same specimen as Pl. 1F). B. Internal view of the posteroventral triangular extension (same specimen). C. Hingement (same specimen as Pl. 1J). D) Dorsal view of *Bairdia aksala* Forel n. sp. (same specimen as Pl. 1Q). E, F) *Bairdia taan* Forel n. sp. (same specimen as Pl. 2F). E. Pores on the anterolateral surface. F. Pores along the posteroventral surface. G, H) *Bairdia yukonensis* Forel n. sp. (same specimen as Pl. 2O). G. 'Openings' along the anterior margin. H. Two 'openings' at the centre of the lateral surface. I) Reticulation pattern on the posterodorsal spine and surrounding lateral surface of *Cornutobairdia yukonella* Forel n. sp. (same specimen as Pl. 3AB, AC). J, K) *Mirabairdia canadia* Forel n. sp. (same specimen as Pl. 4Y). J. Ornamentation along the anteroventral margin and anterolateral area. K. Thick tubercle below posterodorsal angulation terminated by hollow structures. L) Reticulation pattern of *Leviella riedeli* Forel n. sp. (same specimen as Pl. 6M).

All scale bars are 100  $\mu$ m.

Subclass **MYODOCOPA** Sars, 1866  
 Order **Myodocopida** Sars, 1866  
 Suborder **Myodocopina** Sars, 1866  
 Superfamily Polycopoidea Sars, 1866  
 Family Polycopidae Sars, 1866  
 Genus *Polycope* Sars, 1866

**Type species:** *Polycope orbicularis* Sars, 1866 by original designation.

***Polycope pumicosa schleiferae* Kozur in Bunza & Kozur, 1971**

Pl. 6Z, AA

v1971 *Polycope pumicosa schleiferae* Kozur in Bunza & Kozur, p. 14, pl. 2, fig. 17.

v2013 *Polycopsis* n. sp. ex gr. *cinninata* (Apostolescu); Moix et al., pl. 5, fig. 7.

v non 2013 *Polycope pumicosa schleiferae* [sic] Kozur; Monostori & Tóth, p. 308, pl. 1, fig. 2.

v2019b *Polycope pumicosa schleiferae* Kozur; Forel et al., p. 36, fig. 24D.

v2020 *Polycope pumicosa schleiferae* Kozur; Forel & Moix, p. 9, pl. 1G, H.

**Occurrences.** Hungary, ?Cordevolian, early Carnian, Upper Triassic (Bunza & Kozur 1971); Tavuşçayırı Block, Sorgun Ophiolitic Mélange, Huğlu Tuffite, southern Turkey, *Tetraporobrachia haeckeli* radiolarian Zone, Julian, middle Carnian, Upper Triassic (Forel et al. 2019b); Karapınar Formation, Karadağ Unit, Ağlıovası Yayla section, Lycian Nappes, southwestern Turkey, *Pseudofurnishius murcianus murcianus* conodont zone, Cordevolian, Lower Carnian, Upper Triassic (Forel & Moix 2020). Sample OST6, Aksala Formation, Lewes River Group, Stikinia terrane, Whitehorse area, Yukon Territory, Canada, Upper Norian, Upper Triassic (this work).

## RESULTS

### Taxonomic composition of ostracod assemblages

All samples studied from the Norian of Lime Peak provided identifiable ostracods. Ninety species distributed into 31 genera and 11 families have been identified. Seven species were previously known from the Triassic, 9 are new (*Alatobairdia? sobni* n. sp., *Bairdia aksala* n. sp., *Bairdia taan* n. sp., *Bairdia yukonensis* n. sp., *Cornutobairdia yukonella* n. sp., *Lobobairdia whitella* n. sp., *Mirabairdia canadia* n. sp., *Hungarella limella* n. sp., *Leviella riedeli* n. sp.) and 74 are kept in open nomenclature due to poor preservation and/or paucity of material (including *Bairdia* sp. 7 in Forel et al., 2019b, *Bairdia* sp. A in Dépêche

& Crasquin-Soleau, 1992 and *Ptychobairdia?* sp. in Arias & Lord, 2000 which are known from other localities during the Late Triassic). Tab. 1 summarizes all taxonomic information of the studied assemblages and familial composition (number of species per family) is shown in Fig. 3A. The highest familial diversity is observed in samples OST6 and WH227 (8 families), while the lowest level occurs in OST3 (3 families). The observed generic diversity ranges from 5 (WH232) to 34 (OST6) and the species diversity is comprised between 5 (OST3) and 18 (OST6). The size of all samples processed for this investigation was always between 400 and 500 grams so that observed differences are most likely not due to sample size, assuming rather constant rate of sedimentation.

Bairdiidae (*Acratia*, *Alatobairdia?*, *Bairdia*, *Bairdiacypris*, *Carinobairdia*, *Cornutobairdia*, *Hiatobairdia*, *Isobrythocypris*, *Lobobairdia*, *Mirabairdia*, *Petasobairdia*, *Ptychobairdia*) is the most widespread and diversified family, occurring in all studied assemblages. Their proportions range from 11% (OST8) to 67% (OST12) of the species and they exceed 50% in seven assemblages (OST3, 4, 6, 7, 10, 12, WH227). Cytherellidae (*Cytherella*, *Issacharella*, *Leviella*) and Paracyprididae (*Aglaioocypris*, *Paracypris*, *Spinocypris*, *Triassocypris*) are the second and third most represented families. When present, Cytherellidae range from 9% (OST6) to 33% (WH232, 259) and Paracyprididae comprise between 8% (WH236) and 50% (OST9). Cavellinidae (*Bektasia*) are important components of assemblages WH227, 232, 234, 236, 259 in which they range from 4 to 17% of the species. Polycopidae (*Polycope*) range from 3 to 20% of the species in assemblages OST3, 4, 6-10. Accessory families are Healdiidae (*Hungarella*; 3% to 17% when present), Pontocyprididae (*Pontocypris*, *Pseudomacrocypis*; 8 to 25% when present), Sigilliidae (*Cardobairdia*; 4 to 17% when present), Macrocypriidae (*Praemacrocypis*; only in assemblages OST6, 6%, and OST8, 11%), Cytheruridae (*Judabella*; only in OST6, 9%). Bythocytheridae (*Patellacythere?*) and Limnocytheridae (*Lutkevichinella?*) are restricted to WH227 (4%) and WH236 (7%) respectively. An indeterminate family of Cytheroidea is restricted to WH234 where it represents 7% of the species.

Assemblages OST8, 9, WH232 and to a lesser extent WH259 are exceptions to the dominance of Bairdiidae and document 2 distinct patterns: OST8 and 9 show high proportions of Paracyprididae

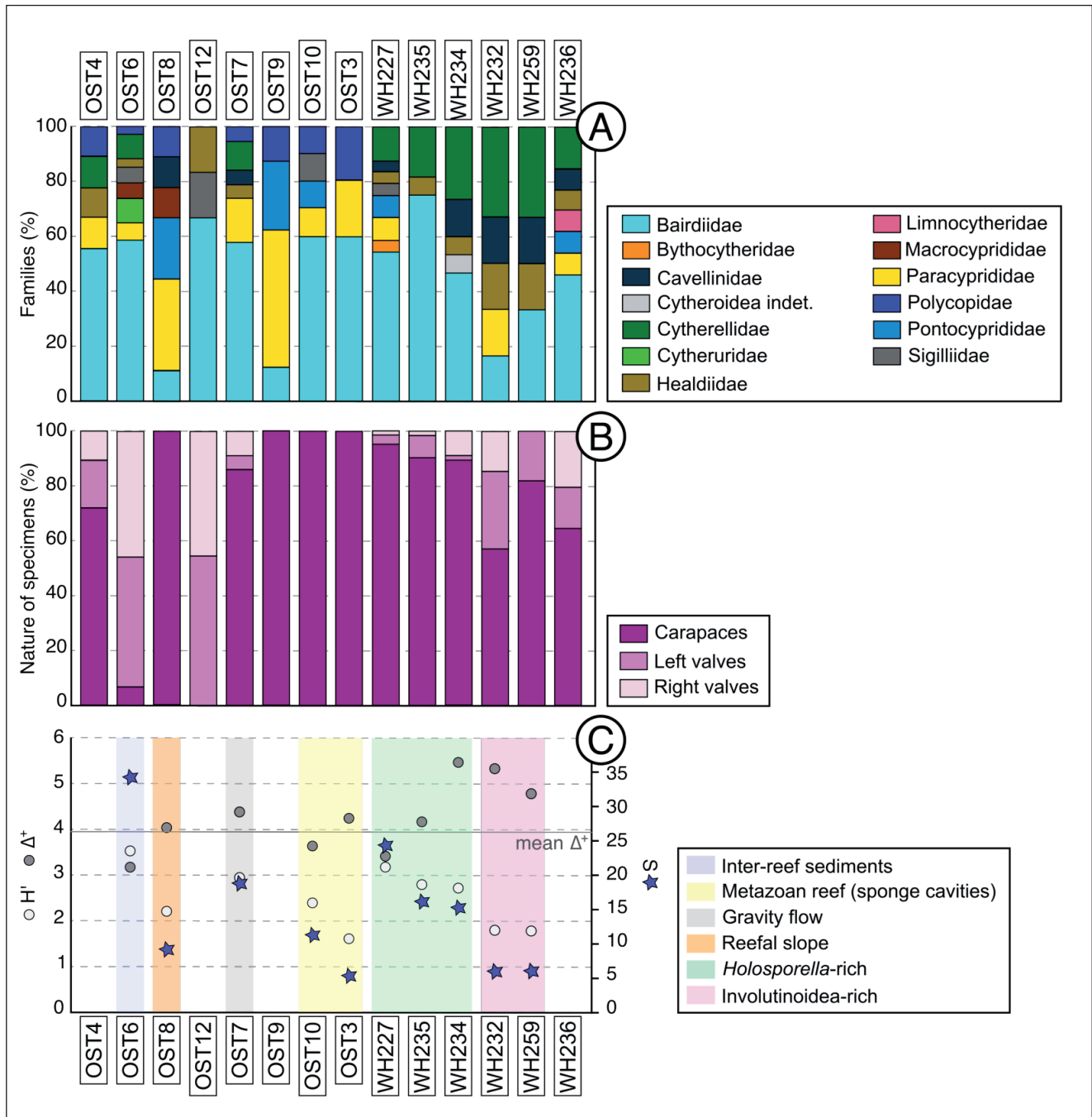


Fig. 3 - Characteristics of the ostracod assemblages (per sample) from the Norian of Lime Peak, Yukon. A. Faunal composition (genera per family). B. Proportions of carapaces, left valves, right valves per sample. C. Species richness (S), Shannon diversity (H'), Taxonomic Distinctness ( $\Delta^*$ ). As detailed in the text, the composite sample OST13 is not considered in faunal analysis and thus not plotted.

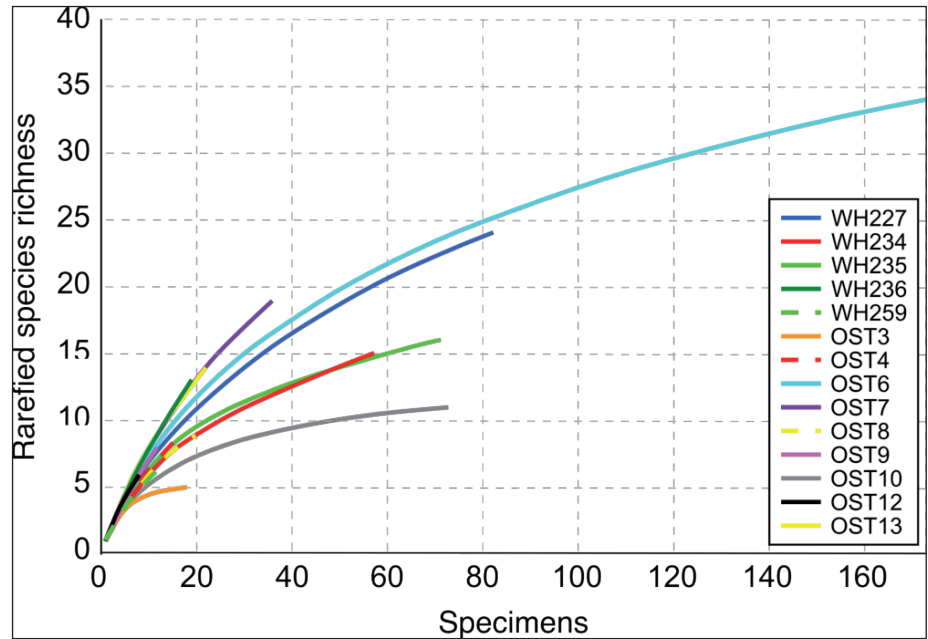
(peak in OST9) and Pontocypridae while WH232 and 259 are characterized by high proportions of Cytherellidae, together with Cavellinidae and Healdiidae.

### Taphonomic analysis

To discuss diversity patterns among Lime Peak assemblages, the specimens of each species

were counted articulated plus higher number of left or right valves (Fürsich & Wendt 1977; Nützel & Kaim 2014; Haussmann & Nützel 2015). Individual rarefaction has been calculated with PAST version 4.04 (Hammer et al. 2001; Hammer & Harper 2005), showing the expected number of taxa as a function of the number of specimens in each of the studied samples (Fig. 4). The rarefaction curves

Fig. 4 - Individual rarefaction curves for ostracod assemblages from the Norian of Lime Peak, Yukon.



show that for most assemblages, more specifically WH236, OST4, WH259, taxa count is not representative of the entire fauna and that a larger sample would have given better counts and higher diversity levels. Only for assemblages OST10, OST3, the curves seem to flatten out gradually demonstrating that further sampling would not have provided a significant number of additional species so that the assemblages in these samples may represent the original diversity of the ostracod fauna.

The proportion of complete carapaces *versus* isolated valves and the demographic structure of populations are tools to determine the autochthonous or allochthonous nature of ostracod assemblages (e.g. Oertli 1971; Boomer et al. 2003). In the Lime Peak assemblages, the proportions of detached valves and complete carapaces are not correlated to taxonomy and vary drastically as shown in Fig. 3B. Assemblages OST3, 8-10 are entirely composed of complete carapaces while OST4, 7, WH227, 232, 234-236, 259 are dominated by carapaces, ranging from 57 to 95% of the specimens analysed. Most assemblages are composed of a mixture of adults and juveniles, as shown by the observed ontogenetic series (Fig. 2), and may consequently correspond to low energy thanatocoenosis with minimal post-mortem disturbance and thus good indicators of the environmental conditions. Of these assemblages, WH232 has only 57% of carapaces and may thus illustrate slightly higher disturbance. Conversely, assemblages OST6 and OST12 have low propor-

tions of carapaces, respectively 12% and 0% of the specimens (Fig. 3B). Considering that these assemblages are also composed of a mixture of juveniles and adults, they may correspond to a high energy thanatocoenosis with some post-mortem disturbance but still considered as good indicators of living conditions. Owing to the patterns of rarefaction curves discussed in the previous paragraph (Fig. 4), the incompleteness of assemblages OST4, 9, 12, WH236 does not reasonably yield robust diversity and palaeoenvironmental inferences: they are not considered in the following discussion.

## DISCUSSION

### Diversity

The diversity of the ostracod assemblages from the Upper Norian of Lime Peak has been approached by two distinct yet complementary indices (Fig. 3C):

- the Shannon diversity index ( $H'$ ; Shannon & Weaver 1949), which is relatively insensitive to sample size and allows for a deep analysis of the species richness taking into account the abundance of each species,
- the Taxonomic Distinctness ( $\Delta^+$ ; Warwick & Clarke 1998), which is a phylogenetic diversity index totally independent of the sampling effort and gives insights into the taxonomic organization of assemblages by considering higher taxonomic levels (up to order here).

At Lime Peak,  $H'$  ranges from 1.6 (OST3) to 3.5 (OST6) and  $\Delta^+$  from 2.5 (WH236) to 5.4 (WH234). The highest  $H'$  value in OST6 may relate to silicification that may have allowed for the preservation of a larger proportion of the original fauna. The assemblage OST7 was also obtained from a silicified sample but its radically different diversity pattern may reflect original differences from OST6, as shown in their taxonomic composition (Fig. 3A). It is worth noting that the individual rarefaction curve for OST6 (Fig. 4) does not really flatten out and that higher diversity may be expected from more sampling. This  $H'$  peak is coupled with the lowest  $\Delta^+$  value, witnessing a relatively poor diversity at higher taxonomic levels. Assemblages WH232 and WH259 are characterized by low  $H'$  and comparatively very high  $\Delta^+$ , indicating that the diversity of these assemblages is ensured by high-taxonomic levels. Samples WH227, 234, 235 are characterized by very similar  $H'$  values while  $\Delta^+$  drastically varies.

#### Palaeoenvironmental implications

At Lime Peak, palaeoenvironmental conditions for samples OST3, 6-8, 10 are relatively well-constrained based on field observations and microfacies: they are attributed to sponge cavities within metazoan reef (OST10 and 3), intra-reef sediments (OST6), slope (OST8) and gravitational beds on the slope (OST7). The rest of the samples discussed in this section were collected from the internal facies of Lime Peak carbonate system: samples WH227, 235, 234 come from *Holosporella*-rich limestone and WH232, 259 from *Involutoidea*-rich limestone (see Bocur et al. 2020 and Del Piero et al. in prep). In this regard, the palaeoenvironmental conditions under which the WH samples were formed are still not completely constrained. The analysis of the composition of ostracod assemblages and their palaeoenvironmental implications can give us new insights regarding the environmental settings associated with these samples and the conditions associated with the OST samples. As a first step in this discussion, we performed an analysis of the similarity of the studied ostracod assemblages. We produced a similarity symmetric matrix, following Q-mode analysis (e.g. Henderson & Heron 1976; Pielou 1979; Janson & Vegelius 1981; Digby & Kempton 1987), based on the occurrence of species per sample shown in Tab. 1. The matrix was analysed using the Jaccard's similarity coefficient

(Jaccard 1912) that was chosen because it emphasises presence instead of absence and is not influenced by differences in sample size (e.g. Cheetham & Hazel 1969; Baroni-Urbani & Buser 1976; Wolda 1981; Magurran 1988). We used the agglomerative clustering method unweighted pair group method with arithmetic mean (UPGMA) which provides an unweighted arithmetic average between individuals (e.g. Hazel 1970; Anderberg 1973; Podam 1989; Shi 1993). All analyses were done using the statistical software package PAST version 4.04 (Hammer et al. 2001; Hammer & Harper 2005). The classification of Lime Peak's assemblages in terms of similarities to their ostracod species and genera composition is shown in Fig. 5. The UPGMA dendrogram displays a rather high cophenetic correlation index of 0.95, demonstrating that it well describes the similarities among-assemblages. This similarity analysis reveals two major groups of assemblages as regard to the similarity of their ostracod species composition (Fig. 5A):

- A first group of 'reef-associated assemblages' (OST3, 7, 8, 10) with the highest similarity between assemblages from sponge cavities in metazoan reefs (OST3, 10) and lower values between samples representing displaced reefal materials (gravity flow, OST7) and autochthonous slope deposits (OST 8).
- A second group of assemblages with a cluster gathering all *Holosporella*-rich samples (WH227, 234, 235) and another one corresponding to *Involutoidea*-rich limestones (WH232, 259). The OST6 assemblage from intra-reef sediments plots with this second group with a very low similarity, highlighting the specificity of this assemblage.

The classification of assemblages in terms of ostracod genera (relatively low cophenetic correlation index of 0.82) also discriminates the two groups of assemblages, with the difference that OST6 is more closely related to 'reef-associated assemblages' (Fig. 5B). These patterns prove that the composition of Norian ostracod assemblages of Lime Peak is closely related to other observations and data, and are therefore good proxies for palaeoenvironmental investigation (see also the taphonomic analysis above).

Numerous physical and chemical factors may influence the distribution of ostracod species, of which salinity, pH,  $O_2$ , food availability, depth, temperature and substrate are considered the most

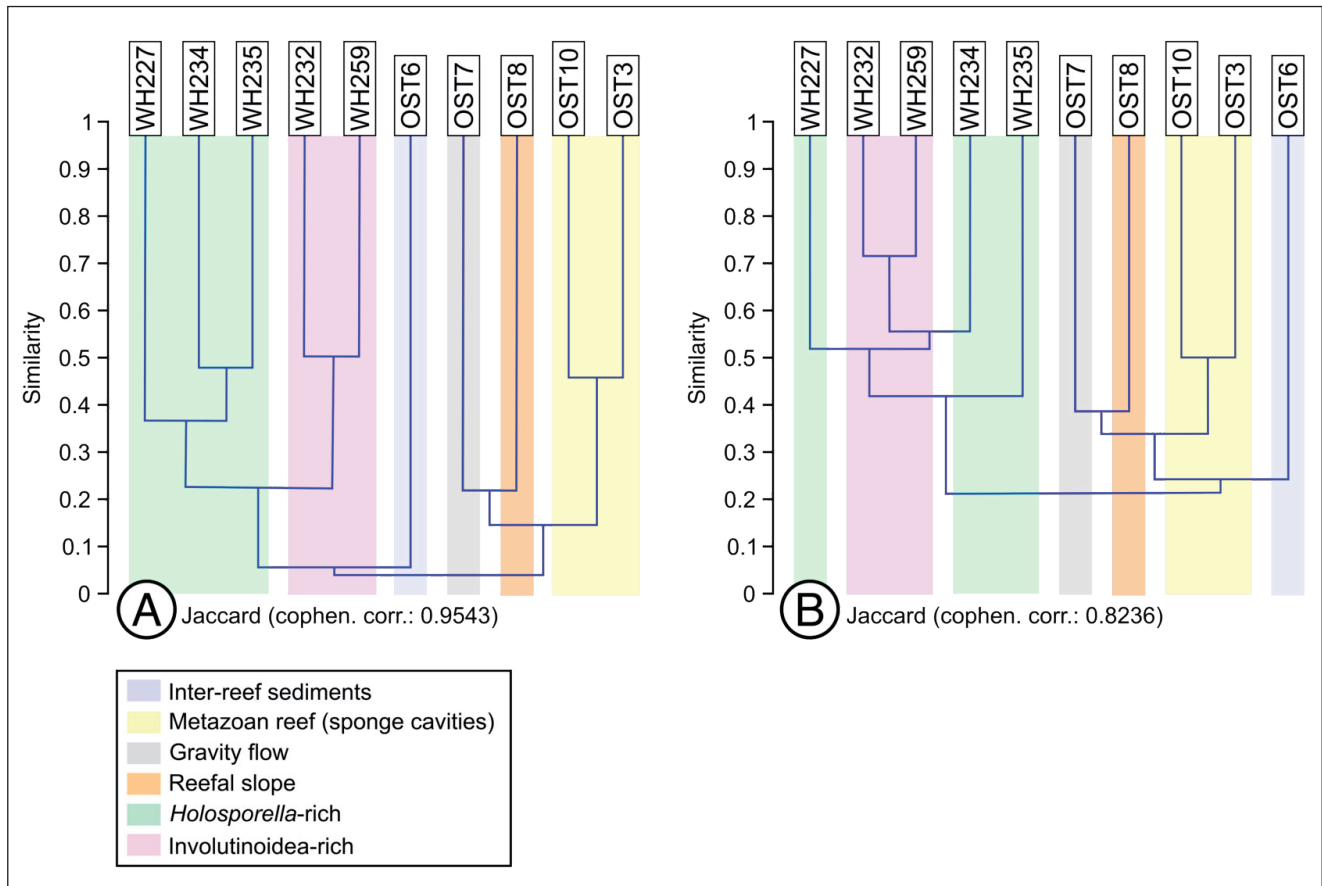


Fig. 5 - Dendrogram of UPGMA analysis based on the species (A) and genera (B) composition of the Norian assemblages of ostracods in Lime Peak.

significant. The influence of depth being principally visible by its effects on other factors such as light intensity and hydrodynamics (e.g. Elofson 1941; Neale 1964; Theisen 1966; Dubovsky 1939; Hirschmann 1909; Tressler & Smith 1948). Paracyprididae and smooth-shelled Bairdiidae (e.g. *Bairdia*, *Bairdiacypris*, *Isobrythocypris*) are suggestive of stable outer shelf conditions with normal salinity and oxygenation. Thick-shelled Bairdiidae (e.g. *Cornutobairdia*, *Carinobairdia*) are generally considered as indicative of relatively high hydrodynamic conditions on the proximal platform (e.g. Urlichs 1972). Some thick-shelled bairdiids are however known from deep-water deposits in the Middle and Upper Triassic (e.g. Kozur 1970, 1971a, b, 1973a; Urlichs 1972; Kristan-Tollmann 1978; Mette et al. 2015) and the traditionally Norian-Rhaetian shallow-water genus *Carinobairdia* may have radiated on the outer shelf during the Carnian (Forel et al. 2019a). In the Norian and Rhaetian of Tethyan realm, *Cornutobairdia* has been for instance reported from reef sediments of Iran (Kristan-Tollmann et al. 1979).

Conversely, *Mirabairdia* is commonly associated with deep-water sediments (e.g. Kozur 1973a; Kristan-Tollmann 1978; Mette et al. 2015). The lateral outline of smooth bairdiids is also of importance as thin, elongate taxa with spinose extremities may be markers of off-shelf conditions. In the Mesozoic, Cytheruridae were restricted to shelf depths and they generally indicate shallow marine conditions with clear and well-oxygenated waters (e.g. Ballent & Whatley 2000, 2009). Cytherellidae are considered as significant of warm water littoral environments in the Mesozoic (e.g. Sohn 1962; Kornicker 1963; Urlichs 1972; Whatley et al. 1995). Healdiidae rather occur in the median zone with euryhaline environments in shallow to very shallow waters and the shallow-water cavellinid genus *Bektasia* tolerated important salinity variations (e.g. Kristan-Tollmann & Hamedani 1973).

The overall dominance of Bairdiidae and Paracyprididae (except for WH232 and to a lesser extent WH259) in the Norian assemblages of Lime Peak is a good indicator of open marine conditions

	OST4	OST6	OST7	OST10	OST3	WH227	WH235	WH259	WH236
Elongate Bairdiidae vs all Bairdiidae	20%	3%	11%	46%	89%	12%	20%	13%	11%
Elongate Bairdiidae vs total assemblage	6%	2%	6%	22%	44%	10%	17%	9%	5%

Tab. 2 - Proportion of elongate Bairdiidae in sample of Lime Peak, Yukon Territory, Canada, Norian, Late Triassic.

over the investigated area. Assessment of off-shelf conditions is complex at the Late Palaeozoic-Early Mesozoic transition due to the gradual disappearance of typical Palaeozoic deep-sea taxa as Rectonariidae, Beecherellidae and deep-sea Bythocytheridae. Although residual, these taxa are commonly reported from Tethyan off-shelf assemblages until the Rhaetian (see Forel in press for a summary). Their absence from all Lime Peak assemblages could be related to palaeogeographic, palaeobathymetric/environmental signals or to their absence in Panthalassa. Nonetheless, the overall composition of the assemblages is similar to coeval Tethyan shelf ones so that we consider that the lack of deep-sea taxa relates to palaeobathymetric/environmental context (of the few sampled levels), which definitively points to neritic conditions. However, thin and elongate bairdiids (*Acratia* sp. 1, *Bairdia aksala*, *B. yukonensis*, *B.* sp. 2) occur in several assemblages, with proportions ranging from 2% (OST6) to 44% (OST3) of the total abundance when present (Tab. 2). Their highest abundance is recorded in assemblages from sponge cavities of metazoan reefs (OST3 and OST10) and implies the influence of offshore conditions. It is worth noting that ostracods associated with sponges have rarely been reported in detail. In the Triassic, they have been described from microbial-sponge mounds that grew below the photic zone during the Carnian in South China (Forel et al. 2019a). Assemblages OST3 and OST10 are much less diversified than the Carnian ones and lack taxa truly indicative of outer shelf conditions (deep-sea Bythocytheridae *Monoceratina* and *Praebythoceratina*). This points to the fact that Lime Peak assemblages developed under much shallower conditions lacking influence of off-shelf water masses compared to those from the Carnian of China.

At Lime Peak, thick-shelled Bairdiidae are represented by the genera *Alatobairdia?*, *Carinobairdia*, *Cornutobairdia*, *Mirabairdia*, *Petasobairdia* and *Ptychobairdia*. The paleoenvironmental significance of *Alatobairdia* is enigmatic as only one species has been reported to date from the Rhaetian of Austria

(Kristan-Tollmann 1971a) and *Alatobairdia? sobni* n. sp. cannot be confirmed as congeneric. *Mirabairdia canadica* n. sp. is restricted to sample OST6 (not considering OST13 from mixed environments), in association with the unique occurrence of Cytheruridae and the lowest proportion of elongate bairdiids (Tab. 2). Although it is considered a relatively off-shore taxon, the implications of the occurrence of *Mirabairdia canadica* are not in line with the two other markers; in addition, owing that most of the specimens of elongate morphology and of *Mirabairdia canadica* found in sample OST6 are single valves, they may have been transported from outer areas. In Lime Peak, Cytherellidae are widespread except in samples OST3, 8-10, 12. Noteworthy, their proportions notably rise in *Holosporella*-rich samples: 12% in WH227, 19% in WH235, 27% in WH234 (Fig. 3A). This increasing pattern is paralleled by a slight decrease in  $H'$  (Fig. 3C). Cavellinidae, genus *Bektasia*, are present in several of the studied samples but they reach their maximum diversity and abundance in WH234. These elements may indicate a trend toward more restricted conditions from WH227 to WH234. It is however interesting to note that this pattern is also paralleled by a major increase in  $\Delta^+$ , indicating high taxonomic level diversity in the most restricted areas. This conclusion is reinforced by the low  $H'$ , here again paralleled by high degrees of diversification at high taxonomic levels (Fig. 3C).

To sum up, a series of conclusions can be drawn for the Norian carbonate deposits of Lime Peak (Fig. 6):

- All studied assemblages document photic conditions.
- The most restricted conditions are reconstructed for all samples WH, as shown by the important proportions of Cytherellidae, Cavellinidae and Healdiidae.
- OST assemblages exhibit a more pronounced influence of open marine waters with the most distal position recorded for those associated with sponge cavities (OST3, 10).
- The assemblages associated with *Holosporella* illustrate a trend toward more restricted conditions

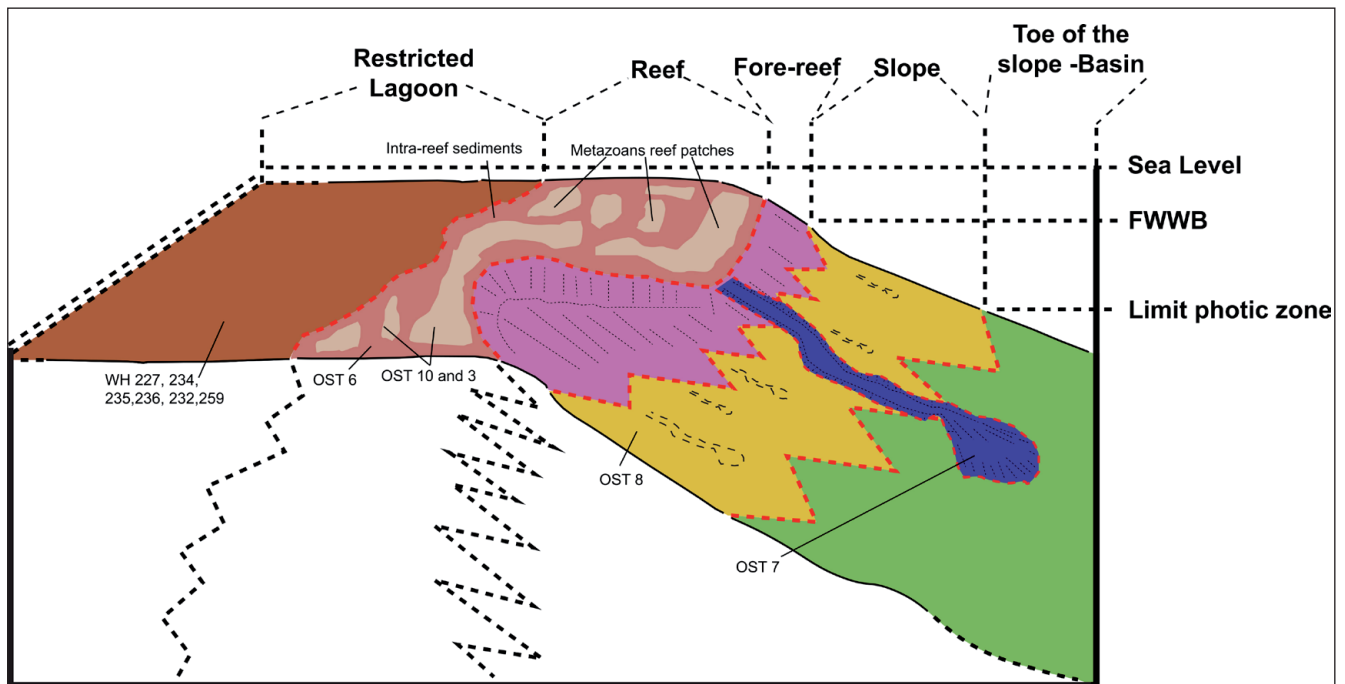


Fig. 6 - Diagram reporting the position of studied samples on a reconstructed model of the platform, based on sedimentological and ostracod analyses (modified from Del Piero et al. in prep.).

from WH227, 235 to 234.

- Assemblages WH232 and WH259, obtained from Involutoidea-rich limestone, represent the climax of this trend associated with relatively restricted conditions.

- Although incomplete, the assemblage WH236 records the more proximal conditions (brackish?), possibly relatively littoral, with the presence of *Limnocytheridae*. This conclusion is in line with lighter values of organic carbon that possibly point to more terrestrial influence (Del Piero et al. in prep.).

### Palaeobiogeographic analysis

Our understanding of the provincialism of marine ostracods during the Triassic is still expanding. Kozur (1973b) distinguished southern boreal, tethyan and northern boreal provinces for Triassic conodonts and ostracods while others considered that the distribution of fossil groups, including ostracods, became homogeneous within the Tethys starting in the Anisian (Kristan-Tollmann & Tollmann 1981, 1982; Kristan-Tollmann 1986, 1988a, b, 1991). In a recent summary, Forel & Crasquin (2020) have shown that the distribution of ostracods was very dynamic in the Triassic, with distinct peri-palaeotethyan and peri-neotethyan biotas in the Early Triassic, followed by a dispersal and a relative

homogenisation from the Anisian onwards. Conversely, a new dating of the opening of communications between the Neo-Tethys and Palaeo-Tethys oceans in the early Carnian (Forel & Moix 2020) rather than middle Carnian as previously thought (e.g. Stampfli & Kozur, 2006; Moix et al. 2007, 2008, 2013) highlights the necessity to investigate the link between this event and the onset of homogenisation of ostracod faunas. Three main hypotheses have been considered for the origin of Mesozoic tethyan ostracods (see Forel & Moix 2020 for further details and references): a western American origin considering a radiation in western America and subsequent trans-Panthalassic migration; a western Tethys origin with European Province as the radiation place for most of the Mesozoic taxa and an eastern Tethys origin for several other taxa (e.g. Kristan-Tollmann 1993; Ketmuangmoon et al. 2018; Forel et al. 2019a).

To investigate the faunal relationship and global palaeobiogeographic patterns during the Norian, we produced a similarity symmetric matrix of genera that has been treated and analysed as described earlier. The history of palaeobiogeographic relationships of marine ostracods in the Triassic has been described in Forel & Crasquin (2020) and the observations for the Norian stage are here refined. The resulting UPGMA dendrogram (Fig. 7A) shows

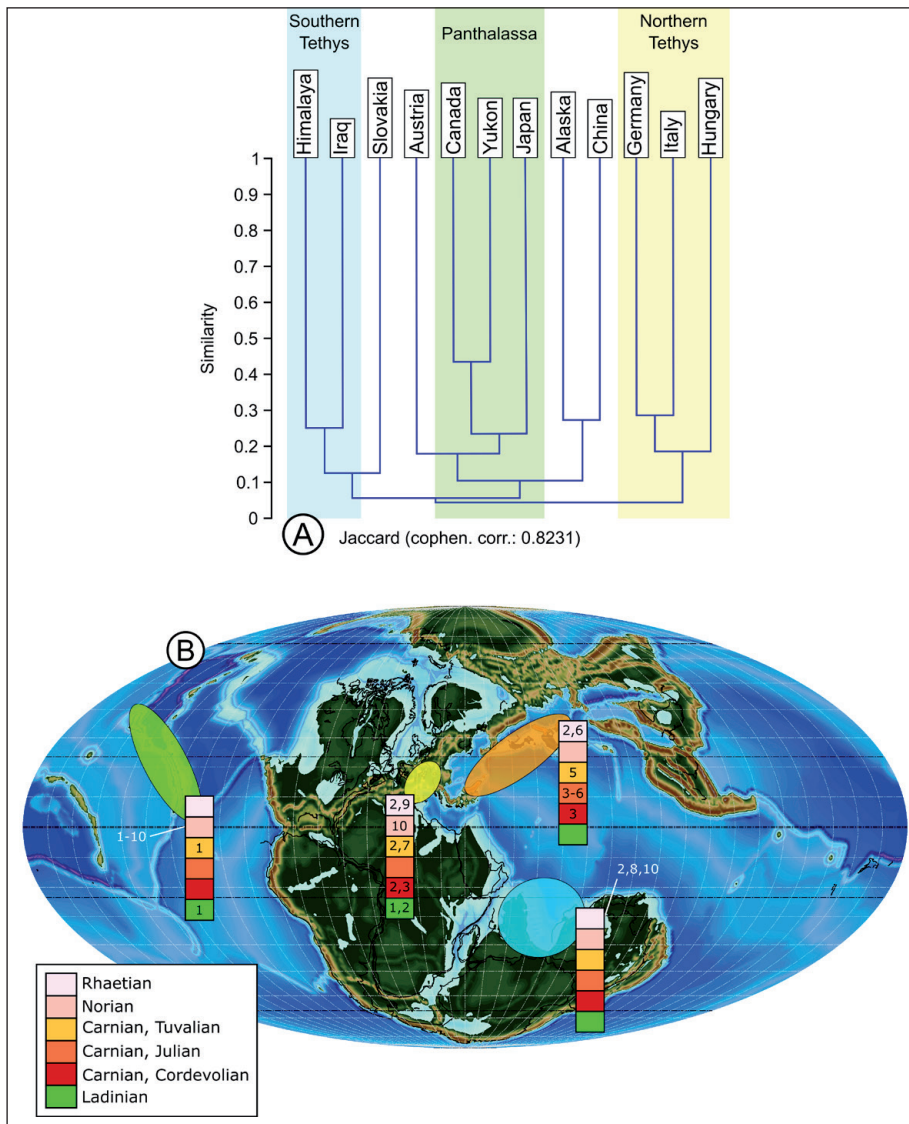


Fig. 7 - A) Dendrogram of UPGMA analysis based on diverse localities for the Norian (generic analysis). B) Palaeogeographic map of the Norian, Late Triassic, showing the geographical and temporal distribution of the species found at Lime Peak. The map was generated from the preliminary version of the Panalexis model (Vérard, 2019). In this model, global tectonic maps have been converted into paleo-DEMs (Digital Elevation Models or 3D surface maps) following the method described in Vérard et al. (2015). Palaeogeographic areas: northern Tethys (yellow), Cimmeria (orange), south-eastern Tethys (blue), eastern Panthalassa (green). 1: *Leviella sobni* Kozur, 1974; 2: *Hiatobairdia subsymmetrica* Kristan-Tollmann, 1970; 3: *Polycopse pumicosa schleiferae* Kozur in Bunza & Kozur, 1971; 4: *Bairdia* sp. 7 in Forel et al., 2019b; 5: *Bairdiacypris sorgunensis* Forel in Forel et al., 2018; 6: *Judabella dizjuense* Kristan-Tollmann in Kristan-Tollmann et al., 1980; 7: *Bairdia taan* Forel n. sp.; 8: *Bairdia* sp. A in Dépêche & Crasquin-Soleau, 1992; 9: *Judabella nodosa nodosa* (Kozur in Bunza & Kozur, 1971 *sensu* Kristan-Tollmann 1989); 10: *Leviella unicostata* (Bolz, 1970).

a rather low cophenetic correlation index of 0.82, indicating that it does not perfectly describe the similarities among assemblages. The dendrogram documents the individualization of 3 important clusters corresponding to Panthalassan localities (British Columbia, Yukon, Japan), Northern Tethys (Germany, Italy, Hungary) and Southern Tethys (Himalaya, Iraq). As expected, the Lime Peak assemblage is more related to the one previously reported from Canada (British Columbia) than to any other assemblage. The individualization of the Panthalassa cluster documents the relationship between eastern Panthalassa and Japan. The link observed between Austrian assemblages and the Panthalassic group fuels discussion on transoceanic Tethyan-Panthalassic faunal migration in the Late Triassic (e.g. Kristan-Tollmann 1988a, b; Peybernes et al. 2016; Forel & Crasquin 2020; Forel & Moix

2020). Conversely, the weaker similarity between Panthalassic group and Alaska raises questions that request investigations of additional localities, complementary quantitative methods and comparison with other taxonomic groups.

As shown in the systematic palaeontology part of this work, ten species found in the Norian of Lime Peak are known from other areas in the Triassic (not considering *Ptychobairdia?* sp. in Arias & Lord, 2000 that is restricted to the Norian of Canada reported by Arias & Lord, 2000): *Bairdia taan*, *B. sp. 7* in Forel et al., 2019b, *B. sp. A* in Dépêche & Crasquin-Soleau, 1992, *Bairdiacypris sorgunensis*, *Hiatobairdia subsymmetrica*, *Judabella dizjuense*, *J. nodosa nodosa*, *Leviella sobni*, *L. unicostata*, *Polycopse pumicosa schleiferae*. To explore their distribution through time and space, they have been grouped into 4 areas: northern Tethys, Cimmeria, south-eastern Te-

thys and eastern Panthalassa (Fig. 7B). *L. sobni* was present in eastern Panthalassa as early as the Ladinian and co-occurred in northern Tethys, implying that this species radiated earlier but its place of origin and the direction of its subsequent dispersal remain unknown. The record of *L. sobni* in the Norian of Lime Peak is the last known occurrence of this species. Conversely, several of these species may have radiated during the Carnian in northern Tethys (*Hiatobairdia subsymmetrica*, *Polycope pumicosa schleiferae*, *Bairdia taan*) and Cimmeria (*Bairdia* sp. 7 in Forel et al., 2019b; *Bairdiacypris sorgumensis*; *Judabella dizluense*) before they migrated to eastern Panthalassa, although Carnian data are scarce in Panthalassa with only isolated specimens reported by Sohn (1987). Only *Judabella nodosa nodosa* may have radiated on the eastern part of Panthalassa before it migrated to the Tethyan area where it is only known from the Rhaetian. This preliminary observation of the Triassic fluxes of species seems very unbalanced with a stronger influx from the Tethys to the Panthalassa. However, this pattern may be partly (or entirely) modified by the addition of new data from the Triassic of the eastern Panthalassa and other regions, especially regarding the Ladinian and Carnian.

An observation at the generic level is here important to make. As detailed in the systematic palaeontology part, *Alatobairdia* is rare and only known from the Rhaetian of western Tethys: if *Alatobairdia? sobni* is proved to be a distinct genus, it may be a precursor of *Alatobairdia* that may have radiated from *Bairdiolites* on the eastern side of the Panthalassa in the Norian and later migrated towards Tethys. Further data from other Middle and Upper Triassic Panthalassan localities are needed to confirm whether this apparent trend is due to sampling bias or is reflecting real dispersal fluxes.

### Phytoplankton ostracods in the Norian?

*Phytoplankton ostracods: a state of the art.* In modern marine environments, most reported phytoplankton taxa are Cytheroidea, such as *Xestoleberis*, *Loxoconcha*, *Paradoxostoma* (e.g. Hartmann 1953; Athersuch 1979; Forsey 2016). Bairdiidae as part of phytoplankton assemblages have been documented for instance by Athersuch (1979) from filamentous (*Cystoseira*, *Caulerpa*), seagrass (*Posidonia*, *Zostera*) and encrusting algae of Cyprus. In shallow water tropical regions, *Neonesidea*, *Bairdoppilata* and *Paranesidea* are

considered characteristic members of epifaunal assemblages living today on marine algae and grasses associated with reefal areas in New Caledonia, Africa, Australia, Hawaii, French Polynesia (e.g. Maddocks 1969, 2015; Hartmann 1974, 1978, 1979, 1980, 1981, 1984; Hartmann-Schröder & Hartmann 1974).

The importance of algae and seagrasses on the distribution of ostracods has been abundantly discussed (e.g. Colman 1940; Dahl 1948; Wieser 1952; Reys 1963; Hagerman 1966, 1968, 1969; Whatley & Wall 1969, 1975; Athersuch 1979; Johnson & Scheibling 1987; Kamiya 1988a; Frenzel et al. 2005; Frame et al. 2007; Forsey 2016). In modern environments, the ostracods/algae relationship is complex and the occurrence and distribution of phytoplankton ostracods are related to the morphology and seasonal development of the algae, sediment content, tidal height and wave exposure in intertidal zone (e.g. Whatley & Wall 1975; Horne 1982; Hull 1999). It has been proposed that calcareous algae are preferred over seagrass or other kinds of algae that offer only little protection (Elofson 1941; Whatley & Wall 1975; Athersuch 1979). Only a few species are restricted to a single type of algae but ostracod communities from different algae types can be distinguished by their relative abundance (e.g. Whatley & Wall 1975; Hull 1997, 1998; Frame et al. 2007). In general, higher abundances are observed with algal types that offer structurally complex microenvironments (e.g. Whatley & Wall 1975; Athersuch 1979; Hull 1997; Frame et al. 2007): algal complexity may provide larger surfaces on which to feed and live and shelter against predation, desiccation and wave action (e.g. Elofson 1941; Hagerman 1966; Whatley & Wall 1975; Coull & Wells 1983; Hicks 1986; Hull 1997). For instance, *Corallina* is thought to provide a protection against fish predators (Coull & Wells 1983). Phytoplankton ostracods graze on bacteria and micro-algae, especially diatoms that grow epiphytically on seaweeds (Elofson 1941; Whatley & Wall 1975; Athersuch 1979). The major food resource of the phytoplankton genus *Paradoxostoma* found on the calcareous algae *Corallina* is composed of diatoms and bacteria associated with the algae (Whatley & Wall 1975) and diatoms have been observed from the stomach of phytoplankton ostracods *Xestoleberis* and *Loxoconcha* (Hagerman 1966). In the littoral zone, the ostracod assemblages from sediment are generally less diverse and less abun-

dant than phytal ones (Hull 1998); in other cases, such as littoral environments of Cyprus, calcareous algae support relatively few but abundant ostracod species (Athersuch 1979). When considering the association of ostracods and calcareous algae, the distribution of species in association with *Corallina* in the intertidal zone is affected by the tide height, the development of instars being faster at high tidal level (Horne 1982).

Phytal ostracods show specialized adaptations, for instance in *Paradoxostoma* that has specialised piercing mouthparts that may be used for feeding on algal sap (Horne & Whittaker 1985). *Loxococoncha* species are also well adapted to their habitat with morphological, ethological adaptations (Kamiya 1988a), adaptation in the mating system (Kamiya 1988c) and population ecology (Kamiya 1988b). Phytal and bottom-dwelling *Loxococoncha* species have distinct morphologies of sieve-pores and distribution of sensory seta that are denser in the ventral area of bottom-dwelling species (Kamiya 1989). Morphological differences include round carapaces with a convex ventral area in phytal species developed on *Zostera* beds and elongate carapaces with flat ventral area in bottom-dwelling species (Kamiya 1988a). Phytal species from *Zostera* beds display important seasonal variation of their diversity with major increase in early summer, while bottom-dwelling species have a much more constant population density through the year (Kamiya 1988b). In sub-fossil assemblages, Kamiya (1988b) furthermore shows that the age structure of the bottom-dwelling and phytal species is different with a much higher juvenile ratio for phytal species, implying that it is more prolific with higher mortality. Noteworthy, no in-depth analysis has ever been performed so far on bairdiids associated with algae in modern tropical environments.

In the fossil record, phytal ostracod assemblages associated with seagrasses have been proposed by Forsey (2016) in the Cretaceous with *Bairdia*, *Bairdoppilata*, *Loxococoncha*, *Xestoleberis* (Campanian; Benson & Tatro 1964; Maastrichtian, Piovesan et al. 2009), Miocene with *Aurila*, *Bairdia*, *Loxococoncha*, *Xestoleberis* (Crespin 1943; Bossio et al. 2006) and Pliocene with *Aurila*, *Bairdoppilata*, *Hemicytherura*, *Loxococoncha*, *Paradoxostoma*, *Xestoleberis* (Swain 1974; Moissette et al. 2007). In all these assemblages, bairdiids are accessory components and Forsey (2016) considered that most of these seagrass records are not convincing.

*The case of Lime Peak.* In the Norian of Lime Peak, two types of ostracod-algae associations are observed:

- three assemblages obtained from dasy-cladales *Holosporella*-rich limestones: WH227, 335, 334, in increasing order of environmental restriction according to the previous discussion,
- two assemblages from Involutinoidea and organic-rich limestone with abundant weakly calcified green algae (i.e. abundance of *Patruluspora pacifica*, see Bocur et al. 2020): WH232 and WH259.

As detailed above, the similarity analysis with regard to the ostracod composition of all studied assemblages documents the uniqueness of the ostracod-algae assemblages, both at the generic and species levels (Fig. 5). In terms of families and genera, the Involutinoidea-rich assemblages provided no endemic taxa, and only Bythocytheridae (*Patellacythere?*) as well as an unidentified Cytheroidea are restricted to *Holosporella*-rich assemblages (WH227 and WH234 respectively; Fig. 3A, Tab. 1). No species is restricted to Involutinoidea-rich assemblages while 15 species are restricted to *Holosporella*-rich ones: *Bairdia* sp. 2, *B.* sp. 8, *B.* sp. 9, *Carinobairdia?* sp., *Hiatobairdia* cf. *senegasi* Forel in Forel et al., 2019a, *Isobythocypris?* sp. 2, *Ptychobairdia?* sp. in Arias & Lord, 2000, *Pt.* cf. *veguae* (Kozur, 1971b), *Paracypris?* sp. 2, *Pa.* sp. 4, *Patellacythere?* sp., *Lutkevichinella?* sp., *Cardobairdia?* sp. 2, *Leviella* sp. 1, Cytheroidea gen. et sp. indet. Only *Cytherella* sp. 2 is restricted to the two types of ostracod-algae assemblages. The  $\Delta^+$  index of the 2 ostracod-algae associations (WH234 and 235) are similar in being above the mean value of all investigated assemblages, with the exception of WH227 (Fig. 3C). The  $H'$  values of *Holosporella*-rich assemblages are the highest with the exception of silicified assemblages OST6 and 7, possibly because of (i) important preservation potential of silicification, (ii) transportation although considered as not sufficient to affect palaeoenvironment inference, (iii) diverse micro-environments associated with sponge reefs in OST6. In contrast,  $H'$  values of Involutinoidea-rich assemblages are among the lowest of this study. This major discrepancy as to  $H'$  may illustrate the distinct algal associations and/or the palaeoenvironmental differences including the possible environmental restriction invoked previously for Involutinoidea-rich samples. Only the analysis of additional samples will allow us to go further into this comparison. The high-taxonomic

level diversification remains a noticeable feature of all algal-ostracod assemblages from the Norian of Lime Peak, possibly witnessing the structural complexity of associated microenvironments. The important diversity at high taxonomic levels described above might, in the case of *Holosporella*-rich samples, be further increased by the restriction trend described from WH227 to WH234. It therefore seems that at Lime Peak, a complex overprinting of signals occurs: a signal of diversity affected by microenvironments associated with algae (Fig. 3C) and a signal of restriction and more generally of palaeoenvironment illustrated for instance by the increase in Cytherellidae and decrease in Bairdiidae from WH227 to WH234 (Fig. 3A).

*Holosporella*-rich samples (WH227, 234, 235) provided rich communities that include *Holosporella* calcified green algae, endobenthic foraminifera, molluscs, gastropods (see Del Piero et al. in prep for in-depth details), possibly involving a multi-layered trophic chain. Unfortunately, the preservation of ostracod specimens does not allow distinguishing possible predation marks, as was done in the Carnian of Turkey (Forel et al. 2018), and to further discuss a possible shelter role of *Holosporella* against predation. It is nevertheless important to notice that thick-shelled ornate Bairdiidae *Alatobairdia?*, *Cornutobairdia* and *Mirabairdia* are absent from these ostracod-algal associations: this observation is reminiscent of modern *Triebelina* that are characteristic of reefs (e.g. Maddocks 1969). All these observations imply that already in the Norian, Bairdiidae were associated with algae and that ornate forms, except for those offshore forms discussed above, may have preferentially been reef-dwellers although it remains obscure whether modern ornate Bairdiidae are lineal descendants of Triassic forms (e.g. Maddocks & Wouters 1990).

## CONCLUSIONS

Ostracods of Norian age, Late Triassic, have been retrieved from samples collected from Lime Peak in the Whitehorse area, Yukon Territory, Canada. They constitute the first complete assemblages so far reported from this area and contribute to fill in the stratigraphic and geographical gaps in the current knowledge of Triassic ostracods. In total, 90 species representing 31 genera and 11 families

are reported, including 9 new species. The analysis of the assemblages composition allowed the refinement of palaeoenvironmental reconstructions, all illustrating a relatively large variety of neritic conditions. The calculation of diversity indices (Shannon diversity and Taxonomic Distinctness) and similarity of assemblages as regard to their generic and species composition demonstrates the distinctness between reef-associated and algae-associated assemblages. The close association of Bairdiidae and algae reported in modern tropical zones appears to have been already established in the Norian, with most ornate forms restricted to reefal conditions. A palaeogeographic analysis identifies a faunal link during the Norian between eastern and western (Japanese terranes) Panthalassa, in line with studies on other taxa. The analysis of widely distributed ostracod species documents an unbalanced flux from Tethyan areas to eastern Panthalassa, but this pattern should be further confirmed by adding to the dataset additional assemblages, especially from the eastern Panthalassic area.

*Acknowledgements:* The first author is deeply grateful to Prof. Dr. Alan Lord (Senckenberg Museum) for his constant availability and for discussion on *Alatobairdia? sobni*. The field mission, allowing the collection of the samples used for the presented research, has been fully financed by the Swiss National Science Foundation, as a part of the REEFCADE long-term project (Grants number 200020\_156422 and 200020\_178908 by R.M.). Sampling in the Yukon was conducted under the Yukon-Canada Scientists and Explorers Act license number 17-60S&E; the authors acknowledge the Government of the Yukon as well as Kwanlin Dün and Ta'an Kwäch'an First Nations for granting us the access to their lands. The authors acknowledge Christian Vérard for his valuable help with the palaeogeographic map and Agathe Martignier for her technical support with the scanning electron microscope. Dr. Maria Cristina Cabral (University of Lisbon, Portugal) and an anonymous reviewer are thanked for their thorough reading and detailed comments that greatly improved an earlier version of this manuscript.

## REFERENCES

- Aberhan M. (1999) - Terrane history of the Canadian Cordillera: Estimating amounts of latitudinal displacement and rotation of Wrangellia and Stikinia. *Geological Magazine*, 136: 481-492.
- Anderberg M.R. (1973) - Cluster Analysis for Applications. Academic Press, 359 pp.
- Arias C. & Lord A. (2000) - Upper Triassic Marine Ostracoda from the Queen Charlotte Islands, British Columbia, Canada. *Revista Española de Micropaleontología*, 32: 175-192.
- Athersuch J. (1979) - The ecology and distribution of the littoral ostracods of Cyprus. *Journal of Natural History*, 13: 135-160.

- Baird W. (1845) - Arrangement of the British Entomostraca, with a list of species, particularly noticing those which have as yet been discovered within the bounds of the club. *Transaction of Berwickshire Naturalists' Club*, 2: 145-158.
- Baird W. (1850) - Description of several new species of Entomostraca. *Annals and Magazine of Natural History*, 2 (10): 56-59.
- Ballent S.C. & Whatley R. (2000) - The composition of Argentinian Jurassic marine ostracod and foraminiferal faunas: environment and zoogeography. *Geobios*, 33(3): 365-376.
- Ballent S.C. & Whatley R. (2009) - Taxonomy and zoogeography of the Mesozoic cytherurid ostracod from west-central Argentina. *Palaeontology*, 52(1): 193-218.
- Baroni-Urbani C. & Buser M.W. (1976) - Similarity of binary data. *Systematic Zoology*, 25: 251-259.
- Bate R.H. (1977) - Jurassic Ostracoda of the Atlantic Basin. In: Swain F.M. (Eds) - Stratigraphic micropaleontology of Atlantic basin and borderlands: 231-244. New York, Elsevier Scientific Pub. Co. Amsterdam.
- Becker G. (2002) - Contributions to Palaeozoic Ostracod Classification [POC], no. 24, Palaeozoic Ostracoda: the standard classification scheme. *Neues Jahrbuch für Geologie und Paläontologie, Abhandlungen*, 226: 165-228.
- Belasky P., Stevens C.H. & Hanger R.A. (2002) - Early Permian location of western North American terranes based on brachiopod, fusulinid, and coral biogeography. *Palaeogeography, Palaeoclimatology, Palaeoecology*, 179: 245-266.
- Benson R.H. & Tatro J.O. (1964) - Faunal description of Ostracoda of the Marlbrook Marl (Campanian), Arkansas. *University of Kansas Paleontological Contributions*, Article 37 Arthropoda 7: 1-32.
- Beranek L.P. & Mortensen J.K. (2011) - The timing and provenance record of the Late Permian Klondike orogeny in northwestern Canada and arc-continent collision along western North America. *Tectonics* 30, TC5017.
- Bocur I., Rigaud S., Del Piero N., Fucelli A., Heerwagen E., Peybernes C., Peyrotty G., Verard C., Chablais J. & Martini R. (2020) - Upper Triassic calcareous algae from the Panthalassa Ocean. *Rivista Italiana di Paleontologia e Stratigrafia*, 126 (2): 499-540.
- Bolz H. (1969) - Der "bairdoppilate" Verschluss und Skulptur-Unterschiede bei Bairdien (Ostrac.) der alpinen Obertrias. *Senckenbergiana Lethaea*, 50: 411-431.
- Bolz H. (1970) - Einige *Cytherelloidea*-Arten (Ostrac.) aus der alpinen Obertrias. *Senckenbergiana Lethaea*, 51(2/3): 239-263.
- Bolz H. (1971a) - Late Triassic Bairdiidae and Healdiidae. In: Oertli, H.J. (Eds) - Paléocologie des Ostracodes. *Bulletin du Centre de Recherche, SNPA*, 5 (Supplement): 717-745.
- Bolz H. (1971b) - Die Zlambach-Schichten (alpine Obertrias) unter besonderer Berücksichtigung der Ostrakoden, 1: Ostrakoden der Zlambach-Schichten, besonders Bairdiidae. *Senckenbergiana Lethaea*, 52: 129-283.
- Boomer I. & Jellinek T. (1996) - On *Ogmoconcha contractula* Triebel. *Stereo-Atlas of Ostracod Shells* 23 (13): 53-60.
- Boomer I., Horne D.J. & Slipper I.J. (2003) - The use of ostracods in palaeoenvironmental studies or what can you do with an Ostracod shell? *Palaeontological Society Papers*, 9: 153-179.
- Bordet E. (2016) - Preliminary results on the Middle Triassic-Middle Jurassic stratigraphy and structure of the Teslin Mountain area, southern Yukon. In: MacFarlane K.E. & Nordling M.G. (Eds) - Yukon Exploration and Geology 2015: 43-61. Yukon Geological Survey.
- Bordet E. (2017) - Updates on the Middle Triassic-Middle Jurassic stratigraphy and structure of the Teslin Mountain and east Lake Laberge areas, south-central Yukon. In: MacFarlane K.E. & Nordling M.G. (Eds) - Yukon Exploration and Geology 2016: 1-24. Yukon Geological Survey.
- Bordet E., Crowley J.L. & Piercey S.J. (2019) - Geology of the eastern Lake Laberge area (105E), south-central Yukon (No. 2019-1), Open File.
- Bossio A., Dall'Antonia B., Da Prato S., Foresi M. L. & Oggiario G. (2006) - Preliminary stratigraphical investigations on the Miocene successions of the Porto Torres Basin (Northern Sardinia, Italy). *Atti Società Toscana di Scienze Naturali, Memorie, Serie A*, 111: 67-74.
- Bradfield H.H. (1935) - Pennsylvanian Ostracoda of Ardmore Basin, Oklahoma. *Bulletin of American Paleontology* 22: 1-145.
- Bunza G. & Kozur H. (1971) - Beiträge zur Ostracodenfauna der tethyalen Trias. *Geologisch-Paläontologische Mitteilungen Innsbruck*, 1: 1-76.
- Cheetham, A.H., Hazel, J.E. (1969) - Binary (presence-absence) similarity coefficients. *Journal of Paleontology*, 43: 1130-1136.
- Colman J. (1940) - The nature of the intertidal zonation of plants and animals. *Journal of the Marine Biological Association of the United Kingdom*, 18: 435-476.
- Colpron M. & Nelson J.L. (2011) - A Digital Atlas of Terranes for the Northern Cordillera, BCGS GeoFile 2011-11.
- Colpron M., Nelson J.L. & Murphy, D.C. (2007) - Northern Cordilleran terranes and their interactions through time. *GSA today*, 17: 4-10.
- Coney P.J., Jones D.L. & Monger J.W.H. (1980) - Cordilleran suspect terranes. *Nature*, 288: 329-333.
- Coull B.C. & Wells J.B.J. (1983) - Refuges from fish predation experiments with phytal meiofauna from the New Zealand rocky intertidal. *Ecology*, 64: 1599-1609.
- Crasquin S. & Forel M.-B. (2014) - Ostracods (Crustacea) through Permian-Triassic events. *Earth-Science Reviews*, 137: 52-64.
- Crasquin S., Sciuto F. & Reitano A. (2018) - Late Carnian (Tuvalian, *Tropites dilleri* zone) ostracods (Crustacea) from the Mufara Formation (Monte Scalpello, Central-Eastern Sicily, Italy). *Annales de Paléontologie*, 104(2): 129-142.
- Crasquin S., Sciuto F., Reitano A. & Coco R.M. (2020) - Late Triassic (Tuvalian-Carnian, *Tropites subbullatus*/*Anatropites spinosus* zones) ostracods from Monte Gambanera (Castel di Iudica, Central-Eastern Sicily, Italy). *Bulletin de la Société Géologique de France*, 191(36).
- Crasquin-Soleau S., Vaslet D. & Le Nindre Y.M. (2005) - Ostracods as markers of the Permian/Triassic boundary in Khuff Formation of Saudi Arabia. *Palaeontology*, 48:

853-868.

- Crespin I. (1943) - Report on a collection of fossils from the Lakes Entrance shaft, Gippsland, Victoria. *Bureau of Mineral Resources, Geology and Geophysics Commonwealth of Australia*, 9: 1-4.
- Croneis C. & Gale A.S. (1939) - New ostracodes from the Golconda formation. *Denison University Bulletin, Science Laboratories*, 33: 251-295.
- Dahl E. (1948) - On the smaller Arthropoda of marine algae, especially in the polyhaline waters off the Swedish west coast. *Undersökningar Över Öresund*, 35: 1-193.
- Dépêche F. & Crasquin-Soleau S. (1992) - 26. Triassic marine ostracodes of the Australian margin (Holes 759B, 760B, 761C, 764A and 764B). *Proceedings of the Ocean Drilling Program, Scientific Results*, 122: 453-462.
- Digby P.G.N. & Kempton, R. (1987) - Multivariate Analysis of Ecological Communities. Chapman & Hall, 206 pp.
- Dubovsky N.W. (1939) - Zur Kenntnis der Ostracoden fauna des Schwarzen Meeres. *Trudy Krardagskoj Biol. Stencil*, 5: 1-68.
- Elofson O. (1941) - Zur Kenntnis der marinen Ostracoden Schwedens mit besonderer Berücksichtigung des Skagerraks. *Zoologiska Bidrag Fran Uppsala*, 19: 215-534. (Marine Ostracoda of Sweden with special consideration of the Skagerrak, Translation from German into English, 1969. Israel Program for Scientific Translations, 286 pp).
- Egorov V.G. (1950) - Ostracodes from the Frasnian stage of the Russian Platform. Part 1: Kloedenellidae. *Trudy VN-IGRI*: 1-175.
- Forel M.-B. & Crasquin S. (2020) - Bounded by crises: an updated view of the evolution of marine ostracods during the Triassic. *Marine Micropaleontology*, <https://doi.org/10.1016/j.marmicro.2020.101925>
- Forel, M.-B. & Grădinaru E. (2020) - Rhaetian (Late Triassic) ostracods from the offshore prolongation of North Dobrogean Orogen into the Romanian Black Sea Shelf. *European Journal of Taxonomy*, 727(1): 1-83.
- Forel M.-B. & Moix, P. (2020) - Late Triassic Ostracods from the Lycian Nappes, Southwestern Turkey: Implications on Taxonomy and Palaeobiogeographical Distribution. *Bulletin de la Société Géologique de France* 191(30).
- Forel M.-B., Ozsvárt P. & Moix P. (2018) - Carnian (late Triassic) ostracods from the Sorgun Ophiolitic Mélange (Southern Turkey): Taxonomy, palaeoenvironment and evidence of predation. *Palaeontologia Electronica*, 21.2 (26A): 1-23.
- Forel M.-B., Thuy B. & Wisshak M. (2019a) - Digging into the ancestral stocks of Jurassic lineages: ostracods (Crustacea) from Carnian (late Triassic) sponge mounds from the Maantang Formation (South China). *Bulletin de la Société Géologique de France*, 190(9).
- Forel M.-B., Tekin U.K., Okuyucu C., Bedi Y., Tuncer A. & Crasquin S. (2019b) - Discovery of a long-term refuge for ostracods (Crustacea) after the end-Permian extinction: a unique Carnian (late Triassic) fauna from the Mersin Mélange, southern Turkey. *Journal of Systematic Palaeontology*, 17: 9-58.
- Forel M.-B., Kolar-Jurkovšek T. & Jurkovšek B. (2020) - Ostracods from the "Raibl Beds" (Carnian, Late Triassic) of Belca section in Karavanke Mountains, northwestern Slovenia. *Geodiversitas*, 42(21): 377-407.
- Forel M.-B. (in press) - Thoughts on the Late Paleozoic-Early Mesozoic records of deep-sea ostracods. *Micropaleontology*.
- Forsey, G.F. (2016) - Ostracods as proxies for past seagrass: A review. *Palaeogeography, Palaeoclimatology, Palaeoecology*, 447: 22-28.
- Frame K., Hunt G. & Roy K. (2007) - Intertidal meiofaunal biodiversity with respect to different algal habitats: a test using phytal ostracodes from Southern California. *Hydrobiologia*, 586: 331-342.
- Frenzel P., Henkel D., Siccha M. & Tschendel L. (2005) - Do ostracod associations reflect macrophyte communities? A case study from the brackish water of the southern Baltic Sea coast. *Aquatic Sciences*, 67: 142-155.
- Fürsich F.T. & Wendt J. (1977) - Biostratigraphy and Palaeoecology of the Cassian Formation (Triassic) of the Southern Alps. *Palaeogeography, Palaeoclimatology, Palaeoecology*, 22: 257-323.
- Golding M.L. (2019) - Evaluating tectonic models for the formation of the North American Cordillera using multivariate statistical analysis of Late Triassic conodont faunas. *Palaeobiodiversity and Palaeoenvironments*, 100: 135-149.
- Golding M.L., Mortensen J.K., Ferri F., Zonneveld J.P. & Orchard M.J. (2016a) - Determining the provenance of Triassic sedimentary rocks in northeastern British Columbia and western Alberta using detrital zircon geochronology, with implications for regional tectonics. *Canadian Journal of Earth Sciences*, 53: 140-155.
- Golding M.L., Mortensen J.K., Zonneveld J.P. & Orchard, M.J. (2016b) - U-Pb isotopic ages of euhedral zircons in the Rhaetian of British Columbia: Implications for Cordilleran tectonics during the Late Triassic. *Geosphere*, 12: 1606-1616.
- Gümbel C.W. (1869) - VII. Ueber Foraminiferen, Ostracoden und mikroskopische Thier-Ueberreste in den St. Cassianer und Raibler Schichten. *Jahrbuch der kaiserlich-königlichen geologischen Reichsanstalt*, 10: 175-186.
- Hagerman L. (1966) - The macro-and micro-fauna associated with *Fucus serratus* L., with some ecological remarks. *Ophelia*, 3(3): 1-43.
- Hagerman L. (1968) - The ostracod fauna of *Corallina officinalis* L. in western Norway. *Sarsia*, 36: 49-54.
- Hagerman L. (1969) - Environmental factors affecting *Hirschmannia viridis* O. F. Müller (Ostracoda) in shallow brackish water. *Ophelia*, 7: 79-99.
- Hammer Ø. & Harper D.A.T. (2005) - Paleontological data analysis. Blackwell, 351 pp.
- Hammer Ø., Harper D.A.T. & Ryan P.D. (2001) - PAST: Paleontological Statistics software package for education and data analysis. *Palaeontologia Electronica*, 4: 9.
- Harloff J. (1993) - Ostracoden des Unter-Pliensbachiums in Baden-Württemberg. *Stuttgarter Beiträge zur Naturkunde, Serie B, Geologie und Paläontologie*, 191: 1-214.
- Harlton B.H. (1933) - Micropaleontology of the Pennsylvanian Johns Valley Shale of Ouachita Mountains, Okla-

- homa and its relationships to the Mississippian Caney Shale. *Journal of Paleontology*, 7: 3-29.
- Hartmann G. (1953) - Les ostracodes de la zone d'algues de l'eulittoral de Banyuls. *Vie et Milieu, Observatoire Ocanologique, Laboratoire Arago*, 4(4): 608-612.
- Hartmann G. (1974) - Zur Kenntnis des Eulitorals der afrikanischen Westkste zwischen Angola und Kap der Guten Hoffnung und der afrikanischen Ostkste von Sdafrika und Moambique unter besonderer Bercksichtigung der Polychaeten und Ostracoden. Teil III. Die Ostracoden des Untersuchungsgebietes. *Mitteilungen aus dem Hamburgischen Zoologischen Museum und Institut, Ergnzungsband*, 69: 229-520.
- Hartmann G. (1978) - Teil 1. Die Ostracoden der Ordnung Podocopida G.W. Mller, 1894 der tropisch-subtropischen Westkste Australiens (Zwischen Derby im Norden und Perth im Sden). *Mitteilungen aus dem Hamburgischen Zoologischen Museum und Institut*, 75: 63-219.
- Hartmann G. (1979) - Teil 3. Die Ostracoden der Ordnung Podocopida G.W. Mller 1894 der warm-temperierten (antiborealen) West- und Sdwestkste Australiens (zwischen Perth im Norden und Eucla im Sden). *Mitteilungen aus dem Hamburgischen Zoologischen Museum und Institut*, 76: 219-301.
- Hartmann G. (1980) - Teil 5. Die Ostracoden der Ordnung Podocopida G.W. Mller 1894 der warmtemperierten und subtropisch-tropischen Kstenabschnitte der Sd- und Sdostkste Australiens (zwischen Ceduna im Westen und Lakes Entrance im Osten). *Mitteilungen aus dem Hamburgischen Zoologischen Museum und Institut*, 77: 111-204.
- Hartmann G. (1981) - Teil 7. Die Ostracoden der Ordnung Podocopida G.W. Mller, 1894 der subtropisch-tropischen Ostkste Australiens (zwischen Eden im Sden und Heron-Island im Norden). *Mitteilungen aus dem Hamburgischen Zoologischen Museum und Institut*, 78: 97-149.
- Hartmann G. (1984) - Zur Kenntnis der Ostracoden der polynesischen Inseln Huahin (Gesellschaftsinseln) und Rangiroa (Tuamotu-Inseln) mit Bemerkungen zur Verbreitung und Ausbreitung litoraler Ostracoden und einer bersicht ber die bislang auf den pazifischen Inseln gefundenen Arten. *Mitteilungen aus dem Hamburgischen Zoologischen Museum und Institut*, 81: 117-169.
- Hartmann-Schrder G. & Hartmann G. (1974) - Zur Kenntnis des Eulitorals der afrikanischen Westkste zwischen Angola und Kap der Guten Hoffnung und der afrikanischen Ostkste von Sdafrika und Moambique unter besonderer Bercksichtigung der Polychaeten und Ostracoden. Teil I. Beschreibung der Lebensrume, kologie und Zoogeographie. *Mitteilungen aus dem Hamburgischen Zoologischen Museum und Institut, Ergnzungsband*, 69: 5-94.
- Hausmann I.M. & Ntzel A. (2015) - Diversity and palaeoecology of a highly diverse Late Triassic marine biota from the Cassian Formation of north Italy. *Lethaia*, 48: 235-255.
- Hazel J.E. (1970) - Binary coefficients and clustering in biostratigraphy. *Geological Society of America Bulletin*, 81: 3237-3252.
- Henderson R.A. & Heron M.L. (1976) - A probabilistic method of palaeobiogeographic analysis. *Lethaia*, 10: 1-15.
- Hicks G.R.F. (1986) - Meiofauna associated with rocky shore algae. In: Moore P.G. & Seed R. (Eds) - *The Ecology of Rocky Coasts*. Columbia University Press, New York, NY: 36-56.
- Hirschmann N. (1909) - Beitrag zur Kenntnis der Ostracoden fauna des Finnischen Meerbusens. *Meddelanden af Societas pro Fauna et Flora Fennica*, 35: 282-296.
- Horne D.J. (1982) - The vertical distribution of phytal ostracods in the intertidal zone at Gore Point, Bristol Channel. *Journal of Micropalaeontology*, 1: 71-84.
- Horne D.J. & Whittaker J.E. (1985) - A revision of the genus *Paradoxostoma* Fischer (Crustacea: Ostracoda) in British waters. *Zoological Journal of the Linnean Society*, 85: 131-203.
- Horne D.J., Cohen A. & Martens K. (2002) - Taxonomy, morphology and biology of Quaternary and living Ostracoda. In: Holmes J.A. & Chivas A. (Eds) - *The Ostracoda: Applications in Quaternary Research*. Geophysical Monograph American Geophysical Union, Washington, DC: 5-36.
- Hull S.L. (1997) - Seasonal changes in ostracod abundance and diversity on four species of algae with differing complexity. *Marine Ecology Progress Series*, 161: 71-82.
- Hull S.L. (1998) - The distribution and assemblage composition of the ostracod fauna (Crustacea: Ostracoda) on Filey Brigg, North Yorkshire. *Journal of Natural History*, 32(4): 501-520.
- Hull S.L. (1999) - Comparison of tidepool phytal ostracod abundance and assemblage structure on three spatial scales. *Marine Ecology Progress Series*, 182: 201-208.
- Jaccard P. (1912) - The distribution of flora in the alpine zone. *The New Physiologist*, 11: 37-50.
- Janson S. & Vegelius J. (1981) - Measures of ecological association. *Oecologia*, 4: 371-376.
- Johnson S.C. & Scheibling R.E. (1987) - Structure and dynamics of epifaunal assemblages on intertidal macroalgae *Ascophyllum nodosum* and *Fucus vesiculosus* in Nova Scotia, Canada. *Marine Ecology Progress Series*, 37(2/3): 209-227.
- Jones D.L., Silberling N.J. & Hillhouse J. (1977) - Wrangellia—A displaced terrane in northwestern North America. *Canadian Journal of Earth Science*, 14: 2565-2577.
- Kamiya T. (1988a) - Morphological and ethological adaptations of Ostracoda to microhabitats in *Zostera* beds. In: Hanai T. et al. (Eds) - *Evolutionary biology of Ostracoda, its fundamentals and applications*: 303-318. Kodansha Scientific, Tokyo.
- Kamiya T. (1988b) - Contrasting population ecology of two species of *Laxoconcha* (Ostracoda, Crustacea) in Recent *Zostera* (eelgrass) beds: adaptive differences between phytal and bottom-dwelling species. *Micropaleontology*, 34(4): 316-331.
- Kamiya T. (1988c) - Different sex-ratios in two recent species of *Laxoconcha* (Ostracoda). *Senckenbergiana Lethaea*, 68(5/6): 337-345.
- Kamiya T. (1989) - Differences between the sensory organs of phytal and bottom-dwelling *Laxoconcha* (Ostracoda,

- Crustacea). *Journal of micropalaeontology*, 8(1): 37-47.
- Ketmuangmoon P., Chitnarin A., Forel M.-B. & Těpnarop P. (2018) - Diversity and paleoenvironmental significance of Middle Triassic ostracods (Crustacea) from northern Thailand: Pha Kan Formation (Anisian, Lampang Group). *Revue de Micropaléontologie*, 61: 3-22.
- Klie W. (1938) - Ostracoda, Muschelkrebse Die Tierwelt Deutschlands und der angrenzenden Meeresteile nach ihren Merkmalen und nach ihrer Lebensweise 34 Teil: Krebstiere oder Crustacea. Gustav Fischer, Jena, pp. 1-230
- Klompaker A.A., Nützel A. & Kaim A. (2016) - Drill hole convergence and a quantitative analysis of drill holes in mollusks and brachiopods from the Triassic of Italy and Poland. *Palaeogeography, Palaeoclimatology, Palaeoecology*, 457: 342-359.
- Kollmann K. (1960) - Ostracoden aus der alpinen Trias. I *Parabairdia* n. g. und *Ptychobairdia* n. g. (Bairdiidae). *Jahrbuch der Geologischen Bundesanstalt*, 5: 79-105.
- Kollmann K. (1963) - Ostracoden aus der alpinen Trias. II Weitere Bairdiidae. *Jahrbuch der Geologischen Bundesanstalt*, 106/121\_203.
- Kornicker L.S. (1963) - Ecology and classification of Bahamian Cytherellidae (Ostracoda). *Micropaleontology*, 9(1): 61-70.
- Kozur H. (1970) - Neue Ostracoden-Arten aus dem Obersten Anis des Bakonyhochlandes (Ungarn). *Berichte des naturwissenschaftlich-medizinischen Vereins in Innsbruck*, 58: 384-428.
- Kozur H. (1971a) - Die Bairdiacea der Trias. Teil I: Skulpturierte Bairdiidae aus Mitteltriassischen Flachwasserablagerungen. *Geologisch-Paläontologische Mitteilungen Innsbruck*, 1(3): 1-27.
- Kozur H. (1971b) - Die Bairdiacea der Trias. Teil II: Skulpturierte Bairdiidae aus mitteltriassischen Teilschelfablagerungen. *Geologisch-Paläontologische Mitteilungen Innsbruck*, 1(5): 1-21.
- Kozur H. (1971c) - Die Bairdiacea der Trias. Teil III: Einige neue Arten triassischer Bairdiacea und Bemerkungen zur Herkunft der Macrocyprididae (Cypridacea). *Geologisch-Paläontologische Mitteilungen Innsbruck* 1(6): 1-18.
- Kozur H. (1973a) - Beiträge zur Stratigraphie und Paläontologie der Trias. *Geologisch-Paläontologische Mitteilungen Innsbruck*, 3(1): 1-30.
- Kozur H. (1973b) - Faunenprovinzen in der Trias und ihre Bedeutung für die Klärung der Paläogeographie. *Geologisch-Paläontologische Mitteilungen Innsbruck*, 3(8): 1-41.
- Kozur H. (1996) - Upper Triassic Punciacea, the connecting link between the Palaeozoic to Lower Triassic Kirkbyacea and the Cretaceous to Cenozoic Punciacea. *Elf Aquitaine Production, Mémoire*, 20: 257-269.
- Kozur H., Kampschuur W., Mulder-Blanken C.W.H. & Simon O.J. (1974) - Contribution to the Triassic ostracode faunas of the betic zone (southern Spain). *Scripta Geologica*, 23: 1-56.
- Kristan-Tollmann E. (1969) - Zur stratigraphischen Reichweite der Ptychobairdien und Anisobairdien (Ostracoda) in der alpinen Trias. *Geologica et Palaeontologica*, 3: 81-95.
- Kristan-Tollmann E. (1970) - Einige neue Bairdien (Ostracoda) aus der alpinen Trias. *Neues Jahrbuch für Geologie und Paläontologie Abhandlungen*, 135: 268-310.
- Kristan-Tollmann E. (1971a) - Weitere Beobachtungen an skulptierten Bairdiidae (Ostrac.) der alpinen Trias. *Neues Jahrbuch für Geologie und Paläontologie Abhandlungen*, 139: 57-81.
- Kristan-Tollmann E. (1971b) - *Torohealdia* n. gen., eine charakteristische Ostracoden-Gattung der obersten alpinen Trias. *Erdoel-Erdgas-Zeitschrift*, 87: 50-54.
- Kristan-Tollmann E. (1973) - Zur phylogenetischen und stratigraphischen Stellung der triadischen Healdiiden (Ostracoda) II. *Erdoel-Erdgas-Zeitschrift*, 89, 150-155.
- Kristan-Tollmann E. (1977a) - On the development of the muscle-scar patterns in Triassic Ostracoda. In: H. Löffler & D. Danielopol (Eds) - Proceedings of the Sixth International Symposium on Ostracoda: 133-143. Saalfelden, Salzburg.
- Kristan-Tollmann E. (1977b) - Zur Evolution des Schließmuskelfeldes bei Healdiidae und Cytherellidae (Ostracoda). *Neues Jahrbuch für Geologie und Paläontologie*, 10: 621-639.
- Kristan-Tollmann E. (1978) - Bairdiidae (Ostracoda) aus den obertriadischen Cassianer Schichten der Ruones-Wiesen bei Corvara in Südtirol. *Schriftenreihe der Erdwissenschaftlichen Kommissionen, Österreichische Akademie der Wissenschaften*, 4: 77-104.
- Kristan-Tollmann E. (1986) - Triassic of the Tethys and its relations with the Triassic of the Pacific realm. In: McKenzie K.G. (Eds) - Shallow Tethys 2: 169-186. Proceedings of the International Symposium on Shallow Tethys 2, Wagga Wagga, Australia.
- Kristan-Tollmann E. (1988a) - Unexpected microfaunal communities within the Triassic Tethys. *Geological Society, London, Special Publications*, 37: 213-223.
- Kristan-Tollmann E. (1988b) - A comparison of late Triassic agglutinated foraminifera of Western and Eastern Tethys. *Abhandlungen der Geologischen Bundesanstalt*, 41: 245-253.
- Kristan-Tollmann E. (1989) - Untersuchungen zum Schloßbau triadischer Cytheracea (Ostracoda). *Courier Forschungsinstitut Senckenberg*, 113: 49-60.
- Kristan-Tollmann E. (1991) - Triassic Tethyan microfauna in Dachstein Limestone blocks in Japan. In: Kotaka T. (Eds) - Shallow Tethys 3: 169-186. International Symposium on Shallow Tethys, Sendai, 1990, Sendai, Saito Ho-on Kai? Special Publication, 3.
- Kristan-Tollmann E. (1993) - Zur paläogeographischen Verbreitung der Ostracoden-Gattung *Hermiella* an der Rhät/Lias-Grenze. *Zitteliana*, 20: 331-342.
- Kristan-Tollmann E. & Hamedani A. (1973) - Eine spezifische Mikrofaunen-Vergesellschaftung aus den Opponitzer Schichten des Oberkarn der niederösterreichischen Kalkvoralpen. *Neues Jahrbuch für Geologie und Paläontologie Abhandlungen*, 143(2): 193-222.
- Kristan-Tollmann E. & Tollmann A. (1981) - Die Stellung der Tethys in der Trias und die Herkunft ihrer Fauna. *Mitteilungen der Österreichischen Geologischen Gesellschaft*, 74(75): 129-135.

- Kristan-Tollmann E. & Tollmann A. (1982) - Die Entwicklung der Tethystris und Herkunft ihrer Fauna. *Geologische Rundschau*, 71(8): 987-1019.
- Kristan-Tollmann E. & Gramann F. (1992) - Paleontological evidence for the Triassic age of rocks dredged from the northern Exmouth Plateau (Tethyan foraminifers, echinoderms and ostracodes). *Proceedings of the Ocean Drilling Program, Scientific Results*, 122: 463-474.
- Kristan-Tollmann E., Tollmann A. & Hamedani A. (1979) - Beiträge zur Kenntnis der Trias von Persien. I. Revision der Triasgliederung. Rhätfazies in Raum von Isfaham und Kossener Fazieseinschlag bei Waliabad SE Abadeh. *Mitteilungen der Österreichischen Geologischen Gesellschaft*, 70: 119-190.
- Kristan-Tollmann E., Tollmann A. & Hamedani A. (1980) - Beiträge zur Kenntnis der Trias von Persien. II. Zur Rhätafauna von Bagerabad bei Isfahan (Korallen, Ostracoden). *Mitteilungen der Österreichischen Geologischen Gesellschaft*, 73: 163-235.
- Latreille P.A. (1806) - Genera crustaceorum et insectorum: secundum ordinem naturalem in familias disposita, iconibus exemplisque plurimis explicata. Tomus 1. Koenig, Paris, 301 pp.
- Lethiers F. & Crasquin-Soleau S. (1988) - Comment extraire des microfossiles à tests calcitiques de roches calcaires dures. *Revue de Micropaléontologie*, 31: 56-61.
- Lord A.R. (1972) - The ostracod genera *Ogmoconcha* and *Procytheridea* in the Lower Jurassic. *Bulletin of the Geological Society of Denmark*, 21: 319-336.
- Lord A.R. (1982) - Metacopine ostracods in the Lower Jurassic. In: Banner E.T. & Lord A.R. (Eds) - Aspects of Micropalaeontology: 262-277. Allen & Unwin, London.
- Lord A.R. (1988) - Ostracoda of the Early Jurassic Tethyan Ocean. In: Hanai T., Ikeya N. & Ishizaki K. (Eds) - Evolutionary biology of Ostracoda, its fundamentals and applications. Proceedings of the 9th International Symposium on Ostracoda, Shizuoka, Japan 1985. Developments in Palaeontology and Stratigraphy, 11: 855-868. Kodansha/Elsevier, Tokyo.
- Lukeneder A., Surmik D., Gorzelak P., Niedźwiedzki R., Brachanec T. & Salamon M.A. (2020) - Bromalites from the Upper Triassic Polzberg section (Austria); insights into trophic interactions and food chains of the Polzberg palaeobiota. *Scientific Reports*, 10: 20545.
- Maddocks R.F. (1969) - Revision of Recent Bairdiidae (Ostracoda). *United States National Museum Bulletin*, 295: 1-126.
- Maddocks R.F. (2015) - New and poorly known species of *Bairdoppilata* and *Paranesidea* (Bairdiidae, Ostracoda) from French Frigate Shoals and O'ahu, the Hawaiian Islands. *Zootaxa*, 4059(6): 277-317.
- Maddocks R.F. & Wouters K.A. (1990) - *Triebelina* ? *pustulata* Keij, 1974 from the Maldive Islands: more homeomorphy in the ornate Bairdiidae (Ostracoda). *Bulletin de l'Institut royal des Sciences naturelles de Belgique, Biology*, 60: 173-180.
- McCoy F. (1844) - A Synopsis of the Characters of the Carboniferous Limestone Fossils of Ireland. Dublin University Press, Dublin, 207 pp.
- McKenzie K.G. (1982) - Palaeozoic-Cenozoic Ostracoda of Tethys. *Bollettino della Società Paleontologica Italiana*, 21(2-3): 311-326.
- Magurran A.E. (1988) - Ecological Diversity and its Measurement. Cambridge University Press, 179 pp.
- Mandelstam M.I. (1960) - [Subfamily Sigilliuminae.] 398. In: Chernysheva N.E. (Eds) - Osnovy paleontologii: Arthropoda, Trilobitomorpha et Crustaceomorpha. State Scientific-Technological Publishing House, Moscow, 515 pp.
- Mehes G. (1911) - Über Trias-Ostrakoden aus dem Bakony. Resultate der wissenschaftlichen Erforschung des Balatonsees. *Anhang zu Band 1, Teil 1, Paläontologie der Umgebung des Balatonsees*, 3: 1-38.
- Mette W. & Mohtat-Aghai P. (1999) - Ostracods and foraminifera from Upper Triassic intrashelf basin deposits in the Northern Calcareous Alps. *Geologisch Paläontologische Mitteilungen Innsbruck*, 24: 45-77.
- Mette W., Honigstein A. & Crasquin S. (2015) - Deep-water ostracods from the Middle Anisian (Reifling Formation) of the Northern Calcareous Alps (Austria). *Journal of Micropalaeontology*, 34: 71-91.
- Moissette P., Koskeridou E., Cornée J.-J., Guillocheau F. & Lécuyer C. (2007) - Spectacular preservation of seagrasses and seagrass-associated communities from the Pliocene of Rhodes, Greece. *Palaios*, 22: 200-211.
- Moix P., Kozur H., Stampfli G.M. & Mostler H. (2007) - New palaeontological, biostratigraphical and palaeogeographical results from the Triassic of the Mersin mélange, SE Turkey. *New Mexico Museum of Natural History and Science, Bulletin* 41: 282-311.
- Moix P., Beccalotto L., Kozur H., Hochard C., Rosselet F. & Stampfli G.M. (2008) - A new classification of the Turkish terranes and sutures and its implication for the paleotectonic history of the region. *Tectonophysics*, 451: 7-39.
- Moix P., Vachard D., Allibon J., Martini R., Wemli R., Kozur H. & Stampfli G.M. (2013) - Palaeotethyan, Neotethyan and Huglu-Pindos series in the Lycian Nappes (SW Turkey): Geodynamical implications. In: Tanner L.H., Spielmann J.A. & Lucas S.G. (Eds) - The Triassic System: 401-444. *New Mexico Museum of Natural History and Science, Bulletin* 61.
- Monostori M. (1996) - Pliensbachian ostracod fauna from condensed limestones of the Bakony Mts. (Transdanubian Central Range, Hungary). *Fragmenta Mineralogica et Palaeontologica*, 18: 31-61.
- Monostori M. & Tóth E. (2013) - Ladinian (Middle Triassic) silicified ostracod faunas from the Balaton Highland (Hungary). *Rivista Italiana di Paleontologia e Stratigrafia*, 119: 303-323.
- Monostori M. & Tóth E. (2014) - Additional Middle to Upper Triassic ostracod faunas from the boreholes of Transdanubian Central Range (Hungary). *Hantkeniana*, 9: 21-43.
- Moore R.C. (1961) - Treatise on Invertebrate Paleontology. In: Arthropoda 3, Crustacea, Ostracoda. Geological Society of America and University of Kansas Press, 442 pp.
- Müller G.W. (1894) - Die Ostracoden des Golfes von Neapel

- und der angrenzenden Meeres Abschnilte. *Fauna und Flora Neapel*, 21: 1-404.
- Müller G.W. (1912) - Crustacea: Ostracoda. *Das Tierreich*, 31: 1-434.
- Neale J.W. (1964) - Some factors influencing the distribution of Recent British Ostracoda. *Pubblcazioni della Stazione Zoologica di Napoli*, 33: 247-307.
- Nützel A. & Kaim A. (2014) - Diversity, palaeoecology and systematics of a marine fossil assemblage from the Late Triassic Cassian Formation at Settsass Scharte, N Italy. *Paläontologische Zeitschrift*, 88(4): 405-431.
- Oertli H.J. (1971) - The aspect of ostracode fauna – a possible new tool in petroleum sedimentology. In: Oertli H.J. (Eds) - Paléocologie des Ostracodes: 137-151. *Bulletin du Centre de Recherches de Pau, SNPA*.
- Piovesan E.K., Bergue C.T. & Fauth G. (2009) - Cretaceous ostracodes from Pará-Maranhão Basin, Brazil: taxonomy and preliminary paleoecological and paleobiogeographical inferences. *Revue de Paléobiologie*, 28: 457-470.
- Peybernes C., Chablais J. Onoue T., Escarguel G. & Martini R. (2016) - Paleocology, biogeography, and evolution of reef ecosystems in the Panthalassa Ocean during the Late Triassic: Insights from reef limestone of the Sambosan Accretionary Complex, Shikoku, Japan. *Palaeogeography, Palaeoclimatology, Palaeoecology*, 457: 31-51.
- Pielou E.C. (1979) - Biogeography. John Wiley & Son, New-York, 351 pp.
- Podam J. (1989) - New combinational clustering methods. *Vegetatio*, 81: 61-77.
- Reid R.P. (1985) - The facies and evolution of an Upper Triassic reef complex in Northern Canada. PhD thesis, University of Miami, Coral Gables, Florida, United States, 370 pp.
- Reid R.P. (1988) - Lime Peak reef complex, Norian age, Yukon. In: H.H.J. Geldsetzer, N.P. James & G.E. Tebbutt (Eds) - Reefs, Canada and Adjacent. Canadian Society of petroleum Geologists, Memoir 13: 758-765.
- Reid R.P. & Ginsburg R.N. (1986) - The Role of Framework in Upper Triassic Patch Reefs in the Yukon Canada. *Palaios*, 1: 590-600.
- Reid R.P. & Tempelman-Kluit D.J. (1987) - Upper Triassic Tethyan-type reefs in the Yukon. *Bulletin of Canadian Petroleum geology*, 35: 316-332.
- Reuss A.E. (1868) - Foraminiferen und Ostracoden aus dem Schichten von St. Cassian. *K. Akademie Wissenschaften, Mathematisch-Naturwissenschaftliche Klasse, Sitzungsberichte*, 57(1): 101-108.
- Reys S. (1963) - Ostracodes de peuplements algaux de l'étage infralittoral de substrat rocheux. *Recueil des travaux de la Station marine d'Endoume*, 28(43): 33-47.
- Sars G.O. (1866) - Oversigt af marine Ostracoder. *Norske Videnskaps-Akademi, Förhandlingar*, 1865: 1-130.
- Sars G.O. (1887) - Nye bidrag til kundskaben om middelhavets invertebrafauna: 4. Ostracods mediterranea (sydeuropæiske ostracoder). *Archiv for Matematik og Naturvidenskab*, 12: 173-324.
- Sars G.O. (1922-1928) - An account of the Crustacea of Norway. Volume 9, Crustacea. *Bergen Museum*, 9: 1-277.
- Schroeder-Adams C. & Haggart J.W. (2006) - Biogeography of Foraminifera in tectonic reconstructions; imitations and constraints on the paleogeographic position of Wrangellia. *Geological Association of Canada Special Paper*, 46: 95-108.
- Senowbari-Daryan B. & Reid R.P. (1987) - Upper Triassic sponges (sphinctozoa) from southern Yukon, Stikinia terrane. *Canadian Journal of Earth Sciences*, 24: 882-902.
- Shannon C.E. & Weaver W. (1949) - The Mathematical Theory of Communication. University of Illinois Press, Urbana, Illinois, USA.
- Shi G.R. (1993) - Multivariate data analysis in palaeology and palaeobiogeography, a review. *Palaeogeography, Palaeoclimatology, Palaeoecology*, 105: 199-234.
- Shi C. & Chen D. (1987) - The Changhsingian ostracodes from Meishan Changxing, Zhejiang. Stratigraphy and palaeontology of systemic boundaries in China. *Permian and Triassic Boundary*, 5: 23-80.
- Smith P.L. (2006) - Paleobiogeography and Early Jurassic molluscs in the context of terrane displacement in western Canada. In: Haggart J.W., Enkin R.J. & Monger J.W.H. (Eds) - Paleogeography of the North American Cordillera: Evidence for and against Large-Scale Displacements: 81-91. Geological Association of Canada.
- Sohn I.G. (1960) - Paleozoic species of *Bairdia* and related genera. *United States Geological Survey Professional Paper*, 330-A: 1-105.
- Sohn I.G. (1962) - The ostracod genus *Cytherelloidea*, a possible indicator of paleotemperature. *United States Geological Survey Professional Paper*, 450D: D-144-D147.
- Sohn I.G. (1964) - Significance of Triassic ostracodes from Alaska and Nevada. *United States Geological Survey Professional Paper*, 501D: D40-D42.
- Sohn I.G. (1968) - Triassic ostracodes from Makhtesh Ramon, Israel. *Bulletin of the Geological Survey of Israel*, 44, 1-71.
- Sohn I.G. (1984) - Tethyan marine Triassic ostracodes in northeastern Alaska. In: Reed K.M. & Bartsch-Winkler S. (Eds) - The United States Geological Survey in Alaska during 1982. *United States Geological Survey Circular*, 939: 21-23.
- Sohn I.G. (1987) - Middle and Upper Triassic Marine Ostracoda From the Shublik Formation, Northeastern Alaska. *United States Geological Survey Bulletin*, 1664: C1-C24.
- Stampfli G.M. & Kozur H. (2006) - Europe from the Variscan to the Alpine cycles. In: Gee D.G. & Stephenson R.A. (Eds) - European Lithosphere Dynamics: 57-82. Memoir of the Geological Society, London.
- Swain F.M. (1974) - Some Upper Miocene and Pliocene(?) Ostracoda of Atlantic Coastal Region for Use in Hydrogeologic Studies. *United States Geological Survey Professional Paper*, 821: 1-50.
- Sylvester-Bradley P.C. (1961) - Suborder Metacopina Sylvester-Bradley, n. suborder. Q358–359. In Moore RC (Ed.) Treatise of invertebrate paleontology. Part Q, Arthropoda 3, Crustacea, Ostracoda. Geological Society of America, Boulder, CO and University of Kansas Press, Lawrence, KS, 442 pp.
- Theisen B.F. (1966) - The life history of seven species of os-

- tracods from a Danish brackish water locality. *Meddelelser fra Danmarks Fiskeri- og Havundersøgelser*, 4: 215-270.
- Tollmann A. (1976) - Analyse des klassischen nordalpinen Mesozoikums. *Monographie des Nördlichen Kalkalpen*, 2: 1-580.
- Tollmann A. & Kristan-Tollmann E. (1970) - Geologische und mikropaläontologische Untersuchungen im Westabschnitt der Hallstätter Zone in den Ostalpen. *Geologica et Palaeontologica*, 4: 87-145.
- Tressler W.L. & Smith E.M. (1948) - An ecological study of seasonal distribution of Ostracoda, Solomons Island, Maryland region. *Chesapeake Biological Laboratory Publication Series/Contribution Series*, 71: 1-61.
- Triebel E. (1941) - Zur Morphologie und Ökologie der fossilen Ostracoden. Mit Beschreibung einiger neuer Gattungen und Arten. *Senckenbergiana* 23, 294-400.
- Ulrich E.O. & Bassler R.S. (1923) - Paleozoic Ostracoda: their morphology, classification and occurrence. In: Maryland Geological Survey (Eds) - Silurian: 271-391. Johns Hopkins Press, Baltimore.
- Ulrichs M. (1971) - Variability of some ostracods from the Cassian Beds (Alpine Triassic) depending on the ecology. *Bulletin du Centre de Recherches Pau-SNP4*, 5: 695-715.
- Ulrichs M. (1972) - Ostracoden aus den Kössener Schichten und ihre Abhängigkeit von der Ökologie. *Mitteilungen der Gesellschaft der Geologie und Bergbaustudenten in Österreich*, 21:661-710.
- Vérard C. (2019) - Panalexis: Towards global synthetic palaeogeographies using integration and coupling of manifold models. *Geological Magazine*, 156 (2), 320-330. doi:10.1017/S0016756817001042.
- Vérard C., Hochard C., Baumgartner P.O. & Stampfli G.M. (2015) - 3D palaeogeographic reconstructions of the Phanerozoic versus sea-level and Sr-ratio variations. *Journal of Palaeogeography*, 4(1): 64-84. doi: 10.3724/SPJ.1261.2015.00068.
- Warne M.T. (1988) - *Neonesidea* and *Bairdoppilata* (Ostracoda) from the Miocene of the Port Phillip and Western Port Basins, Victoria, Australia. *Alcheringa: An Australasian Journal of Palaeontology*, 12(1): 7-26.
- Warwick R.M. & Clarke K.R. (1995) - New 'biodiversity' measures reveal a decrease in taxonomic distinctness with increasing stress. *Marine Ecology Progress Series*, 129: 301-305.
- Warwick R.M. & Clarke K.R. (1998) - Taxonomic distinctness and environmental assessment. *Journal of Applied Ecology*, 35(4): 532-543.
- Wei M., Li Y.W., Jiang Z.W. & Xie L.C. (1983) - Subclass Ostracoda. In: Chengdu Institute of Geology and Mineral Resources (Eds) - Palaeontological Atlas of Southwest China, Guizhou. Volume of Microfossils: 23-254. Geological Publishing House, Beijing, China [in Chinese].
- Whatley R.C. & Boomer I. (2000) - Systematic review and evolution of the early Cytheruridae (Ostracoda). *Journal of Micropalaeontology*, 19: 139-151.
- Whatley R.C. & Wall D.R. (1969) - A preliminary account of the ecology and distribution of Ostracoda in the southern Irish Sea. In: Neale J. (Eds) - Taxonomy, Morphology and Ecology of Recent Ostracoda: 268-298. Edinburgh: Oliver & Boyd.
- Whatley R.C. & Wall D.R. (1975) - The relationship between Ostracoda and algae in littoral and sublittoral marine environments. In: Swain F.M. (Eds) - Biology and Palaeobiology of Ostracoda. *Bulletin of the American Palaeontology Society*, 5: 173-203.
- Whatley R.C. Cooke P.C.B. & Warne M.T. (1995) - Ostracoda from Lee Point on Shoal Bay, Northern Australia: Part 1 - Cladocopina and Platycopina. *Revista Española de Micropalaeontología*, 27: 69-89.
- Wheeler J.O. & McFeeely P. (1991) - Tectonic assemblage map of the Canadian Cordillera and adjacent part of the United States of America. Geological Survey of Canada Map.
- White D., Colpron M. & Buffett G. (2012) - Seismic and geological constraints on the structure and hydrocarbon potential of the northern Whitehorse trough, Yukon, Canada. *Bulletin of Canadian Petroleum Geology*, 60: 239-255.
- Wieser W. (1952) - Investigations of the microfauna inhabiting seaweeds on rocky coasts IV. Studies on the vertical distribution of the fauna inhabiting seaweeds below the Plymouth laboratory. *Journal of Marine Biology*, 31: 145-174.
- Wolda H. (1981) - Similarity indices, sample size and diversity. *Oecologia*, 50: 296-302.
- Zorn I. (2010) - Ostracodal type specimens stored in the paleontological collection of the Geological Survey of Austria. *Jahrbuch der Geologischen Bundesanstalt*, 150(1+2): 263-299.